THE IMPACT OF IMPOUNDMENT AND URBANIZATION ON SHALLOW GROUNDWATER CONDITIONS IN THE JOE POOL LAKE CATCHMENT, TEXAS

by

MANOJ KUMAR GHIMIRE

Presented to the Faculty of the Graduate School of

The University of Texas at Arlington in Partial Fulfillment

of the Requirements

for the Degree of

DOCTOR OF PHILOSOPHY

THE UNIVERSITY OF TEXAS AT ARLINGTON

December 2014

In memory of my mother and dedicated to my father, brothers, and teachers,

“teachers of different phases of my life”, who opened my eyes,

inspired, and amalgamated the “Continuum Light of Knowledge”

and helped me

to stand who I am now and what I will be in future.

Acknowledgements

Numerous contributions from many individuals have aided the completion of this dissertation research; without their help my work would have been impossible. The space permitted in this dissertation would be insufficient to describe their contribution. I am obliged to them for contributions and my genuine thanks go to all of them!!!

My genuine thanks go to Gordon D. Bennett, volunteer in the Department of Earth and Environmental Sciences, and retired hydrogeologist at the U.S. Geological Survey and S. S. Papadopulos and Associates, Inc., for his guidance in all aspects of modeling since the beginning of my dissertation research, and for proof reading my initial manuscript. I am indebted for his help.

My sincere thanks go to my advisor Dr. Qinhong Hu for his guidance, comments, and support from the beginning of my Ph. D. work. Thanks to the committee members, Dr. James P. Grover, Dr. Merlynd K. Nestell, Dr. Arne M. Winguth, and Dr. Nick Z. Fang for their comments, guidance, and time in serving on my dissertation committee. I am indebted with Professor Dr. Merlynd K. Nestell, for his time and generous support and final proof reading of my manuscript. Without his help I would not have completed on time.

I am indebted to Mr. Josh Been, GIS librarian of University of Texas at Arlington (UTA) library. His guidance in processing land-use data, digital elevation data, and demographic data using GIS analysis has indeed helped me to integrate GIS applications with groundwater modeling, and to automate data processing and visualization.

I would like to thank my beloved wife Sabita, who has always encouraged and inspired me to do my best. Her emotional help and unspoken eyes have played a vital role in completion of this dissertation. Thanks to my son Abhash, my brothers, and sisters in law. Thanks go to my father, father in law and mother in law; their help and emotional support have been supreme during this research work.

The following agencies and individuals assisted directly and indirectly in the research completion with their personal support, data, and resources: US Army Corps of Engineers (USACE) Fort Worth District; City of Arlington; City of Grand Prairie; City of Mansfield; City of Midlothian; City of Cedar Hill; City of Burleson; City of Alvarado; Texas Department of Transportation (Fort Worth and Dallas Regions); Texas Water Development Board (TWDB); Texas Commission on Environmental Quality (TCEQ); North

Central Texas Council of Government (NCTCOG); US Geological Survey (USGS); Texas Natural Resources Information Systems (TNRIS); Texas Bureau of Economic Geology (BEG); Trinity River Authority (TRA); Railroad Commission of Texas (RRC); Tarrant County; Johnson County; Ellis County; Dallas County; Minnesota Population Center National Historical Geographical Information System (MPC-NHGIS); US Census Bureau (USCB); National Weather Services (NWS-NOAA).

November 19, 2014

Abstract

THE IMPACT OF IMPOUNDMENT AND URBANIZATION ON SHALLOW GROUNDWATER CONDITIONS IN THE JOE POOL LAKE CATCHMENT, TEXAS

Manoj Kumar Ghimire, PhD

The University of Texas at Arlington, 2014

Supervising Professor: Qinhong Hu

This dissertation is an assessment of the shallow groundwater (SGW) regime within the drainage area of Joe Pool Lake (JPL), an impoundment on Mountain Creek (MC) located in Grand Prairie, Texas. A thin zone of highly-weathered consolidated rock is normally found at the upper surface of the bedrock in north-central Texas; the SGW regime, or shallow aquifer, as defined for this study, extends vertically downward from the water table to the base of this highly-weathered layer, and extends laterally over the surface water drainage area of JPL and its tributaries. Geologically, the shallow aquifer thus consists largely of unconsolidated material, chiefly Holocene and Quaternary deposits on the floodplains and terraces of MC, Walnut Creek, and other creeks of the MC drainage system. The creation of JPL has, in itself, had a significant impact on the shallow groundwater regime; rapid urbanization has occurred in the vicinity of JPL since the completion of the impoundment, and questions exist as to the effects, current or potential, of this urbanization on the SGW. The objective of the research reported herein was to examine and analyze the impact of the lake itself on the SGW, and to evaluate the impacts of the subsequent urbanization on the hydrology of the JPL watershed.

The research utilized finite-difference simulation of groundwater flow, applied in an investigative sense, to gain an understanding of the hydraulics of the groundwater regime, and used Geographic Information System (GIS) technology to prepare simulation input data, to process and interpret supporting data, and to analyze and evaluate simulation results. The flow simulations were undertaken using the U.S. Geological Survey's MODFLOW-2005 software to calculate heads and model-wide flow totals, and using the MODFLOW postprocessor ZONEBUDGET-1996 to calculate internal flows and sub-regional

groundwater budgets. Two steady-state simulations were performed with the objective of determining the rates and directions of groundwater (GW) flow throughout the SGW, in an average or long-term sense, first as the system now exists, with the lake in place, and then as the system existed prior to construction of the lake. In each simulation, it was assumed that the GW flow regime was in hydrologic equilibrium, and was limited by GW divides coinciding with the topographic divides surrounding the study area. The model was calibrated by comparing the observed borehole water level with calculated heads and comparing the baseflow per unit area of the catchment with the model calculated flow from SGW into the river. The optimum model thus obtained was again simulated using an unconfined approach so that the heads above the land surface and dry heads were kept within 25% of total. Finally the head distribution was found to be a replica of the subdued image of the topography.

Based on the results of simulation and the information supported by land-use, streamflow analysis, and demographic data, it appears that whereas the SGW in general is sensitive to the external systems and factors, to date the impact of impoundment and urbanization have been moderate. Obviously, in any natural setting the effect of recharge due to population-based water is trivial compared to the effect of land-use change and urbanization; the impact of rainfall is utmost.

The presence of the lake has had an impact on the area hydrology and GW-SW interaction has changed. Prior to lake construction, GW discharged directly to the streams, and by near-surface discharge processes from the water table. In the present regime, GW discharge is primarily into the lake. From there discharge is by lake evaporation, gated discharge, municipal use, etc. The model results provide information that, the recharge to the GW regime has increased by about 5%, whereas the volume of SGW has increased by about 4%, although the distribution of GW has changed. Water levels are higher around the lake, but tend to be lower farther from the lake. The recharge from the shallow aquifer into the strata of the Woodbine is approximately similar in pre and post-lake conditions. Urbanization has imported extra water, but much of the import is either lost by near-surface discharge processes, or exported through sanitary sewer systems, or directly discharged to the SW system through storm sewer network. More work with well distributed observed water table data, improved versions of MODFLOW 2005 such as MODFLOW NWT and MODFLOW USG, and transient simulation would be required for an improvement of the model.

Table of Contents

List of Illustrations

List of Tables

List of Acronyms

ArcMap - the main component of Esri's ArcGIS Geospatial Processing Programs

BOT – Bottom of the finite difference-cell

CBD – Central Business District

CFD – Cubic Feet Per Day

CFS – Cubic Feet Per Second

CFY – Cubic Feet Per Year

CHD – Constant Head Boundary

CSV – Comma-Separated Values

DEM – Digital Elevation Model

EFS – Eagle Ford Shale

EOS – Earth Observing System

ESRI – Environmental Systems Research Institute

ET – Evapotranspiration

EVT – MODFLOW Evapotranspiration Package

FID – Field Identification Number used in GIS

ft – feet

gal – gallons

GHB – General Head Boundary

GIS – Geographic Information System

GMS – Groundwater Modeling System

GW – Groundwater

GWF – Groundwater Flow

GWM – Groundwater Management

CH – High Plasticity Clay

CL – Low Plasticity Clay

ID – Identification Number used in GIS

in – inches

JPL – Joe Pool Lake

LSD – Land Surface

LUCODE – Land-Use Code

MC – Mountain Creek

MCL – Mountain Creek Lake

MCRWS – Mountain Creek Regional Wastewater System

MGD – Million Gallons Per Day

MNA – Monitored Natural Attenuation

MPC – Minnesota Population Center

MOD16 – Evapotranspiration component of MODIS

MODFLOW – Modular Three-dimensional Groundwater Flow Model

MODFLOW-DCM – MODFLOW Dual Conductivity Model

MODIS – Moderate Resolution Imaging Spectroradiometer

MODPATH – Modular Three-dimensional Particle Tracking Post-Processing Program

MSL/msl – Mean Sea Level

MT3DMS – MODFLOW Modular Three-dimensional Transport Model

NA – Not Available

NASA – National Aeronautics and Space Administration

NASD – Naval Air Station Dallas

NCTCOG – North Central Texas Council of Government

NHGIS – National Historical Geographic Information System

NLDAS – North American Land Data Assimilation System

NTSG – Numerical Terradynamic Simulation Group

NTW-GAM – Northern Trinity Woodbine Groundwater Availability Model

NWIRP – Naval Weapons Industrial Reserve Plant

NWS-NOAA – National Weather Services - National Oceanic and Atmospheric Administration

OSSF – On-site Sewage Facility

OPR-PPR – Observation-Prediction (OPR) and Parameter-Prediction (PPR)

PART – USGS Baseflow Separation Program

PCPN – Precipitation

PDE – Partial Differential Equation

PHREEQC – pH-REdox-EQuilibrium

PEST – Parameter Estimation

PMF – Probable Maximum Flood

PMPH – Probable maximum Flood Hydrograph

Quasi-3D – Quasi Three-dimensional Approach

RCH – Recharge Package

REV – Representative Elementary Volume

RIV – MODFLOW River Package

RRC – Railroad Commission of Texas

RT3D – MODFLOW Reactive Transport in 3 Dimensions

SGW – Shallow Groundwater

SIM_ADJUST – Simulated Adjustment, A computer Code that Adjusts Simulated Equivalents for Observations

SSC – Superconducting Super Collider

SUH – Synthetic Unit Hydrograph

SW – Surface Water

TCEQ – Texas Commission on Environmental Quality

TNRIS – Texas Natural Resources Information Systems

TRA – Trinity River Authority

TU – Tribhuvan University

TWDB – Texas Water Development Board

TxDOT – Texas Department of Transportation

UCODE – Universal Inverse Modeling Post-processors for sensitivity analysis, data assessment, calibration, prediction, and uncertainty analysis

UH – Unit Hydrograph

USACE – U. S. Army Corps of Engineers

USCB – US Census Bureau

USGS – U. S. Geological Survey

UTA – University of Texas at Arlington

WC – Walnut Creek

WEL – MODFLOW Well Package

WHAT – Web-based Hydrograph Analysis Tool

ZONEBUDGET – MODFLOW - Zone Budget Post-processor Program

Chapter 1

Introduction

1.1 Background

Joe Pool Lake (JPL) is one of many artificial lakes in northern Texas. Along with Mountain Creek Lake (MCL), it is one of two major impoundments on Mountain Creek (MC), a tributary to the West Fork of the Trinity River. JPL lies a short distance south (upstream) of MCL, in the city of Grand Prairie. It is fed primarily by MC and its tributary, Walnut Creek (WC), although several smaller streams also feed into the JPL. MCL is fed primarily by MC as it flows northward from the JPL dam, although a minor input is also provided by small streams flowing directly into the lake.

The area of JPL watershed is alone approximately 224 square miles. JPL has surface area of 11.67 square miles at normal pool level of 522 feet msl (USACE, 1991; Sterner, 1994). Figure 1-1 shows the drainage area of JPL, which is the study area of this research. The JPL dam is located at the river mile of 11.2 miles on MC (USACE, 1979). The area of JPL is divided into two arms, corresponding to the valleys of MC and WC. The lake serves the city of Midlothian as one of its sources of water supply, and is also extensively used for recreation. Having an area of about 4.23 square miles, MCL is the smaller and older of the two lakes. The total area draining directly into MCL (downstream of the JPL dam), and draining into the reach of MC between the two lakes, is about 63 square miles, giving an area of about 287 square miles for the combined watershed. Construction of MCL was initiated in 1929 (Table 1-1), but the reservoir was apparently not completely full until 1938. Construction of JPL was initiated in 1981, and impoundment was initiated in 1986; the reservoir was completely filled by 1989.

Table 1-1 The Evolution of MCL and JPL Through Time

Event	MCL	JPL
Start Construction	1929[1]	1981[2]
Complete Construction	1936[1]	December 1985[2]
Begin Impoundment	January 1937[1]	January 1986[2]
Achieve Full Impoundment	June 1938[1]	June 1989[2]
Hensley Field and Subsequent NASD Operation	1928[3]	NA
NWIRP Operation	1941[3]	NA
Resource Conservation and Recovery Act (RCRA) Facility Investigation (RFI)	1998[4]	NA

Note: NA = Not Applicable

(Sources: [1] Dowell, 1964; [2] USACE, 1991; [3] Van Metre and others, 2003; [4] EnSafe/Allen & Hoshall, 1996 a; b; 1997 a; b)

The drainage area of JPL, as shown in Figure 1-1, is the area of study for this research. The alluvium of this area consists of unconsolidated terrace and floodplain deposits of the WC and MC drainage systems. As used in this dissertation, the shallow groundwater regime, or shallow aquifer, refers to groundwater within the JPL catchment area, and occurring in the alluvial materials, or in a thin zone of enhanced permeability normally found at the upper surface of the underlying bedrock.

The strata of the Woodbine Group subcrop and outcrop locally on the western side of the project area and dips below the Eagle Ford Shale (EFS) at the eastern boundary of the WC watershed. The EFS is the dominant bedrock unit in the project area, forming the subcrop over approximately 70% of the study area. This unit downdips under the Austin Chalk unit along the eastern margin of the JPL watershed, in the vicinity of Cedar Hill. The Austin Chalk outcrops along the eastern boundary of the project area (Figures 1-2 and 1-3). The Quaternary units are found primarily in the stream valleys, terraces, upstream of JPL, and between the two arms of JPL. Hydrogeologically, the Woodbine Group strata is a relatively minor aquifer (George and others, 2011), and the EFS and Austin Chalk are considered aquitards. The overburden above these units forms the shallow aquifer. Further details of the geology and hydrogeologic setting are given in Section 1.3 of Chapter 1, and in Chapter 2.

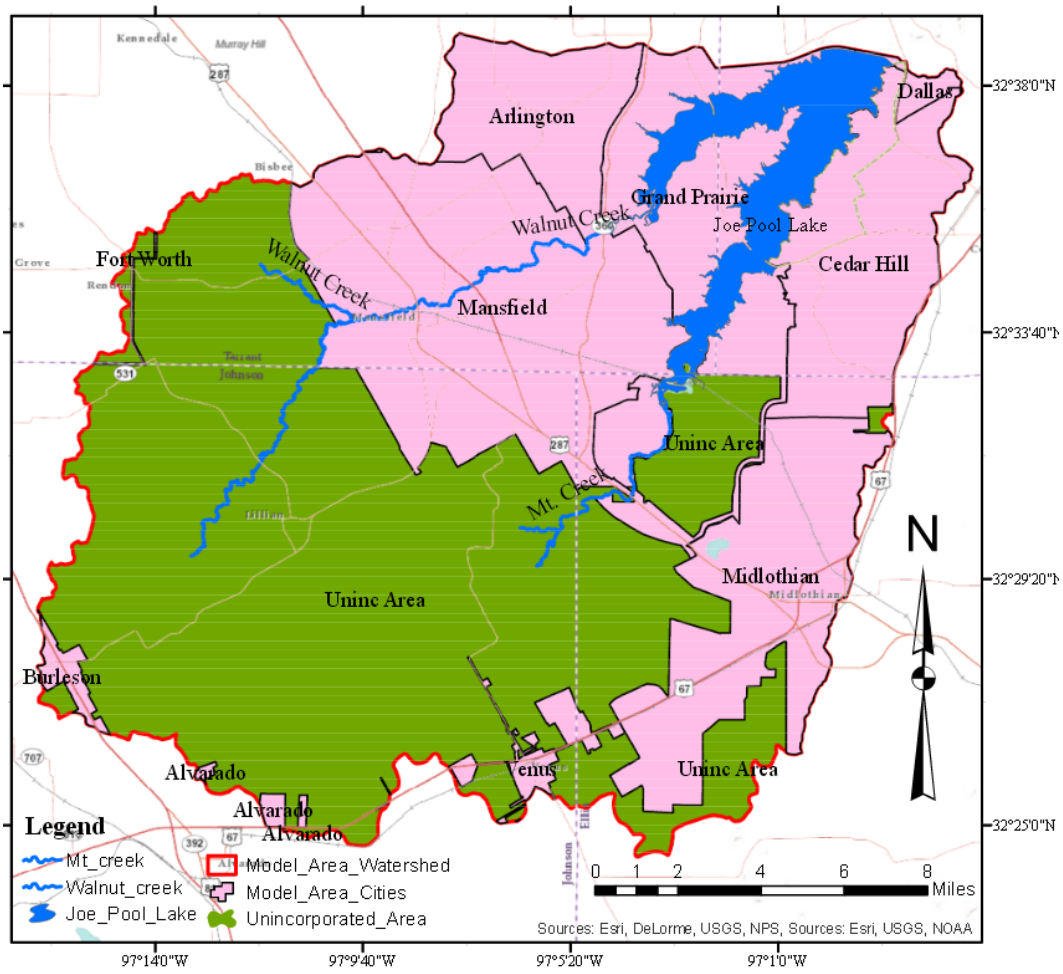

Figure 1-1 Map of the study area; JPL is located southeast of Arlington, primarily in the City of Grand Prairie. MCL lies to the north, outside the proposed study area

Prior to the creation of MCL and JPL, the region shown in Figure 1-1 largely consisted of agricultural land, largely unused or undeveloped land. Beginning some years prior to World War II, areas near the northern shore of MCL were occupied by military aviation facilities, and by electric power generation facilities (Van Metre and others, 2003); MCL was in fact built as a source of power plant cooling water. During and after World War II, the military aviation activities near MCL were expanded into the (now-decommissioned) Naval Air Station Dallas (NASD) and the Naval Weapons Industrial Reserve Plant (NWIRP). The operation of these facilities through the years caused local contamination of groundwater and MCL sediment with organic chemicals and trace elements (Van Metre and others,

2003). Numerous investigations of these problems have been carried out in recent years, and the hydrologic information of those investigations is a significant resource for the research described herein. Similarly, an area at a short distance southeast of JPL project area, as shown in Figure 1-1, was at one time considered a potential site for the proposed Superconducting Super Collider (SSC). A detailed hydrogeological study of a part of that site (Wickham, 1991) also is a significant resource for this research.

The study area incorporates parts of four counties: Dallas, Tarrant, Ellis, and Johnson. The Dallas County segment falls in the northeast quadrant of the project area; Ellis County covers the southeast quadrant of the project area and Johnson County extends into the southwest quadrant. Tarrant County covers the northwest quadrant of the project area. In addition, the project area includes some portion of ten cities of the Dallas-Fort Worth Metroplex: Dallas, Arlington, Fort Worth, Grand Prairie, Mansfield, Midlothian, Cedar Hill, Venus, Burleson, and Alvarado. Almost all of the City of Mansfield lies within the study area, whereas relatively small parts of Dallas, Fort Worth, Venus, Alvarado, and Burleson lie in the project area. About half of the project area is unincorporated, which lies mostly in Johnson County and Ellis County (Figure 1-1).

1.2 Factors Affecting the Hydrogeology of the Study Area

The area of study for this research, i.e., the catchment area of JPL, remained relatively undeveloped until the completion of the lake in 1989; since that time, rapid urbanization has characterized the area. The alluvial deposits are generally thin and of relatively low hydraulic conductivity, and are little used for water supply; most of the groundwater used in the study area is derived from aquifers of the underlying consolidated-rock sequence.

As noted above, most of the study area is underlain by the EFS (see for example, Figure 1-2 and Jones and Paillet, 1995). Vertical flow through the EFS must be downward under prevailing hydraulic gradients, but is generally assumed to be very small relative to the flows in the shallow aquifer and/or in deeper bedrock aquifers. An estimate of the magnitude of this downward flow was made in the course of the research reported herein, but is subject to uncertainty because of the sparse data on the vertical

hydraulic conductivity of the EFS. Production of water from wells in the study area is almost entirely from bedrock aquifers below the EFS. These aquifers include strata of the Woodbine Group, which directly underlie the EFS wherever the EFS is present; the Paluxy Formation, which is separated from the Woodbine Group strata by confining units of the Washita and Fredericksburg groups; and the Twin Mountains Formation, which is separated from the Paluxy by aquitards of the Glen Rose Formation. The EFS has been removed by erosion in the western portion of the study area, so that the shallow aquifer directly overlies the strata of the Woodbine Group in that vicinity. The Austin Chalk overlies the EFS in a narrow zone in the eastern part of the study area, and thus directly underlies the alluvium in that area (see Figures 1-2 and 1-3, and Table 1-2).

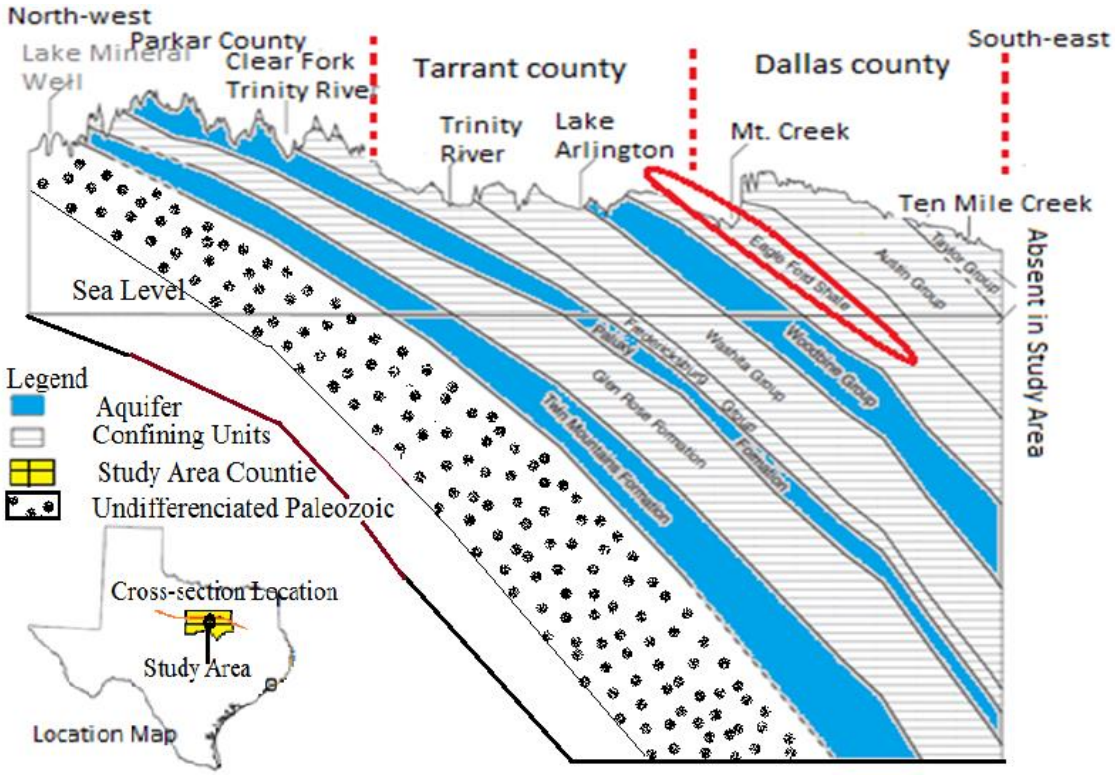

Figure 1-2 Generalized cross-section showing the consolidated rock units near the study area. The cross-section is not to the scale (Source: Jones and Paillet, 1995)

The impoundment of MCL and JPL necessarily had significant impacts on the local hydrology, including in particular a major change in the surface water base level against which groundwater

discharge occurs. After the lake impoundment, the water balance in the catchment was changed due to changes in infiltration, lake evaporation, evapotranspiration (ET), and other factors. One of the questions addressed by this research was whether, or to what extent, the urbanization in recent years has generated additional hydrologic impacts, such as further changes in ET, changes in the patterns and intensity of runoff and infiltration, and changes in sedimentation (which could affect both the thickness and permeability of the lake-aquifer interconnection). One of the conclusions of this research is that the total impact of urbanization on hydraulic aspects of the shallow groundwater regime has, to date, been relatively modest. As discussed above, the industrial development began to the north of the study area with power generation, the NASD activities, and the NWIRP facility. Land-use data available in GIS format through the North Central Texas Council of Governments (NCTCOG) indicates that there has been little overall change in the fraction of land devoted to industry within the study area, and this observation is consistent with the hydrologic interpretations of this research.

1.3 General Geology and Hydrogeological Setting

Table 1-2 and Figures 1-2 and 1-3 illustrate the geology and hydrogeological setting of the water-bearing formations within the project area.

The geology of the JPL project area is dominated by the Upper Cretaceous Formations, namely Woodbine Group strata, EFS, and Austin Chalk. Holocene and Quaternary Alluvium overlie the bedrock of these Upper Cretaceous Formations. The older formations subcrop and outcrop on the wstern side of the project area, and younger formations are on the eastern side. In this pattern, the strata of the Woodbine Group subcrop under the unconsolidated overburden on the western side along the WC watershed and also along the thalweg of the MC. The EFS, as noted above, subcrops under the unconsolidated overburden in the central part of the study area, mostly in the MC Valley. The Austin Chalk subcrops on the eastern edge of the project area, along the Cedar Hill Ridge. The Quaternary and Holocene deposits appear along the river valleys of the MC and WC and between the two arms of JPL. Thus, the shallow aquifer functions as a recharge pathway for the deeper aquifers. Lower Cretaceous

deposits below the Woodbine Group strata include the Washita Formation, the Fredericksburg Formation, and the Trinity Formation. However, these units are not included in the present research.

Table 1-2 The Geologic Units in the Study Area

Era	System	Series	Group	Stratigraphic Unit	
Cenozoic	Quaternary	Holocene		Alluvium	
		Pleistocene		Fluvial Terrace Deposits	
Mesozoic	Cretaceous	Gulf	Austin		
			Eagle Ford		
			Woodbine	Undifferentiated	
		Comanche	Washita	Undifferentiated	
			Fredericksburg	Undifferentiated	
			Trinity	Antlers Formation	Paluxy Formation
					Glen Rose Formation
					Twin Mountain Formation

The strata of the Woodbine Group (Kwb) form the lowest unit of the Upper Cretaceous deposits. This unit is often referred to as sandstone, and is composed of sandstone, clay, and shale. The upper part is basically sandstone, fine grained and well sorted. Ripple marks, and large scale cross bedding are visible in the strata of the various parts of this group. The Woodbine Group strata is acidic, with reddish brown iron-oxide concretions near the top (BEG, 1972). The Woodbine Group strata downdip below the EFS in the eastern part of the WC drainage at a slope of 50 feet per mile.

The EFS (Kef) subcrops over a large part of the project area and dips below the Austin Chalk near the base of Cedar Hill Ridge, in the eastern part of the watershed. The EFS is composed of shale,

sandstone, and limestone. Its upper part contains shale and selenite; it is bituminous with calcareous concretions and large septaria. Sandstone and sandy limestone are common in the upper part. The middle part is composed of platy, medium to dark gray shale. The lower part has a number of bentonite beds (BEG, 1972). The EFS functions as an aquitard. In the simulations carried out in this research, horizontal flow through it is neglected, whereas the vertical flow is represented by reducing the vertical conductance of the interval between the shallow aquifer and the Woodbine Aquifer (Layer 1 and Layer 2, respectively), using an appropriate MODFLOW option, popularly known as U.S. Geological Survey modular three-dimensional finite-difference flow model.

The Austin Chalk (Kau) is the youngest of the three Upper Cretaceous formations inside the project area. It subcrops along the eastern margin of the JPL watershed near the Cedar Hill Ridge. It is composed of marine microfossils and is mostly microgrannular calcite or chalk. Massive layers of chalk and calcareous clay and thin layers of bentonite can be seen in the lower part. The middle part is mostly thin-bedded marl with inter-bedded chalk. It weathers white and forms a white rock cuesta (BEG, 1972).

The perennial creeks that discharge into JPL, as well as some intermittent creeks in the study area, exhibit Holocene (Qal) sedimentary deposits on their banks. Terrace deposits of the Pleistocene fluvial process (Qt) are found along river terraces. The Pleistocene is composed of gravel, sand, silt, and clay, whereas the Holocene deposits are composed mostly of alluvium and are found on the flood-plains of perennial and intermittent creeks, and on the lowest terrace deposits. The latter are composed of gravel, sand, silt, silty-clay, and organic matter, either eroded or transported by overland flow, direct runoff, or flood (BEG, 1972).

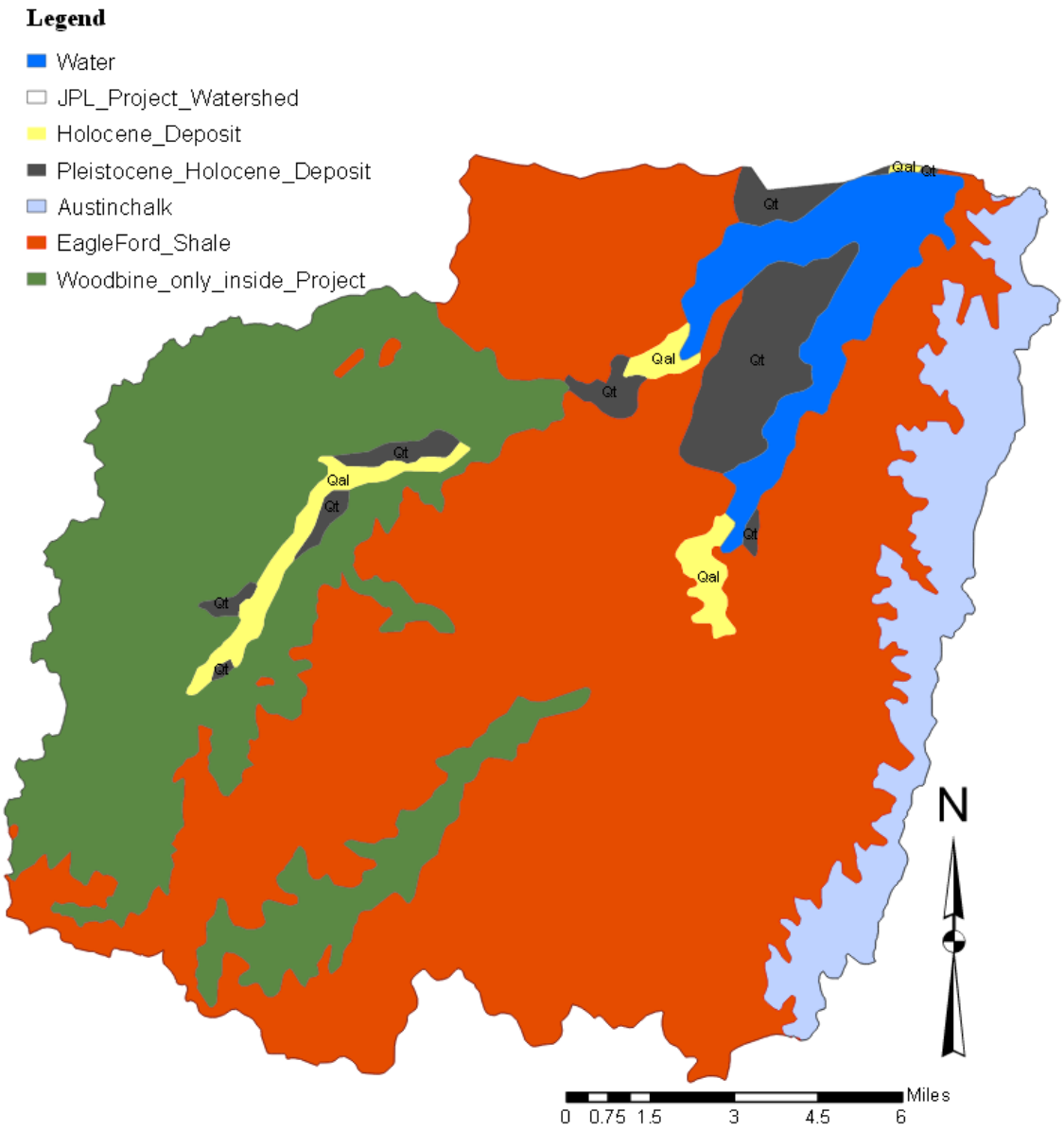

Figure 1-3 Geologic map of the project area (Source: BEG____, Bureau of Economic Geology, UT Austin)

1.4 Research Objectives

The main objectives of this research were to understand the impact of the lake itself on shallow groundwater, and to understand also the impacts of urbanization on hydrology of the JPL watershed. Some specific objectives of this research can be summarized as follows:

1. Develop detailed water balances for the JPL catchment, both for current conditions and for conditions as they were before impoundment;
2. Expand and quantify the present understanding of the shallow groundwater regime in the JPL catchment, by developing detailed descriptions of recharge patterns, discharge patterns, and rates and directions of groundwater flow within the system;
3. Quantify the relationship between the shallow groundwater regime and the surface water regime, and between the shallow groundwater regime and deeper consolidated-rock aquifers;
4. Provide an estimate of the average annual recharge to the groundwater regime by determining the spatial distribution of recharge over the JPL catchment, and developing information on the factors controlling recharge;
5. Develop information on the relationship between land-use and ET; and
6. Evaluate the impact of urbanization on the shallow groundwater system and on its relationship to JPL.

1.5 Research Scope

The aim of this research was to understand the shallow groundwater regime. The models that were developed were not intended for prediction of the future status of the groundwater regime, but may nevertheless be helpful in water resource management, urban and regional planning, and groundwater resource development. The simulations do not deal with contaminant transport, particle tracking analysis or groundwater quality problems. The research does not deal with aspects of groundwater and surface water interaction related to water management issues.

1.6 General Approach

The general approach to this research falls into two major categories:

1.6.1 Data Interpretation through GIS

GIS technology was used to prepare, organize, interpret, and interrelate data on precipitation, land-use, population, urban development, ET, streamflow, and other factors affecting the shallow groundwater regime, its relation to JPL, and the overall hydrologic balance. GIS tools and technology have proven very effective for the automation of database preparation tasks.

1.6.2 Groundwater Flow Simulation

Finite-difference groundwater flow simulation was used to study the shallow groundwater system and its relation to the lake -- in particular, to estimate the distribution and rates of recharge, the mechanisms and rates of groundwater discharge and the directions and rates of groundwater flow throughout the system, both prior to and after the lake impoundment and, if possible to identify specific causes of the changes that are identified.

1.7 Organization of Dissertation Report

Chapter 1 of the dissertation is an introduction to the project area; it focuses on the geography and geology of the catchment. It also focuses on the objectives, scope, and general approach of the modeling exercise. Chapter 2 is a review of prior work related to the project area, from which basic concepts of groundwater, the parameters to be used in the MODFLOW simulations, and the geographic, geologic, and hydrogeologic characteristics of the project area are inferred. Chapter 3 deals with procedures for extracting land-use information inside the project area. This chapter also provides a step-by-step procedure for calculating cell-by-cell population distribution and cell-by-cell values of ET; the results thus derived were used to estimate the net applied water for the simulations pertaining to pre-lake (1981) and post-lake (2010) conditions of the shallow aquifer. The techniques of streamflow analysis used to extract the baseflow of the WC gage catchment are described in Chapter 4. The discussion covers evaluating the streamflow and baseflow per unit area of land surface, and using the results in the evaluation of model calculations. Chapter 5 begins with a discussion of groundwater flow simulation and an overview of simulation theory. In this chapter, the “overall hydrologic system in the JPL catchment” is explained as a part of the conceptualization of the JPL shallow groundwater modeling approach. Detailed

discussions of the MODFLOW approach, the model characteristics, model constructions, and of the simulation approach in general are also provided, and the vertical and horizontal discretization of the model is described; Chapter 5 also discusses the approach of using two steady-state finite-difference simulations for the model years 1981 and 2010 to compare pre-lake and post-lake conditions. Chapter 6 provides the results and discussion of the model; the results of the finite-difference simulation and of the "ZONEBUDGET" post-processing analyses are presented, and discussed in relation to the streamflow, land-use, and population distribution results. The conclusions of the research and further studies are presented in Chapter 7. A derivation of the groundwater flow equation is provided in Appendix A; Appendix B discusses the solution of this equation by finite-difference approximations. Appendix C contains miscellaneous graphs developed during the research. A bibliography of the citations used in the dissertation is presented in the Reference Section.

Chapter 2

Review of Prior Work

2.1 Introduction

An understanding of the geology, hydrogeology, and other characteristics of the JPL catchment and adjacent areas is required to develop a conceptually and numerically sound model. To this end, various reports related to geology, hydrology, hydrogeology, and groundwater modeling are reviewed and their conclusions are summarized in this chapter.

2.2 General Groundwater Investigations

The USGS has played a major role in groundwater modeling since the 1960's, and worked much to make simulation a standard approach of groundwater investigations through the development of the flow simulator MODFLOW (Harbaugh, 2005; McDonald and Harbaugh, 1988; see Chapter 5, Sections 5.2 and 5.3 for details). A great number of groundwater modeling studies have been carried out by USGS personnel using MODFLOW, throughout all parts of the United States. These studies have addressed both shallow and deep aquifers, in contexts relating to groundwater development, groundwater contamination, groundwater management, and water-rights issues.

The geology and groundwater hydrology of Tarrant County have been summarized by Leggat (1957). Thompson (1967 and 1969) has summarized information on the groundwater resources of Johnson and Ellis counties. These reports discuss the status of groundwater resources before the planning or development of JPL. Thompson (1967 and 1969) in his reports "Groundwater Resources of Johnson County, Texas" (Thomson, 1969) and "Groundwater Resources of Ellis County, Texas" (Thomson, 1967) has described the location and extent of important aquifers in Johnson and Ellis counties, their hydraulic properties, and the quantity and chemical quality of groundwater withdrawn at that time. The work of Thompson illustrates the value of groundwater management, and the requirement of quantitative analysis to understand these problems. The relevance of the reports "Ground-Water Resources of Ellis County" (Thomson, 1967) and "Ground-Water Resources of Johnson County" (Thomson, 1969) to the present study is based on the assessment of the author on (1) the physical and

hydraulic characteristics of aquifer materials, and (2) the availability, use, and movement of groundwater. Thompson (1967 and 1969) has described that the shallow aquifer materials in Ellis Counties and Johnson County has thin deposits of quaternary alluvium (mixtures of gravel, sand, and clay) covering Cretaceous strata, chiefly the EFS and the Woodbine Sand (Figures 1-2 and 1-3). The alluvial materials exhibit their maximum thickness along the rivers, approximately 45 feet in Ellis County and 30 feet in Johnson County. Among the bedrock aquifers, the Woodbine Aquifer is dominant in Johnson County, whereas other Cretaceous water-bearing sandstone such as the Hossten Formation and the Paluxy Sand, as well as to some extent the Woodbine Aquifer, are the principal aquifers in Ellis County. The Hossten and Paluxy aquifers are much deeper than the Woodbine Aquifer in the project area. The saturated thickness of the Woodbine Sand in Johnson County is about 88 feet. The average hydraulic conductivity of the Woodbine Aquifer is 5.35 feet/day in Johnson County. In Ellis County, the Woodbine sand has a saturated thickness of about 135 feet, and the average hydraulic conductivity of the formation is estimated as 9.36 feet/day. The average recharge reaching the Woodbine Aquifer, according to these early studies, is 0.5 inches per year.

The report of Leggat (1957) “Geology and Groundwater Resources of Tarrant County, Texas” has described the approximate amount of groundwater in storage, the ability of aquifers to yield water, the use of groundwater during the year 1950, and the impact on the groundwater of Johnson County due to the pumping of groundwater outside the county. The report also addressed the sources of recharge, the chemical quality of groundwater, and the future outlook for groundwater development. Winton and Scott (1922) in their report “The Geology of Johnson County” explained that stratigraphically, lower and older beds outcrop towards the west; in the eastern part of the study area, these older deposits lie below younger formations, which in turn subcrop beneath the alluvium. These authors described the Woodbine Group strata as a distinctly sandy, acidic, and iron-stained rock. The report of Shuler (1918) “The Geology of Dallas County” has provided a geologic overview of the county; the northeast portion of the JPL study area lies within Dallas County. In the eastern part of the study area, the Austin Chalk overlies the EFS, and subcrops beneath the Holocene and Pleistocene deposits.

2.3 Groundwater Contamination Studies at NASD and NWIRP by USGS, Tetratech, and EnSafe

As noted previously, military aviation activities began near MCL as early as 1929, at a facility then known as Hensley Field; during and after World War II, these activities developed into the NASD and the NWIRP. NASD was decommissioned in 1998 and was later re-commissioned as the Grand Prairie Armed Forces Reserve Complex. The NWIRP was established as a government-owned contractor-operated facility for the development, testing, and manufacture of weapons and equipment associated with naval aviation (Van Metre, 2003; Kalthoff, 2011). A variety of fuels, solvents, and other industrial chemicals were used at NASD and at NWIRP over a period of several decades, leading eventually to contamination of soil, groundwater, and lake sediment in the vicinity of both facilities. Numerous studies of these problems have been carried out over the years, leading to a much-improved understanding of the shallow groundwater regime in the MC drainage system.

Barker and Braun (2000) developed a computer model of the groundwater flow regime in the vicinity of the NASD and NWIRP using the USGS MODFLOW simulation code (McDonald and Harbaugh, 1988; Harbaugh and McDonald, 1996) and used the results of the particle tracking postprocessor MODPATH (Pollack, 1989) to estimate contaminant pathways. Calibration of the flow model helped to define the aquifer properties of the alluvium, and the model results in general provided groundwater budget computations, major flow path delineations, and simulations of remedial operations. Barker and Braun (2000) used calibrated values of hydraulic conductivity ranging from 0.75 to 7.5 feet/day, and averaging about 4 feet/day. Calibrated specific yield values ranged from 0.005 to 0.15, and averaged about 0.08; recharge rates ranged from 0 to 2.5 inches per year. A porosity of 0.15 was used in the particle-tracking calculations to estimate minimal times that might be required to remove contaminants from the shallow aquifer. Baker and Braun (2000) noted that the calibrated hydraulic conductivity was somewhat lower than that inferred from specific capacity testing of shallow wells. They attribute the difference to the fact that the simulated hydraulic conductivity represents an average value for the full thickness of the aquifer, whereas the test results may reflect the specific character of more permeable intervals supplying the wells.

Jones and Paillet (1997) used geophysical log analysis to investigate the potential for contamination of bedrock aquifers by vertical transport of shallow contaminants through or around existing wells on the NWIRP site, and to evaluate the effectiveness of the EFS as a deterrent to direct vertical contaminant migration in general. Their results show little evidence that significant vertical movement through or around existing wells has occurred, and confirm the character of the EFS as a confining unit of very low hydraulic conductivity.

Remedial investigations at both NASD and NWIRP by private consulting firms, e.g., those by EnSafe, Inc. (formerly EnSafe Allen and Hoshall, Inc.) and by Tetratech Nus, Inc., have also contributed extensively to the overall understanding of alluvial groundwater in the MC drainage. An excellent example of this work is summarized in Tetratech Nus (2004), in which groundwater flow simulation is discussed using MODFLOW, followed by transport simulation to predict contaminant concentrations under proposed remediation by natural attenuation. The primary significance of these studies to the present research is the insight they have provided about the modeling parameters such as hydraulic conductivity, recharge rates, and the overall character of the shallow groundwater system in the alluvium of the JPL catchment.

2.4 Groundwater Investigations at the Proposed Superconducting Supercollider Project Site

In the 1990's, the US Department of Energy was considering the development of a major particle accelerator facility, to be known as the Superconducting Super Collider (SSC). The project was abandoned in 1993, but site characterization studies had already been undertaken at a proposed site in Ellis County, located to the southeast of the JPL project area. Because the facility was to involve extensive underground installations, these studies included geologic investigations of many types, as noted by Nance and others (1994), the Pb/MK Team (1991), Mace and Dutton (1994), Collins and others (1992), Romero and others (1994), Raney and others (1987), Reaser (1991), and Wickham (1991). Two of these studies have particular reference to groundwater, and are summarized below.

Mace and Dutton (1994) studied the Austin Chalk of the SSC site. Their study area lies just to the southeast of this dissertation study area, and their findings are important to the research reported here, in that the Austin Chalk directly underlies the shallow alluvium in the eastern part of the dissertation area. In

the simulations carried out for the present dissertation (see Chapter 5), the shallow aquifer was represented by the uppermost layer (Layer 1) of the model mesh (see Figure 3-1 in Chapter 3 and Section 3.2), and was assumed to include both the alluvium and a thin zone of highly-weathered consolidated material commonly found at the upper surface of the bedrock. Immediately deeper bedrock strata were simulated as semi-confining material, beneath which a bedrock source-or-sink aquifer, representing the Woodbine Group strata, was simulated as a separate layer (Layer 2) and as a Constant Head Boundary (CHD) layer. The semi-confining material in the interval between Layer 1 and Layer 2 was simulated by reducing the hydraulic conductivity between Layer 1 and Layer 2, using the MODFLOW "quasi-3D" approach (see Section 5.7.9 in Chapter 5). In the central part of the dissertation area, the semi-confining zone corresponds to the EFS; in the western part of the dissertation area, where the EFS is missing, the semi-confining zone corresponds to low-permeability strata within the upper Woodbine Group itself, whereas deeper and more permeable strata of the Woodbine represent the underlying source-sink aquifer. In the eastern part of our study area, less-weathered zones of the Austin Chalk were assumed to function together with the EFS as the semi-confining material, and again the Woodbine Aquifer was considered the source-sink aquifer. Mace and Dutton (1994) summarize the hydrogeologic controls on contaminant transport in the Austin Chalk, and assess the danger that may be posed by the SSC itself and by associated urbanization. Their study showed that the permeability of the shallow fractured-and-weathered Austin Chalk is indeed three to four orders of magnitude higher than that of the deeper and less-weathered chalk, but that the influence of oxide coatings, Liesegang band, soil transported from the surface, calcite fill, and clay coatings on the fracture-solution zones is complex; these features may reduce secondary permeability and increase solute retardation, but may also speed up solute transport by reducing porosity and limiting matrix diffusion. Mace and Dutton (1994) cited the importance of fracture intensity, water table elevation, rainfall intensity, and fracture coating as controlling factors on the transport of solutes in a fracture-solution environment.

Wickham (1991) studied the shallow unconsolidated aquifers of Ellis County in the northern part of the proposed SSC site. This study involved extensive field studies, including test drilling, geophysical surveying, aquifer testing, streamflow measurement, water level monitoring, and collection of water

samples for chemical analysis; data interpretation was based on flow simulation using MODFLOW, and particle tracking using the MODPATH postprocessor. The alluvium of Wickham's study consists primarily of a terrace deposit containing stratified calcium-rich clay, clayey sand, granules, and pebbles. It exhibits many similarities to the shallow alluvium in the eastern part of the JPL project area, having a saturated thickness that varies seasonally from 7 to 40 feet. Hydraulic conductivity testing of the aquifer yielded results ranging from 2.3 to 37.4 feet/day. The study found that most of the groundwater flow discharges to local streams through springs and seeps. The model-simulated discharge from the aquifer (43,200 Cubic Feet per Day (CFD)) was found to be of the same order as measured local gains in streamflow (155,520 CFD). Geochemical studies involving tritium, coupled with fluid particle time-of-flow calculations based on the simulations, indicated groundwater residence times ranging from of one to a few decades.

2.5 Northern Trinity-Woodbine Groundwater Availability Model

The Woodbine Aquifer is of interest to this research because, throughout most of the study area, it represents the uppermost permeable bedrock aquifer below the alluvium, and to the extent that vertical flow between the shallow aquifer and deeper aquifers occurs, either directly, or through the EFS, or through some combination of the EFS and the Austin Chalk; the Woodbine Group strata can be expected to act as the underlying source or sink layer. As an important source of public water supply in the Dallas-Fort Worth area, the Woodbine Group strata has been studied extensively, both in the field and through simulation. The Northern Trinity/Woodbine Groundwater Availability Model (NTW-GAM) was developed for the Texas Water Development Board by a consortium of consultants, with the cooperation of the USGS, and is thoroughly documented in a report bearing the same title (Bene and others, 2004, 2007; Kelley and others, 2014). In this report, their model simulated groundwater flow in the outcrop and downdip portions of the Cretaceous Woodbine and Trinity Aquifer, which they visualized as extending from Central Texas to 40 miles north of the Red River, and (following the subdivisions used in their model), included the Hosston, Hensell, Paluxy, and Woodbine Aquifers.

The aquifer system is characterized by sandy units, which are generally confined and separated by low permeability clay and carbonate rocks (Bene and others, 2004; Bene and others, 2007; Kelley and

others, 2014). The NTW-GAM study provides estimates of current and future pumping requirements in the simulated area, and documents the hydraulic parameters, hydrologic inputs and outputs, and modeling assumptions used in simulation. Because of the extensive hydrologic information and interpretation available through the NTW-GAM, it was decided to exclude bedrock aquifers from active simulation as separate layers in the models developed for this dissertation. Rather, the Woodbine group strata was represented simply as a layer of fixed and unchanging water level below the semi-confining zone, capable of providing upward flow or receiving downward flow during each simulation run, but not itself subject to the iterative recalculation of heads inherent in the numerical simulation process. In the models developed for this dissertation, the heads specified for the Woodbine Aquifer were interpolated from water level contour maps provided in the NTW-GAM report of Kelley and others (2014), and in Mace and others (1994), and the aquifer parameters used for the layer representing the Woodbine Group strata were similarly taken from the NTW-GAM report. These data included a horizontal hydraulic conductivity of 1 foot/day and a vertical hydraulic conductivity of 0.0001 feet/day. Streambed hydraulic conductivities used in the NTW-GAM model ranged from 0.001 to 0.1 feet/day, but the recharge used in that model is not clearly defined. The MODFLOW evapotranspiration (EVT) function, as used in the NTW-GAM model, is interpreted to represent the removal of water due to various near-surface processes: transpiration, direct evaporation from the water table, springs and seeps, and flow into ditches or gullies. As used in the NTW-GAM report, the goal of simulation appears to be to “understand historical changes and future response” of the Trinity/Woodbine system rather than to predict the response of the aquifer system to hypothetical stresses.

2.6 USACE Pre-Impoundment Studies

The United States Army Corps of Engineers (USACE) surveyed the hydrological, climatological, and general conditions of the JPL catchment to evaluate the feasibility of impoundment before the construction of the dam. The results of these investigations appear in a series of documents issued by USACE. One of these is summarized below; two additional reports of the series are reviewed in Section 2.7.

The document “Design Memorandum No. 1, Lakeview Lake, Hydrology” (USACE, 1979) provides a detailed discussion of factors related to the surface water hydrology of the site, including the area of the JPL catchment, the annual runoff, the maximum flood recorded at MCL, and at the discontinued gaging station at Grand Prairie. USACE (1979) also provides the probable maximum flood (PMF), the probable maximum flood Hydrograph (PMPH), the unit hydrograph (UH), a synthetic unit hydrograph (SUH), etc., as prepared from the design rainfall. In addition, USACE (1979) provides the elevation of the top of the dam, the conservation pool elevation, the top of flood control elevation, the maximum design water surface, and the spillway crest elevation, with the volume of water at those elevations and the equivalent runoff in inches. USACE (1979) also describes the physiography, soils, geology, stream characteristics, and channel capacity of major tributaries in the JPL catchment, and gives a climatological summary including precipitation, evaporation, major floods, infiltration indices, discharge frequencies and runoff records. USACE (1979) also provides analytical tools relating to flood forecasting, including a rating curve of the JPL dam, envelope curves of backwater for flood levels corresponding to different return periods, an area capacity curve, a frequency curve for pool elevation and discharge, and mass runoff curves.

2.7 USACE Embankment Criteria and Performance Report of JPL Dam

In 1991, USACE has prepared an “Embankment Criteria and Performance Report” for the JPL Dam. The dam was constructed for purposes of flood control, water supply, recreation, and fish and wildlife enhancement (USACE, 1991). The completion of the “Embankment and Spillway Report” prepared by USACE (1988) presents a detailed review of the physiography and geology of the dam site and surrounding area, giving the thickness and nature of overburden, the depth of bedrock from the surface, the locations of buried channels, and the nature of flood plain deposits. At the location of the dam, the average depth of overburden is 45 feet. The overburden is predominantly medium to high plasticity clay, 35-40 feet in thickness and is underlain by 5 to 10 feet of semi-pervious clayey sand and gravel, immediately overlying the bedrock. Along the west side of the dam a “Quaternary Terrace Deposit”, approximately 30 feet in thickness and consisting of sandy clay and clayey sand, directly overlies the bedrock. The primary bedrock stratum beneath the dam is the Britton Member of the

Cretaceous EFS. The layer below the EFS is upper part of the Woodbine Group strata, described previously. The EFS displays a monoclinal structure, dipping about 50 feet per mile to the east-southeast; it is about 225 feet thick at the dam location. In the vicinity of Dallas, both the EFS and the overlying Austin Chalk, described previously, display normal faulting due to the consolidation and differential settlement of individual beds. The western limit of the outcrop area of the Austin Chalk follows approximately the east side of JPL along Cedar Hill, and forms a white rock cuesta. The bedrock below the overburden, as observed in the deep inspection trench and in the spillway excavation, shows two different intensities of weathering. A highly weathered zone is found in the upper 3 to 10 feet of bedrock, and is probably due to high moisture content and the resulting enhanced solution along fractures. A more moderately-weathered zone is typically found in the next 5 to 20 feet of depth, characterized by the presence of joints and fractures. A transitional zone is observed between these weathered zones and the underlying un-weathered material. USACE (1988) reports that groundwater was encountered in test holes and excavations in semi-pervious clayey sand at an average depth of 40 feet; however, the piezometric level, as measured in piezometers installed to this depth, later rose to within 20 feet of land surface. In contrast, only a very small amount of free water was found in the joints and fractures of the Eagle Ford Formation, suggesting that the formation is of very low permeability.

In the “Embankment Criteria and Performance Report of October, 1991”, USACE (1991) reports that the embankment is founded on a clay base that lies above the EFS, and that the material composition of this overburden includes high plasticity clays (CH) and low plasticity clays (CL) interbedded with clayey sand, clayey gravel, and silty sand. The CH clay type has significant plasticity, whereas the CL clay has lower plasticity (USACE, 1991). The construction materials used for the dam were all of medium and high plasticity, were erosion and piping resistant, and were of low permeability. After the impoundment, no visible seepage was observed into a deep inspection trench installed on the right side below the dam.

USACE (1991) reports the results of seepage analyses corresponding to various post-impoundment stages and conditions, and to different sections of the structure, such as the foundation, the right abutment, the buried channel area, the western segment, the floodplain, and east of the center of

the dam. The seepage calculations were performed using a range of hydraulic conductivity (*K*) values. For the buried channel area, the *K* value was taken as 0.2834 feet/day and the level of the lake as 522 feet, yielding a seepage rate of 3 gal/day per linear foot of dam. Similarly, at the right abutment, using the horizontal hydraulic conductivity (*K*) as 2.834 X 10^{-5} feet/day, and the ratio of horizontal to vertical hydraulic conductivity as 25, the seepage rate is computed as 6 X10^{-4} gal/day per linear foot of embankment. For the flood plain with the same *K* value the computed seepage is 1.6 X10^{-3} gal/day per linear foot of embankment. Remaining results are tabulated in Table 2-1. The report also describes the piezometers are installed around the dam, but due to the observed direct impact of the lake on the piezometers they have not been used in this study for the evaluation of simulation results.

Table 2-1 Permeability Study Results for JPL Dam, Flood Plain, and Buried Channel

(Source: USACE 1991)

SN	Identified Section	Horizontal Hydraulic Conductivity	Computed Seepage Quantity
1	Right Abutment	2.834 X 10^{-5} feet/day	6X10^{-4} gal/day/linear foot of embankment
2	Flood Plain	2.834 X 10^{-5} feet/day	1.6X10^{-3} gal/day/linear foot of embankment
3	Buried Channel	0.2834 feet/day	3 gal/day/linear foot of dam

2.8 Austin Chalk

The Austin Chalk is an Upper Cretaceous marine deposit stratigraphically overlying the EFS (Figure 1-3 and Table 1-2). It crops out on the eastern side of the project area along the Cedar Hill Ridge, and extends south and east to Midlothian. The Austin Chalk is a fine-grained chalk and marl deposit, characteristic of a shallow shelf depositional environment. In the slope of Cedar Hill Ridge it forms white rock cuestas. Wickham (1991) studied the alluvial aquifer to the east of the JPL project area, outside the JPL watershed boundary, and within the Austin Chalk and overlyingTaylor Marl outcrop area. The then-proposed SSC project to the south of Wickham's (1991) study area gave rise to numerous geological

studies; some of these have involved investigation of faulting and fracturing in the Austin Chalk. The bottom and top of the formation are characterized by chalk and interbedded calcareous clay. The middle of the formation is however a thin-bedded marl with interbeds of massive chalk. The unit stratigraphically above the Austin Chalk is the Taylor Marl. Reaser (1957) pointed out the presence of an unconformity between the Austin Chalk and the lower part of the Taylor Marl. Numerous faults, developed during the Late Cretaceous, now extend into the study area as a part of the Balcones Fault Zone (Reaser and Collins, 1988; Weeks, 1945). Hydrogeologically, the Austin Chalk is not a good aquifer, although it may be adequate for short-term or limited water supply.

Chapter 3

Development of Information on the Model Grid, Cell, Land-use, Evapotranspiration, Population, and Net Applied Water for 2010 and 1981

3.1 Introduction

This chapter will focus on the divisions of the project area into an array or "grid" of rectangular cells for the study purposes – both for describing and correlating detailed distributions of population, land-use, and ET, and subsequently for use as the map-view component of a finite-difference simulation mesh.

3.2 Division of the Project an Area into Array or Grid of Cells

Early in the planning stages of this research, it became clear that groundwater flow simulation would be central to understanding the impacts of the lake itself on the shallow groundwater regime, and possibly also to understanding the impacts of subsequent urbanization on the groundwater system. At the same time, it became clear that very large volumes of information on population, land-use, and evapotranspiration (ET) were available, and would have to be brought together and interpreted using a GIS approach. Finite-difference (see Section 5.3 in Chapter 5 and also Appendix B) flow simulation requires, initially, the development of a calculation mesh, which generally takes the form of an array of points or nodes, at each of which head or pressure is to be calculated by numerical means. Typically, each node is assumed to lie at the centroid of a "cell", i.e., an area or volume over which hydraulic parameters and conditions are assumed to be uniform; and commonly the cells are assumed to be rectangular in map view, and to form a continuous array over the area of study, as shown in Figure 3-1. A spatial array or mesh such as that in Figure 3-1 also provides a convenient framework for the representation and processing of all sorts of geographic data, for example the data noted above on population, land-use, and ET.

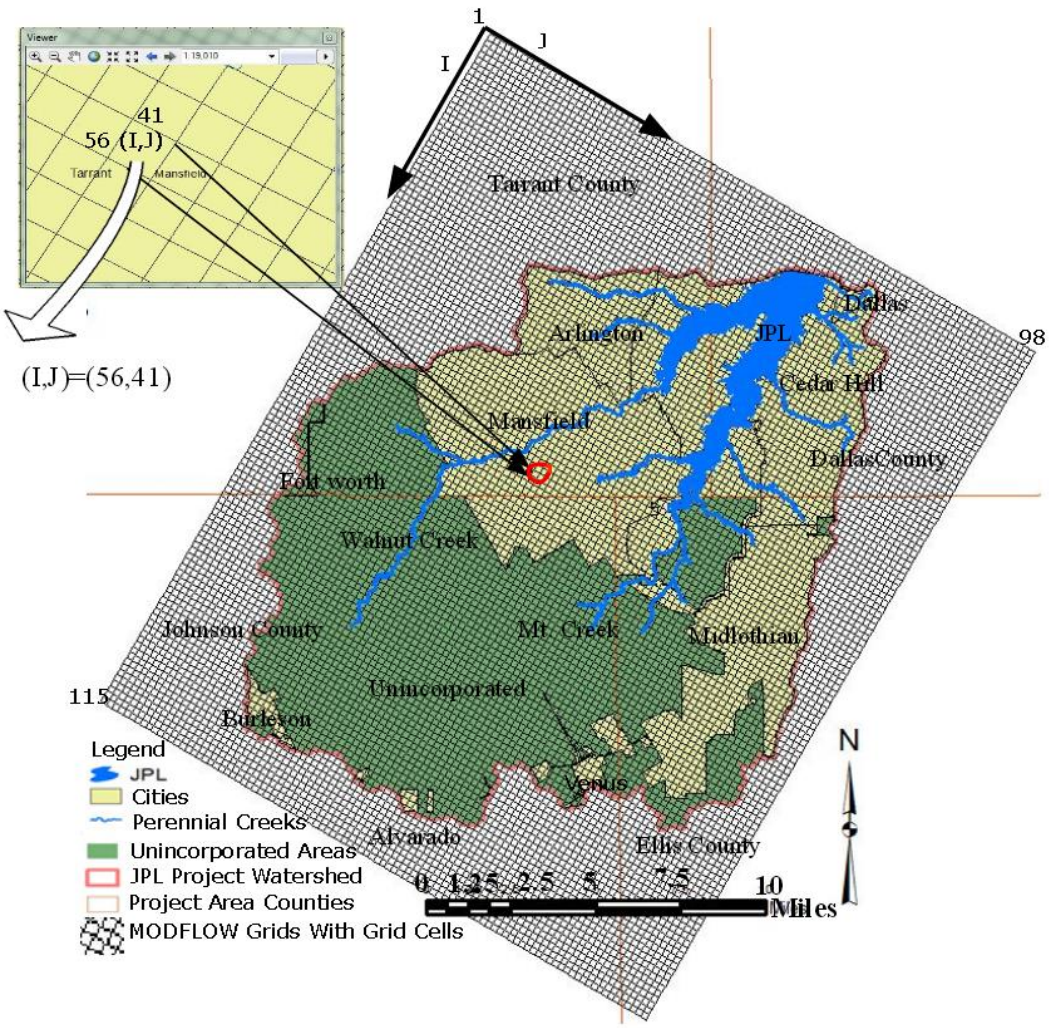

Figure 3-1 Map view of the model mesh. Horizontal array of grid cells used in simulation indicating row (i) and column (j); the horizontal grid size is 1,000 feet X 1,000 feet, but the vertical layer thickness (which is shown in Figures 3-3 and 3-4) is variable in almost all cells

Thus, it was convenient to use the array shown in Figure 3-1 both as the map-view component of the finite-difference simulation mesh and as the framework for GIS storage and processing of relevant data. The cells in Figure 3-1 are square, measuring 1,000 feet on each side, and are arranged in 115 rows, trending northwest to southeast and 98 columns, trending northeast to southwest. As discussed in Chapter 6, the finite-difference model is actually three-dimensional, consisting of two layers, so that

Figure 3-1 is only a partial (two-dimensional) representation of the simulation mesh, although it offers a full representation of the GIS data storage arrays.

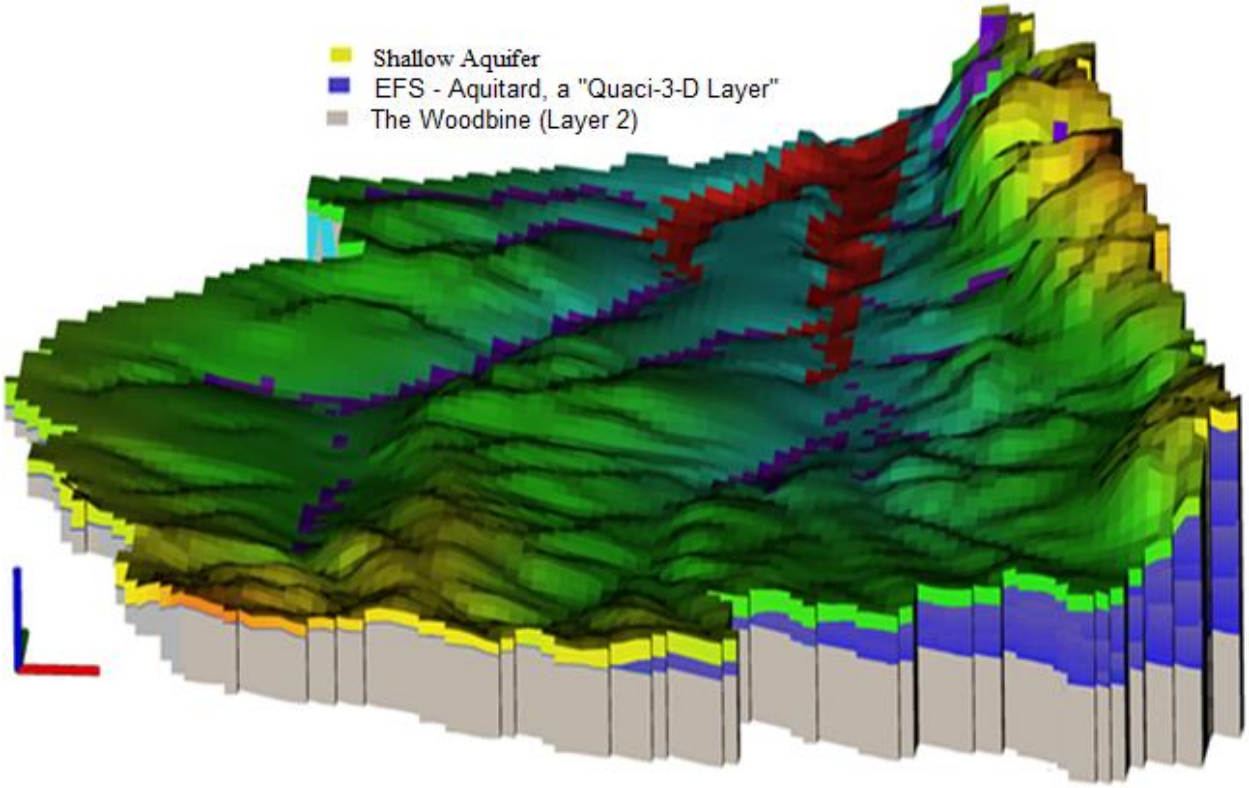

Figure 3-2 Three-dimensional model visualization of the JPL project watershed using USGS Model Viewer (figure is not to the Scale)

The USGS MODFLOW-2005 program is a 3-D finite-difference generic model, or simulator. The flow of groundwater is in general a three-dimensional process, and the model structure in terms of its horizontal discretization (Figure 3-1) and vertical discretization (Figures 3-2, 3-3, and 3-4) is best viewed in 3-dimensions. Using the USGS model viewer (Hsieh and Winston, 2002), the optimum run of each of the simulated models were visualized from the top and the covering entire watershed as shown in Figure 3-2. The blue color are the locations of the cells that contain perennial river reaches as represented in MODFLOW River (RIV) Package in the simulations of this research. The red color shows the cells under the lake in the post-lake (2010) simulations, as represented using the MODFLOW General Head

Boundary (GHB) Package. For the pre-lake (1981) simulation, the GHB Package was deactivated and these cells became unmodified shallow aquifer cells.

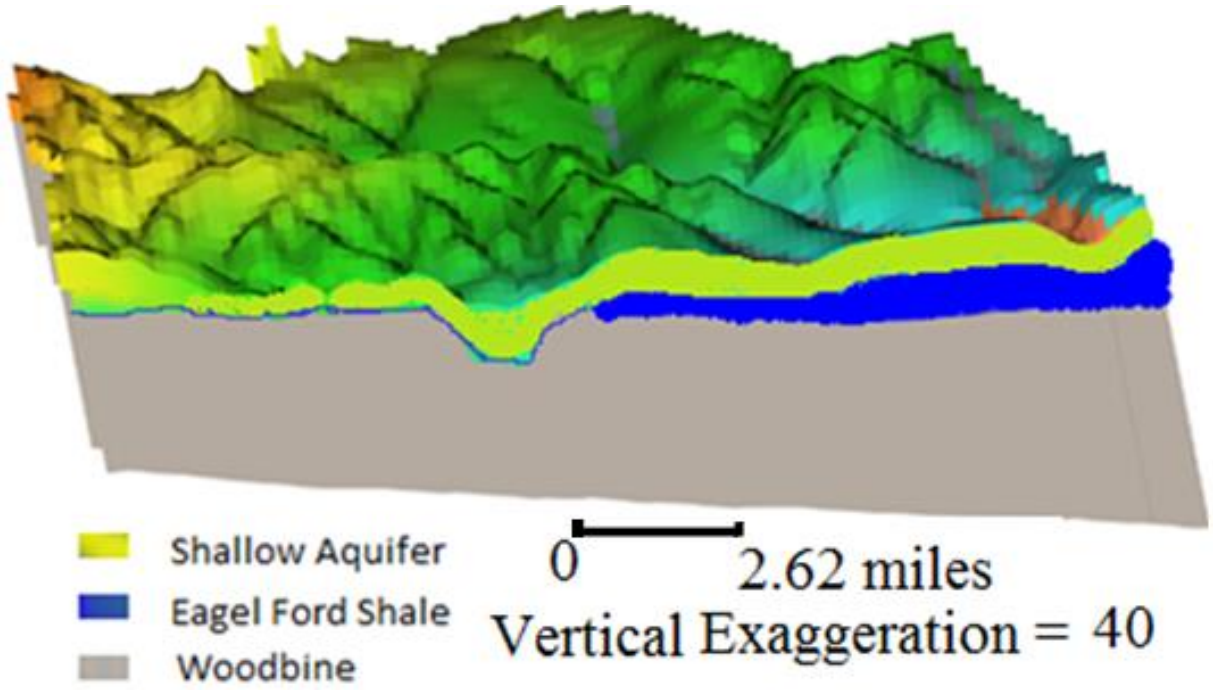

Figure 3-3 The model cross section along the column 55 that passes between the two arms of JPL

Figures 3-3 and 3-4 are two model cross-sections as viewed using the USGS model viewer software (Hsieh and Winston, 2002). As observed in the cross-section, the shallow aquifer (Layer 1) is thinner than the Woodbine Group strata (Layer 2), and the EFS gradually thins out toward the west, and is generally missing in the drainage area of WC (Figures 1-3, 3-2, and 3-3). Again, the EFS is not represented as a separate model layer in the simulation of this research, but rather as a zone within Layer 1 in which the vertical conductance has been drastically reduced. In this approach, which is termed the “quasi-3D” method, horizontal flow in the EFS is not simulated—i.e., an assumption is made that the EFS acts only as a transmitter of vertical flow between the two layers. To avoid numerical problems in the iteration process, areas in which the EFS is missing are represented as areas in which the EFS is actually present, but at a nominal thickness (taken as 1 foot), and as having hydraulic properties the same as those of the underlying layer, i.e., the Woodbine Group strata.

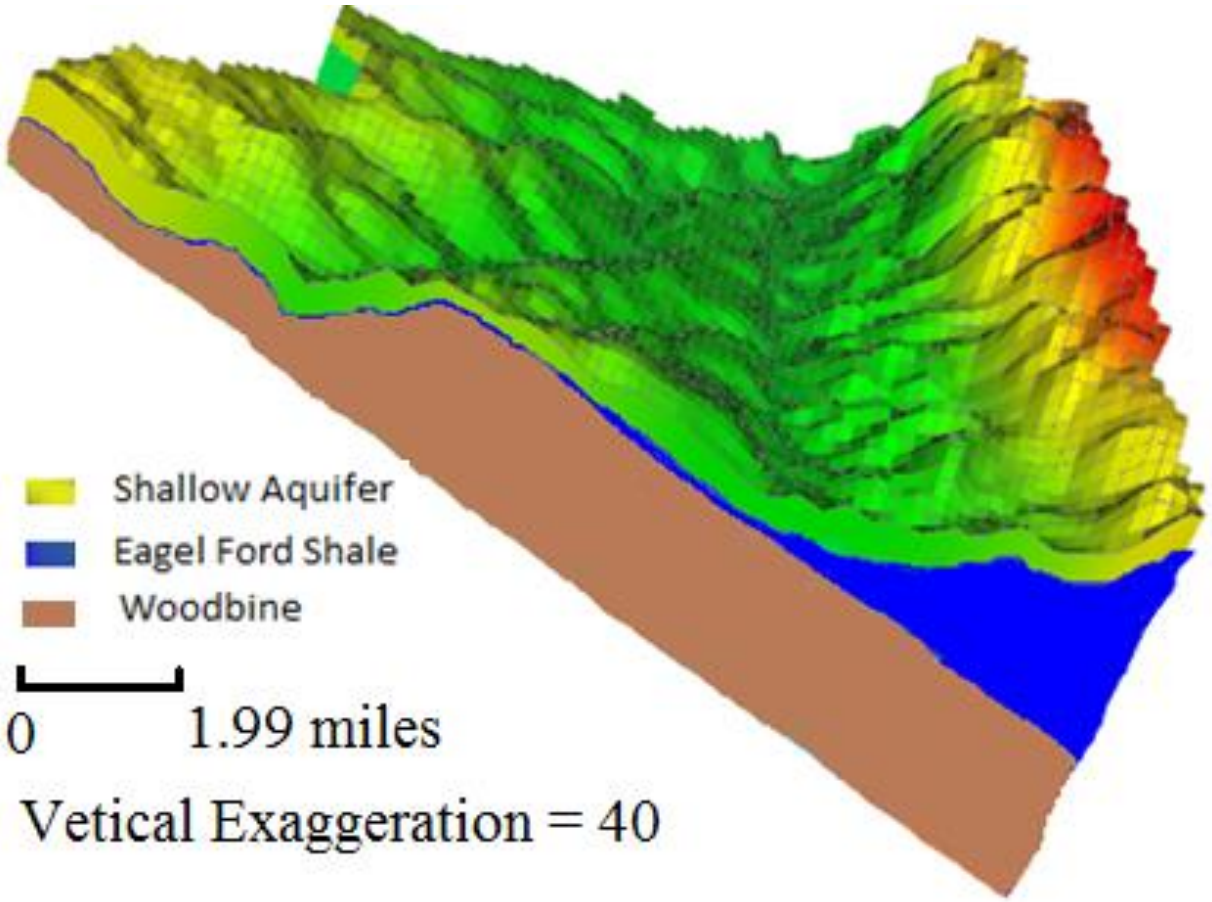

Figure 3-4 A model cross-section viewed along the row 55, which crosses both the WC and the MC

3.3 Development of Detailed Information on Land-use in the Study Area for 1981 and 2010

Land-use changes in the Dallas-Fort Worth Metroplex have in general occurred rapidly as the local population has risen. In any hydrologic environment, the conversion of agricultural or vacant land to other uses typically has immediate impacts on hydrologic processes occurring at or near land surface, and these impacts may lead in turn to broader and more permanent changes in the overall regional hydrology. For these reasons, a review of the available information on land-use change in the project area during recent years was undertaken early in the study.

The North Central Texas Council of Governments (NCTCOG) initially prepared a summary of land-use as of 1990. This summary was updated at five-year intervals, i.e., for the years 1995, 2000,

2005, and 2010; in the research reported here, the data for each of those years were downloaded from the NCTCOG website (http://www.nctcog.org/ris/demographics/landuse.asp). The data for 1990 were used in estimating the land-use for 1981. Because most of the land-use change in the project area occurred after the completion of impoundment, the error in this approximation is considered minor. The NCTCOG data were represented in map form through ArcMap software using an unique Identification Number (ID) for each land-use polygon (popularly known as FID in GIS terminology). The land-use data were tabulated using specific land-use categories according to the summary in Table 3-1. The table reflects the fact that the number of land-use categories was increased over time, as NCTCOG refined and expanded the database. In particular, many categories not used in preceding years were introduced in 2010 (Table 3-1). Thus, the land-use category for a particular parcel of land may change from one 5-year survey to the next, even where no actual change has occurred on the ground.

The data as presented by NCTCOG were uploaded on ArcMap software and were processed using GIS tools. The land-use information was first redistributed in the cell-by-cell format of Figure 3-1 (i.e., the project grid or cells). In this process, the project grid of Figure 3-1 was in effect overlain on the land-use map through GIS. The land-use data were then processed to obtain: (1) the total area of each land-use category inside both the overall JPL Project area, and inside the catchment area of the WC gage; and (2) a cell-by-cell land-use distribution inside each project grid cell, in the form of a set of land-use fractions for that cell, each giving the fraction of the cell area occupied by an individual land-use category. The land-use fraction as used herein is defined as the ratio of the area devoted to a particular land-use within a cell, to the total area of the cell, which is equal to 1,000,000 square feet. The steps involved in calculating these results through GIS are outlined in Section 3.3.2. Procedures for calculating total area of each land-use category in the JPL project area and in the WC gage catchment area are given in Section 3.3.1.

Table 3-1 Evolution of the Land-use Code and Category from 1990 to 2010 (Source: NCTCOG, 2010)

Land-use Code (LUCODE)	Category	Example Use	Year				
			1990	1995	2000	2005	2010
111	Single family	Single family detached units and duplex					
112	Multi-family	Apartments, condominiums, residential hotels, converted apartments and townhouses (single family and attached					
113	Mobile home	Mobile homes inside mobile home parks and free standing units outside park					
114	Group quarters	Nursing homes, group homes, college dormitories, jails, military base personnel quarters					
120	Commercial	Unspecified office or retail uses or a combination of office and retail uses, excludes office and retail uses when residential use is present (see mixed use)	NA	NA	NA	NA	
121	Office	Generally includes any administration functions include corporate and government offices, banks*					
122	Retail	Retail trade and services, such as departmental stores, repair shops, supermarkets, restaurants*					

Table 3-1-Continued

123	Institutional	Churches, governmental facilities and offices, museums, education, hospitals, medical clinics, libraries and military bases*					NA
124	Hotel/motel	Hotels and motels					
125	Institutional/semi-public	Churches, governmental facilities and offices, museums, hospitals, medical clinics, libraries and military bases	NA	NA	NA	NA	
126	Education	All public and private schools	NA	NA	NA	NA	
131	Industrial	Manufacturing plants, warehouses, office showrooms*					
141	Transportation	Railroads, radio and television communications stations, truck terminals					
142	Roadway	Roadways and right-of-ways					NA
143	Utilities	Sewage treatment and power plants, power line easements, pump stations, water treatment plants and water systems					
144	Airport	Airport terminals*					
145	Parking garage	Parking garages	NA	NA			NA

Table 3-1-Continued

146	Runway	Airport runways	NA	NA			
147	Large stadium	Large venue for organized events	NA	NA			
148	Railroad	Railroad lines and stations, rail to truck transfer facilities, freight only	NA	NA	NA	NA	
149	Communication	Radio and television communications stations	NA	NA	NA	NA	
151	Transit	Passenger rail and bus lines and facilities	NA	NA	NA	NA	
160	Mixed use	Areas that contain both commercial (office and retail) and residential uses either in the same facility or in very close proximity	NA	NA	NA		
170	Parks or recreation	Public and private parks, golf courses, public and private tennis courts and swimming pools, amusement parks	NA	NA	NA	NA	
171	Parks or recreation	Public and private parks, golf courses, cemeteries, public and private tennis courts and swimming pools, amusement parks					NA
172	Landfill	Sanitary landfills, land applications, and similar waste management facilities					

Table 3-1-Continued

173	Under construction	Land that has undergone site preparation and construction has begun					
174	Cemeteries	Dedicated burial places					
181	Flood control	Major flood control structures including levies and flood channels	NA	NA	NA	NA	
300	Vacant	Undeveloped land					NA
301	Vacant	Undeveloped land, can be either urban or rural	NA	NA	NA	NA	
302	Residential Acreage	Land that is mostly undeveloped, yet includes a residence, either house or mobile home, as a minor part of the use	NA	NA	NA	NA	
303	Ranch land	Land that is either devoted to or suited to raising livestock	NA	NA	NA	NA	
304	Timberland	Land that is wooded or forested	NA	NA	NA	NA	
305	Farmland	Land that is either devoted to or suited to cultivation of crops	NA	NA	NA	NA	
306	Parking CBD	Parking in Central Business Districts	NA				NA

Table 3-1-Continued

308	Expanded parking	Parking areas adjacent to or near large event venues and other large parking lots	NA	NA			NA
309	Improved acreage	Open land that has a non-residential structure	NA	NA	NA	NA	
401	Parking	Paved areas dedicated to vehicle parking, includes parking structures	NA	NA	NA	NA	NA
500	Water	Lakes, rivers, ponds					
501	Water	Lakes, rivers, ponds of at least 10 acres	NA	NA	NA	NA	
502	Small water bodies	Water bodies less than 10 acres	NA	NA	NA	NA	

3.3.1 Procedure for Calculating the Total Area of Each Land-use Category Inside the WC Catchment and Inside the JPL Project Area

The area of each land-use category inside the WC catchment, and area of each land-use category within the entire JPL catchment, were calculated using the following steps:

1. The project watershed maps (both for the full JPL project area and for the WC gage catchment area) were added in ArcMap using the add-data ('+') tool
2. The land-use map of the four counties, which comes as a separate file, were merged into a single shape file (ArcToolbox/Data Management Tools/General/Merge)
3. The merged file was clipped with the JPL watershed boundaries (ArcToolbox/Analysis Tools/Extract/Clip)
4. The clipped file was then intersected with the watershed boundaries files (ArcToolbox/Analysis Tools/Overlay/Intersect)
5. The intersected file was then dissolved (ArcToolbox/DataManagementTools/Generalization/Dissolve) with the dissolve criteria on (1) watershed boundary and (2) land-use code (see Table 3-1)
6. The area of the dissolved polygon corresponding to each land-use category (Table 3-1) inside the JPL project watershed was then then calculated using (ArcToolbox/Spatial Statistics Tools/Utilities/Calculate Areas)
7. Finally, the attribute table of the result of step 6 is exported to Excel (Open "attribute table/select all/export file"). The file is then exported to either comma separated version (csv) or text, which can be opened easily in Excel spreadsheet

3.3.2 Procedure for the Determination of the Cell-by-cell Land-use Fraction Inside the Project Area

To address the issues of recharge, ET loss, and other hydrologic losses from outdoor water use and onsite sewage disposal, the cell-by-cell land-use fractions were calculated from the raw land-use data using ArcMap/GIS tools. The steps followed in the calculations were:

1. The land-use shape files of four counties (Dallas, Tarrant, Ellis, and Johnson), project watershed maps (JPL and WC), and project grid file were added in ArcMap using the add-data (‘+’) tool
2. The land-use files of four counties, which come as a separate file, were merged into a single shape file (ArcToolbox/Data Management Tools/General/Merge)
3. The land-use file was then clipped with the project grid (ArcToolbox/Analysis Tools/Extract/Clip) file.
4. The clipped land-use and project grid files were then intersected (ArcToolbox/Analysis Tools/Overlay/Intersect)
5. The intersected layer was dissolved (Arc Toolbox/Data Management Tools/Generalization/Dissolve) so that features with identical cell id’s and land-use category were merged together
6. The merged total area (in square feet) of the polygons representing an individual land-use category within a given grid cell was then calculated
7. This procedure was repeated for all land-use categories in that cell, and then for all cells in the mesh, in effect creating an attribute table providing the area of each individual land-use category in each grid cell (ArcToolbox/ Spatial Statistics Tools/Utilities/Calculate areas)
8. The resulting attribute table of land-use data file in step 7 was exported to “Excel”. (Open attribute table/select all/export file). For this purpose first selecting the .txt as the file format and adding a .CSV as the file extension was followed. Now in “Excel” for each project cell, a running total area was calculated, representing the total area of all land-use categories in that cell, as a check to ensure that this total area was approximately 1,000,000 square feet
9. In the “Excel” program, a new column containing the total sum area of each land-use category within each cell was created
10. The total area of each category within each grid cell was divided by the cell area (1,000,000 square feet) to get the land-use area fraction for that category in that cell

11. Finally, the data in the “Excel” file was imported to ArcMap using add data (‘+’) tool. The imported data file is joined with the FID field of the model grid layer.

The processes discussed above for extracting the area of each land-use type inside the JPL project area and inside the WC gage area, and for calculating the cell-by-cell land-use fraction were applied to the NCTCOG land-use categories (Table 3-1) for each of the years 1990, 1995, 2000, 2005, and 2010; the results were used to analyze the trends of the different land-use categories through time, both for the entire JPL watershed and for the WC gage catchment.

The results provide a detailed database suitable for various applications in research on the hydrologic impacts of land-use change. For the purpose of the current dissertation, it proved helpful to combine the NCTCOG land-use categories into three more general merged categories as shown in Table 3-2, i.e. (1) residential land-use, (2) non-residential land-use without major influence of water distribution systems or waste-water collection systems, and (3) non-residential land-use, but with significant possible influence of water distribution systems or waste-water collection systems. In the correlations attempted in this research, these broader combined categories proved more useful.

The land-use change inside the JPL catchment through time since 1990 to 2010 is given in Appendix C, Figures C-1 through C-4. The land-use fraction developed in Section 3.3.2 is however, used for the estimation of cell-by-cell population and finally to calculate the population-based applied-water.

Tables 3-3, 3-4, 3-5, and 3-6 and the land-use change plots in Figures C-1 through C-4 visualize the land-use change through time in the JPL catchment and WC watershed. The map view of these land-use dynamics through time from 1990 to 2010 both representing the pre-lake and post-lake era are shown in a separate supplemental Figures 3-5, 3-6, 3-7, 3-9, and 3-10. The land-use data of the year 1990, representing immediately after the JPL impoundment is assumed to be the land-use condition before the lake impoundment and used as the reference land-use for the model year 1981 to calculate the cell-by-cell population of that year. All other land-use years from 1995 through 2010 are considered as post-impoundment land-use. Obviously, there is a huge change in land-use in the study area. The vacant land is significantly decreased and residential and developed land-use is increased. The detailed

description about the change in land use type through years is presented on the results and discussion section of this dissertation.

Table 3-2 The Derived Broader Land-use Category for the Use of Hydrological Analysis

Broad/Lumped category	Land-use code	Category
Residential Land-use	111	Single family
	112	Multi family
	113	Mobile homes
	114	Group quarters
Non-Residential Land-use, Without Major Influence of Water or Wastewater Collection Systems	141	Transportation
	171	Parks
	173	Under construction
	500	Water
	300	Vacant
Non-Residential Land-use, but with Significant Possible Influence of Water Distribution and Wastewater Collection Systems	122	Retail
	121	Office
	131	Industrial
	123	Institutional
	143	Utilities
	142	Roadways

The statistics of the land-use change of the WC watershed and JPL watershed are given in Tables 3-3 and 3-4, respectively.

Table 3-3 Land-use Change over Time in Walnut Creek Watershed

	Land Use Area Square feet					Land-use in percentage of total land area				
LU Category	1990	1995	2000	2005	2010	1990	1995	2000	2005	2010
111	233631968	269850782	398376743	536946029	506345961	12.33%	14.24%	21.02%	28.33%	26.72%
112	480198	990373	1117924	2802910	4383367	0.03%	0.05%	0.06%	0.15%	0.23%
113	39808959	45747937	49644651	141044007	239197016	2.10%	2.41%	2.62%	7.44%	12.62%
121	163766	163742	271113	2443267	68539353	0.01%	0.01%	0.01%	0.13%	3.62%
122	14402736	15575633	19591863	19778686	4746373	0.76%	0.82%	1.03%	1.04%	0.25%
123	9947385	10029319	11597220	23142263	31273555	0.52%	0.53%	0.61%	1.22%	1.65%
131	46839490	53341961	58128852	38270637	23896272	2.47%	2.81%	3.07%	2.02%	1.26%
141	0	2037446	1973763	1973763	2845563	0.00%	0.11%	0.10%	0.10%	0.15%
142	16683166	16683186	115904692	118326602	111867488	0.88%	0.88%	6.11%	6.24%	5.90%
143	14676118	11924819	11234365	6804611	12091538	0.77%	0.63%	0.59%	0.36%	0.64%
171	18896693	15164208	14466767	26243789	22951345	1.00%	0.80%	0.76%	1.38%	1.21%
173	9309953	1538756	9334633	11130123	1616188	0.49%	0.08%	0.49%	0.59%	0.09%
300	1488377360	1450215035	1195095472	955458779	852645007	78.53%	76.51%	63.04%	50.41%	45.00%
500	2073429	2073428	8912294	13114429	12330102	0.11%	0.11%	0.47%	0.69%	0.65%

Table 3-4 Land-use Change over Time in JPL Watershed

	Land-use Area Square feet					Land-use in percentage of total land area				
LU Category	1990	1995	2000	2005	2010	1990	1995	2000	2005	2010
111	400981021	461138308	684862924	914364294	972064758	6.17%	7.10%	10.49%	14.08%	14.97%
112	1203907	1714088	2227349	5904198	23602126	0.02%	0.03%	0.03%	0.09%	0.36%
113	146726630	154780779	158072660	344634693	614503210	2.26%	2.38%	2.42%	5.31%	9.46%
121	1705014	1438794	18099359	6829038	133093253	0.03%	0.02%	0.28%	0.11%	2.05%
122	22854722	24006510	80364373	28510824	7824367	0.35%	0.37%	1.23%	0.44%	0.12%
123	15377683	16577039	32703590	78797509	113757701	0.24%	0.26%	0.50%	1.21%	1.75%
131	128131813	136490755	179970492	126251887	175853932	1.97%	2.10%	2.76%	1.94%	2.71%
141	15417357	18794923	2819420	9473585	14085646	0.24%	0.29%	0.04%	0.15%	0.22%
142	45403882	37170602	322877067	364147772	346705760	0.70%	0.57%	4.94%	5.61%	5.34%
143	50666395	50176791	43807912	21802449	39909429	0.78%	0.77%	0.67%	0.34%	0.61%
171	246511303	286610562	131922154	302117422	467435492	3.80%	4.41%	2.02%	4.65%	7.20%
173	42706771	21138605	13315765	54003589	4468010	0.66%	0.33%	0.20%	0.83%	0.07%
300	5146785793	5009102618	4571165494	3911079957	3260879158	79.24%	77.12%	69.99%	60.22%	50.20%
500	230558172	275890090	289014028	327221402	320968182	3.55%	4.25%	4.43%	5.04%	4.94%

Table 3-5 Land-use Change over Time in Walnut Creek Watershed Expressed as a Lumped Category

	Walnut Creek Watershed Lumped Land-use, Square Feet					
Lumped Category Description	Lumped Category Abbreviation	1990	1995	2000	2005	2010
Residential Land-use (111, 112, 113, 114)	RLU	273921125 (14.52%)	316589092 (16.72%)	449139318 (23.81%)	680792946 (36.13%)	749926345 (39.61%)
Non Residential Land-use With Water Distribution and Wastewater Collection Systems (121, 122, 131, 123, 143, 141)	NRLU+W-WWD	71353378 (5.45%)	811480100 (5.69%)	91562811 (11.49%)	83634852 (11.08%)	131301115 (13.33%)
Non Residential Land-use Without Water Distribution and Wastewater Collection Systems (142, 171, 300, 500)	NRLU-W/O-WWD	1550016719 (80.13%)	1497599432 (77.61%)	1354948222 (64.87%)	1131078334 (53.07%)	1013501668 (47.10%)

Number inside the Parenthesis is the Percentage of Land-use of that Category of the Total Land Area of the Watershed

Table 3-6 Land-use Change over Time in JPL Watershed expressed as a Lumped Category

	JPL Watershed Lumped Land-use, Square Feet					
Lumped Category Description	Lumped Category Abbreviation	1990	1995	2000	2005	2010
Residential Land-use (111, 112, 113, 114)	RLU	548911558 (8.51%)	617633174.6 (9.54%)	845162932.1 (12.97%)	1264903185 (19.64%)	1610170095 (24.81%)
Non Residential Land-use With Water Distribution and Wastewater Collection Systems (121, 122, 131, 123, 143, 141)	NRLU+W-WWD	183486590 (4.09%)	197308021 (4.11%)	313957234 (10.40%)	249862843 (9.72%)	444614898 (12.59%)
Non Residential Land-use Without Water Distribution and Wastewater Collection Systems (142, 171, 300, 500)	NRLU+W/O-WWD	5762632316 (87.48%)	5680089268 (86.40%)	5372102419 (76.68%)	4980372591 (70.88%)	4440366031 (62.63%)

Number inside the Parenthesis is the Percentage of Land-use of that Category of the Total Land Area of the Watershed

3.4 Estimation of Cell-by-cell Population Distribution for 2010 and 1981

The presence or growth of urban population centers always impacts near-surface groundwater conditions. Evaluation of those impacts, particularly through simulation, requires that the population distribution be understood in detail. In the case of the research presented here, both the simulation and the processing of data were based on the project grid of Figure 3-1. In contrast, the original population data were derived from census data collected by the U.S. Census Bureau, and were presented originally in terms of census blocks, in general much larger than the cells of the project grid. It was therefore necessary to redistribute the population data in terms of the cells of Figure 3-1, by combining the census information with the land-use distribution as developed in terms of the project grid.

The JPL watershed lies within the Dallas-Fort Worth Metroplex area. Rapid population growth has characterized the area for several decades, particularly in the mid-cities area between Dallas and Fort Worth. The cities of Mansfield, Arlington, Midlothian, and Grand Prairie, all located in close proximity to JPL, have shown particularly rapid growth. This growth has required the development of additional water supplies, in almost all cases involving the import of water from sources outside the JPL catchment or from deep aquifers below the shallow aquifer. Because these cities (as well as several others in the catchment) generally provide sewer services in the neighborhoods to which they supply municipal water, a mechanism is in place to remove some part of the wastewater. However, much of the new housing has been developed in unincorporated areas, i.e., areas outside any political jurisdiction that currently provides either municipal water supply or sewer services. In these areas, developers of the housing have generally provided community water supply systems utilizing imported water, but wastewater disposal has generally been provided through the installation of onsite septic systems and “drywells” at each residence, or in the case of large housing complexes or commercial establishments, an On-Site Sewage Facility (OSSF). In general, facilities of the latter type provide a degree of treatment but dispose the processed wastewater locally, often by terrestrial application, rather than by transportation outside the catchment or injection into deep aquifers. Thus, in areas not served by municipal sewer systems, virtually all the “imported” water, and/or that provided from deep pumping, eventually reaches the land surface or the shallow soil, and is in effect added to the incident precipitation. Furthermore, even in areas where

municipal sewer service exists, some part of the municipal water supply inevitably reaches the land surface or the shallow soil, through outdoor use, sewer leakage, or water main leakage (Putra and Bair, 2008; Howard, 2002; Lerner, 2002).

It follows that in any hydrologic investigation, some effort must be made to estimate the additional water application resulting from human activities, and that in this effort, a distinction must generally be made between sewered and un-sewered areas. In the JPL area, the task is complicated by the fact that several large municipal systems serve areas both within and outside the catchment, and do not keep records on deliveries to specific neighborhoods. Estimates of the total water supplied have therefore necessarily been based on population and per capita use figures. In turn, this estimate has required the development of a detailed population distribution within the catchment; this population distribution was done on a cell-by-cell basis using the project grid of Figure 3-1. The approach implied the following assumptions: (1) most of the water imported into the JPL catchment or pumped from deeper aquifers is distributed for residential use; (2) the geographic distribution of population, which is indicated only approximately in the census data, can be refined adequately by using land-use data in conjunction with census data; (3) the available estimates of per capita residential water use in North Texas are adequate for the purposes of this research. Further assumptions, ultimately adopted as the population estimates were applied in estimating the amount of water distributed to the land surface or shallow soil, include the following: (1) on average, about 31 percent of residential water use occurs outdoors for purposes of lawn irrigation, car wash, general cleaning, etc. (Lerner, 2002; Putra and Bair, 2008); (2) in areas not served by municipal sewer systems, virtually all water imported to the catchment is eventually applied to the land surface or disposed in the shallow subsurface; (3) in areas served by municipal sewer systems, approximately 69 percent of the water distributed to users is collected into the sewer system, but of this total about 6 percent is eventually returned to the shallow subsurface within the catchment through sewer leakage (Garcia-Fresca, 2004; Garcia-Fresca and Sharp, 2005; Vazquez-Sune, 2003; Yang and others, 1999; Lerner, 1997(b); Grischek and others, 1996); (4) in both sewered and un-sewered areas, leakage from water mains causes a small additional increase in the total applied water, estimated as about 20-30 percent of the amount as inferred from the per capita use figures (Garcia-Fresca, 2004; Garcia-Fresca

and Sharp, 2005; Lerner and others, 1990; Thornton, 2002; Foster and others, 1994); (5) the water collected into municipal sewer systems is either transported out of the JPL catchment for treatment, or is treated within the catchment at the Mountain Creek Regional Wastewater System (MCRWS). The total discharge (1.6 million gallons per day, MGD) of that facility is evaluated separately as an input to JPL through MC, based on the Trinity River Authority; (6) all areas of the catchment lying within incorporated municipal jurisdictions currently providing sewer service to residents were assumed to be sanitary-sewered; (7) all other areas of the catchment (outside the municipal jurisdictions) were assumed to be without sanitary- sewered service. The distinction between sewered and unsewered areas was therefore based on political boundaries (incorporated vs. unincorporated jurisdiction) and was not related to land-use data.

US census data are available in various forms, but for the present research the data presented in the form of census blocks were used. Census blocks are the smallest geographic area for which the Bureau of the Census collects and tabulates decennial census data. Streets, roads, railroads, streams and other bodies of water, other visible physical and cultural features, and legal boundaries generally form the boundaries of census blocks. The next higher level of census data subdivision, above the census block, is the census block group; the level above which is the census track.

The county-based US Decennial Census Data for the years 1980, 1990, 2000, and 2010 as recorded in the US Census Block was obtained from the National Historical Geographic Information System (NHGIS) through the Minnesota Population Center (NHGIS.ORG, 2011). The original source of the NHGIS data is the U.S. Census. The NHGIS has been obtaining and archiving digital data directly from the Census Bureau since 1970. The population data for the year 2005 was obtained from the Texas Bureau of Statistics. Population for the year 1995 was derived by interpolation from a graph of population vs. year (Figure 3-10). NHGIS provides time series data covering real count of US Census data (popularly called a “100% count statistics”) for the period 1970-2010, a period for which several popular sample-based statistical summaries are available. For the year 1981, the cell-by-cell population was assumed equal to that for 1980. The graph shows the population is increased exponentially, both inside the WC watershed and inside the JPL project area.

These NHGIS data are available in digital GIS format and can be added through GIS, avoiding the necessity for time-consuming manual entry and the associated risk of human error. For the pre-1990 era, which preceded the evolution of GIS tools, NHGIS staff manually edited the census maps showing census block boundaries. In preparing the cell-by-cell population estimates, it was assumed that the entire population listed for a given census block lived in the areas of that block for which the land-use was listed as residential in the land-use map for that year or the closest available year, and that the water use was confined to those years.

The assumptions for cell-by-cell population estimation were (1) the entire population live on one of the four residential land-use categories, i.e., Single Family (111), Multi Family (112), Group Quarters (113), and Mobile Homes (114) (Tables 3-1 and 3-2) and perform most of their water-use activities, where they reside, and (2) this population is uniformly distributed on the residential land-use area inside the census-block. The Census Bureau always tries to ensure that each block represents primarily either urban or rural conditions; this assumption has both simplified and increased confidence in the cell-by-cell population estimation.

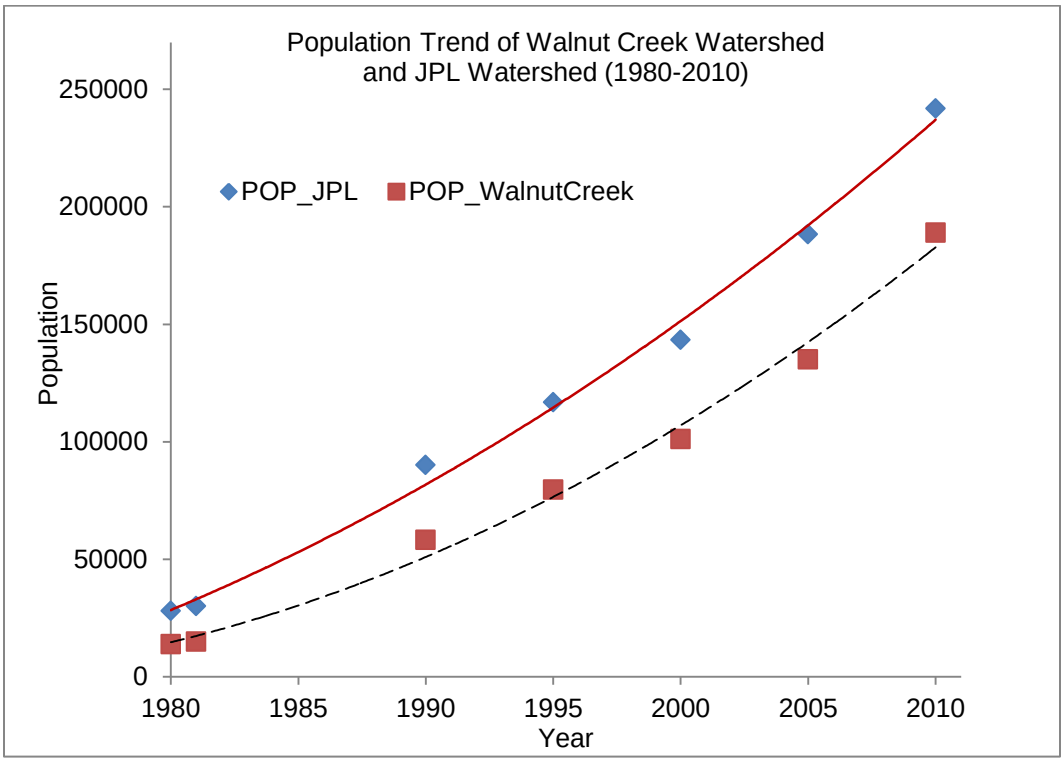

Figure 3-10 Population trend of the WC gaging station (Pop_WalnutCreek) and the JPL project area (POP_JPL; (Source: NHGIS, 2011)

Also, it should be noted that information on the daily migratory population from one part of the census block to another, and on parts of the population in business, offices, and schools is available, but was not considered in this analysis. For example, whereas NHGIS has census data related to business activities (known as “Institutional Census Data”) and these data was not included in formulating the present cell-by-cell population distribution.

Typically, each census block contains several of the (1,000 feet x 1,000 feet) cells making up the project grid of Figure 3-1. Creation of a cell-by-cell population distribution requires that the total population of each census block be distributed among the various cells lying within the boundary of that census block.

For this purpose, the NCTCOG land-use maps were first used to estimate the total land area classified as residential within each census block, and to calculate the population density inside the

census block. The population density was then used to calculate the number of people living inside the grid cell, using the cell-by-cell land-use fractions developed in the Section 3.3.2. This procedure was done inside the ArcMap environment using the steps summarized below:

1. The land-use map was added using the add data (+) button in the ArcMap environment
2. All the land-use polygons inside the census block representing any of the four residential categories (i.e., Single Family, Multi-Family, Mobile Home, or Group Quarters) were selected. (in the menu bar of GIS, go to selection/Selection By Attributes/Select from the land-use layer where land-use code =111,112, 113, and 114)
3. The census block and residential land-use map were then intersected so that each census block would separate the residential land-use area inside the census block from the rest. (ArcToolbox/Analysis Tools/Overlay/Intersect)
4. These land-use types were then dissolved based on land-use and the census block ID (ArcToolbox/DataManagementTools/Generalization/Dissolve)
5. The area of the land-use polygons inside the census block in step 3 was determined (see step 7 in Section 3.3.2)
6. The population inside the census block was divided by the total land-use area of the block to get the population density inside the block
7. The land-use fraction map created by using the procedure in Section 3.3.2 was added using add data (+) tool
8. A separate layer of residential land-use fraction was created by using the selection tool as in step 2 above
9. The population density map of the census block was then intersected with residential land-use fraction map.
10. Now, for all the cells totally within the census blocks, the population density and land-use fraction were multiplied to get the cell-by-cell population, i.e., population = population density*residential land-use fraction inside the cell

11. Step 10 is clear for cells that lie completely inside a census block, but cells on the boundary that share more than one census block will have more than one population density figure, related to another census block which has a different population density. For these cells, the dissolve tool with the statistics field was used to calculate an average population density, and hence the cell-by cell population.
12. The cell-by-cell population will add up to a nearest integer

The resulting cell by cell population distribution is clearly an approximation for several reasons, but appears to be the best estimate possible.

The cell-by-cell population developed in Sections 3.4.1 and 3.4.2 were used to calculate the cell-by-cell population-based water as discussed in Sections 3.6 and 3.7. The population trend developed for the cities and counties inside the JPL watershed using the US Census data, NCTCOG data and NHGIS population is illustrated in Appendix C, Figures C-8 and C-9. The result of population analysis shows that the population inside the catchment is steadily increasing.

3.5 Cell-by-cell ET Estimation from MODIS and NLDAS

ET loss from plants and evaporation loss of water from open water bodies are both high in North Central Texas, and must be considered in any water-related modeling exercise. Varieties of ET data are available (Dougherty, 1975; McDaniels, 1960; Texas AgriLife Extension and Irrigation Technology Program; USGS; MODIS and NLDAS). ET can also be calculated from cimatological data using the relations developed by Penman (1948), Thornthwaite (1948), or Monteith (1965). Some of these approaches involve direct estimation based on vegetation, some utilize empirical calculations, and others utilize remotely sensed data. Moderate Resolution Imaging Spectroradiometer (MODIS) is a satellite based remote sensing project that estimates global terrestrial ET from the land surface. This project is under the National Aeronautics and Space Administration's (NASA) Earth Observing System (EOS). MODIS data have been made public from 2000 to date; before 2000 the North American Land Data Assimilation System (NLDAS) provided remotely sensed ET data. NLDAS utilizes remotely-sensed collective land-surface data in a combined data collection and modeling approach. Information on ET, soil

moisture, snow cover, precipitation, baseflow, and gage flow and other hydrologic and ecological factors are assembled and combined in a coherent overall approach.

For the present purpose these data sets are used to remove the ET loss from the total annual precipitation and population-based applied water that reaches land surface in the JPL catchment, so as to estimate the resultant flow that can reach the groundwater regime on a cell-by-cell basis. Thus, MODIS data was downloaded from the University of Minnesota Numerical Terradynamic Simulation Group (NTSG) MODIS Global Evapotranspiration (MOD16) website. The data comes in raster file and can be added on ArcMap using the add data tool.

3.5.1 Cell-by-cell ET Estimation from MODIS

First of all, the downloaded MODIS ET data, project watershed shape file, and MODFLOW GRID were added on ArcMap using the add data tool. The MODIS data was projected to the same projection as the MODFLOW grid or watershed shape file. The raster data layer of the MODIS ET value was then converted into polygon (ArcToolbox/Conversion Tools/From Raster/Raster to Polygon) so that each polygon represents the annual ET in mm on that part of the watershed. The polygon was then intersected (Arc Toolbox /Analysis Tools/Overlay/Intersect) with the project grid file. As a result, the cell may contain a single ET value or may contain multiple ET values with multiple land-use areas represented by these ET values. Next, the area of all the shape files contained within the grid cell was calculated using (Arc Toolbox/Spatial Statistics tools/Utilities/Calculate areas). The area was now multiplied by the corresponding ET value (open attribute table/table option dropdown menu/create field/use field calculator tool) and the result was kept in a separate field in the attribute data table. Next, the result of the last step was dissolved (ArcToolbox/DataManagementTools/Generalization/Dissolve) with dissolve field(s) (1) cell FID, and (2) ET value inside it and using the statistics field(s) as the last field created by multiplying the ET value with the area, and the statistics type was sum. This procedure will give the cell-by-cell area weighted ET value. If there is any ET value on a lake cell, that value was deleted later on.

MODIS ET is popularly known as MOD16 ET. It includes the measurements of evaporation from saturated and moist soil, evaporation of water intercepted by the canopy, and transpiration from plants.

The evaporation from the soil is calculated two ways depending on whether the soil is "moist" or "saturated". Saturated areas are those areas where the relative humidity is 100%. Moist areas are those with 70-99% relative humidity. Soil moisture and direct ET from the water table is not included in the MOD16 calculation. Calculations of ET are only run on those pixels which are classified as vegetation (evergreen needle leaf forest, evergreen broad leaf forest, deciduous needle leaf forest, deciduous broad leaf forest, mixed forest, closed shrub land, open shrub land, woody savannas, savannas, grasslands and cropland). All pixels containing land cover types other than vegetation (permanent ice/snow, permanent wetland, water bodies, "out of earth boundaries", barren/sparsely vegetated, urban/build up and unclassified) are not included in the ET calculations and are instead given fill values.

The reasons for using ET values from MODIS or NLDAS in the modeling exercise is that the ET loss from the catchment is a very high value and needs to be addressed separately outside the model. MODFLOW in its basic form, doesn't address the ET loss from the vadose zone. The ET Package (EVT) in the MODFLOW is an empirical approach which is designed to estimate direct transpiration or evaporation from the water table, normally a small component of the total water balance, except when the water table rises to within a few feet of land surface. Most of the actual water loss from ET represents water which infiltrates the soil, but does not reach the water table, and which should therefore be subtracted from the precipitation and population-based applied water before any attempt is made to estimate the recharge. The remaining water is either groundwater recharge or becomes surface water through direct runoff or through near-surface (gully flow) processes. These processes may actually be calculated by the MODFLOW EVT Package as explained in Chapter 5, Section 5.7.5.

The MODIS ET obtained for the year 2010 was used to calculate the cell-by-cell ET loss for the post-lake model year (2010) and which eventually used to estimate the net applied-water that is used as recharge starting value for the 2010 simulation. The change of MODIS ET through 2000 to 2012 as a function of time is shown in Appendix C, Figure C-5. The result shows that the ET is fairly uniform and is affected by rainfall and other climatic conditions.

3.5.2 Cell-by-cell ET Estimation from NLDAS

The data required for the cell-by-cell ET calculation for the pre-lake year 1981 was obtained through the NLDAS data source. The procedure of distributing the cell-by-cell ET from NLDAS data is similar to that for the MODIS and is described as follows:

First, the data required for the NLDAS ET is downloaded from the source, known as Mirador (http://mirador.gsfc.nasa.gov/). The time span of the data and the keyword for the data type are needed to download the data. The key word used in this data search was “EVPsfc_110SFC_acc1m”. The data type to be downloaded will be in the format of NetCDF, which can be added to the ArcMap program using the multidimensional tool (ArcToolbox/MultidimensionalTools/MakeNetCDFRasterLayer) and extracting the value of the required parameter. The details of the procedure of data extraction from the raw data downloaded from the Mirador website into the cell-by-cell ET estimation is given below:

1. In the ArcMap program, the multi-dimensional tool was used to add the raw data for analysis (ArcToolbox/MultidimensionalTools/MakeNetCDFRasterLayer). The data files come in a monthly data format so there will be 12 such files for a year of data. The total annual ET is a cumulative sum of the 12 months data.
2. In the popup window after the activation of “MakeNetCDFRasterLayer tool”, the variables field is “EVPsfc_110SFC_acc1m”, which refers to the total monthly accumulated ET in units of mass per square meter (kg/m^2). The equivalent NLDAS ET expressed as a depth of water is in millimeters. The NetCDF Feature Layer was then created by clicking the OK radio button.
3. The layer was zoomed to the area of interest and raster data was converted into point data using the tool (ArcToolbox/ConversionTools/FromRaster/Raster to Point). The point vector data in the JPL project area were selected using the selection tool, and the selected data were copied from the attribute table and saved in excel. The same method was repeated for the remaining 11 months of data, and values corresponding to their ID’s were added together to get cumulative total ET in mm/year.
4. The method used for cell-by-cell ET estimation from the MODIS data was repeated exactly to obtain the cell by cell ET from the total ET data obtained from the NLDAS.

Similarly, the NLDAS ET obtained for the year 1981 was used to calculate the cell-by-cell ET loss for the pre-lake model year 1981 and eventually was used to estimate the net applied-water to be used as starting recharge value for the 1981 simulation. The change of NLDAS ET through 1979 to 2012 as a function of time is shown in Appendix C, Figure C-6. The result shows that the ET is fairly uniform and is affected by rainfall and other climatic conditions.

3.6 Components of Net Applied Water for 1981 and 2010

In estimating the net-applied water for the post-lake model year, 2010, and pre-lake year, 1981, different components of net-applied water were evaluated over the project area. Some of these components must be determined cell-by-cell, and are based on population, where population refers to number of residents in a cell within the MODFLOW grid (see Section 3.4). A cell that does not have residential land-use or recorded population within it will have zero population-based water. With respect to waste water collection/disposal two conditions must be distinguished: (1) public water supply with no sanitary-sewage collection system, and (2) public water supply with sanitary-sewer collection system.

The first of the two conditions (1) public water supply with no sanitary-sewage collection system is normally found in the unincorporated parts of the watershed. The study area is presently more than 50 percent unincorporated, and most of the water used for public and industrial purposes is imported either from sources outside the watershed or pumped from the Woodbine Aquifer or from deeper aquifers. Because the unincorporated areas do not in general have wastewater collection systems, all the water used by the population or by industrial activities is disposed through septic systems or On-site Sewage Facilities (OSSF). In either case the disposed water is assumed to reach the land surface or the shallow subsurface. The second condition (2) public water supply with sanitary-sewer collection system, is found in incorporated areas. Most of the indoor-use wastewater in this category is transported to a wastewater treatment facility, from which the treated effluent is usually released to surface streams. However, there are two ways in which population-based water supply from these areas may reach the soil or groundwater. These ways include water which is used outdoors (e.g., lawn watering or vehicle washing)

and leakage from the sewer collection network. In estimating applied water, these components are treated as fractions of the cell-by-cell water use figures, based on the literature.

During the calculation of net-applied water, some practices were followed to eliminate the redundancy and provide reasonable confidence in results. These data included: (1) any water withdrawal from shallow groundwater was excluded, and (2) any groundwater withdrawal from the Woodbine Aquifer or deeper aquifers was considered an import.

3.7 Estimation of Net Applied Water on Cell-by-cell Basis for 1981 and 2010

A value of net-applied water was calculated for each cell in the present-day MODFLOW array of Layer 1 (Figure 3-1). For each cell the net-applied water was taken as “precipitation plus population-based applied-water, plus sanitary sewer leakage, minus ET loss”. For incorporated areas the population-based applied-water was taken as the population within the cell, multiplied by a per capita water use figure (taken as 140 GPD), and by a land-application fraction, taken as 0.31. The land-application fraction represents the fraction of the estimated household supply which is either used outdoors, or has leaked from the water distribution system before reaching the residence. Sanitary sewer leakage was assumed to be six percent of the total indoor water use in the cell, which in turn was taken as approximately seventy percent of the total water use. The ET valued used in the net applied-water calculations were the cell-by-cell values calculated as in Section 3.5.

For unincorporated areas it was assumed that in the absence of sewer collection systems, all population-based water-use, both indoor and outdoor, eventually reached the land surface or the shallow subsurface. Thus, the total applied water was taken as precipitation plus population-based applied water, minus ET loss. In each simulation series, the net-applied water was take as the starting value for recharge, and was decreased through the calibration process until the calibration criteria were satisfied (see Chapter 5, Section 5.8).The above procedures for estimation of net applied water were repeated for the pre-lake simulations, using the ET and population data appropriate to that period. The results were again used as the starting values for recharge in the various simulation series, and were reduced progressively in calibration.

Chapter 4

USGS Streamflow Record and Analysis

4.1 Introduction

Assessment of the hydrologic impacts of urbanization is always a challenging task. Records of streamflow vs. time are arguably the most valuable kinds of data for assessing those impacts. This chapter describes the stream-gaging activities at USGS gaging stations in the JPL catchment, baseflow separation, the processing and interpretation of results, and the conclusions derived from these tasks.

4.2 USGS Stream Gaging Records

Currently there are two USGS stream gaging stations operating inside the JPL catchment. One is located on WC near Mansfield (USGS 08049700) and the other on MC near Venus (USGS 08049580). Before the construction of the JPL Dam, there was one additional stream gaging station within the JPL catchment (USGS 08049600) at the upstream site of JPL near Cedar Hill. This station was discontinued in 1984 (Figure 4-1), because its location fell within the projected area of the lake. Of the two currently-operating stations in the catchment, only the one on WC has continuously measured streamflow since the time of its establishment. The gaging station on MC (USGS 08049580) records streamflow only when the flow exceeds the base discharge of 580 Cubic Feet Per Second (cfs), apparently because the data is used only for flood forecasting and warning. Thus, the records of this station are not suitable for general hydrologic analysis, or for evaluating hydrologic change associated with the creation of JPL. Note that the outflows of both JPL and MCL are recorded continuously at the respective lake outlet. These records are helpful for catchment water budget estimates, but cannot be used for baseflow separation.

4.3 Reasons for Using of WC Records

Thus, the gaging station on WC near Mansfield is the only gage in the JPL catchment which provides a continuous record of streamflow of suitable quality for baseflow separation and other techniques of hydrologic interpretation, and with continuously available data for the periods before,

during, and since the construction of the lake. The record is continuous from 1961 through 2012, is considered of good quality by the USGS, and has been used extensively in this research. The record provides the daily mean streamflow in cfs, as well as other statistics of the flow regime. The data is provided together with precipitation data from a nearby station. Because there is no apparent impoundment upstream of the gaging station, baseflow separation using the record of this gage appears reliable.

The catchment of the WC gage (see Figure 4-1) occupies roughly the western third of the full catchment of JPL, and coincides approximately with the outcrop area of the Woodbine Group strata, i.e., the area in which the EFS is missing. The gage catchment measures approximately 62.8 square miles, vs. about 224 square miles for the full JPL catchment. As noted above, records of the outflow from the JPL dam are available, and have been supplemented with lake evaporation data (see Figure C-7 in Appendix C), records of diversions from the lake, information on water imports and exports for the JPL catchment and outflow from the MCRWS to provide estimates of total runoff per unit land surface area in the JPL catchment. Estimates of this kind are not themselves suitable for stream baseflow analysis, but have served to confirm that total runoff per unit land surface area for the full JPL catchment is comparable to that for the WC catchment alone. In turn, these data imply that it is reasonable to assume that baseflow studies using the WC data may be accepted as yielding information applicable to the full JPL catchment. Accordingly, baseflow analyses were undertaken using the records of the WC gage. The goals were: (1) to improve overall understanding of the hydrology of the JPL catchment; (2) to determine whether any characteristic of the calculated baseflow could shed light on hydrologic changes associated with either the creation of JPL, or with the urbanization which followed; and (3) to provide information with which the output of groundwater models could be compared.

4.4 Streamflow Analysis and Baseflow Separation

Baseflow is often assumed to represent the long-term drainage of groundwater into the stream network, and for this reason the separation of total streamflow into baseflow and peakflow components is

of interest. The process of baseflow separation is always somewhat subjective; there is an extensive literature on the subject, including for example: Chow (1964), Linsley and others (1958), Horton (1933), Hall (1968), Nathan and McMahon (1990), Tallaksen (1995), and Smakhtin (2001). The calculations undertaken in this research utilized a computer-based method of baseflow separation, the USGS program PART (Rutledge, 1998; Rutledge, 2007(a)). This procedure was used to reduce subjectivity and ensure the use of a common technique of separation throughout the analysis. The baseflow result given by PART is expressed as inches (i.e. cubic inches of water per square inch of catchment area) on a monthly, seasonal (quarter year), or annual basis. Another common method of baseflow analysis, popularly known as Web-based Hydrograph Analysis Tool (WHAT) developed by Purdue University (Lim and others, 2005) has also been used for comparison with the results of PART. The results obtained from the two techniques were the same. The result of the baseflow separation and further relationships with precipitation are presented below: Figure 4-2, Tables 4-1 and 4-2.

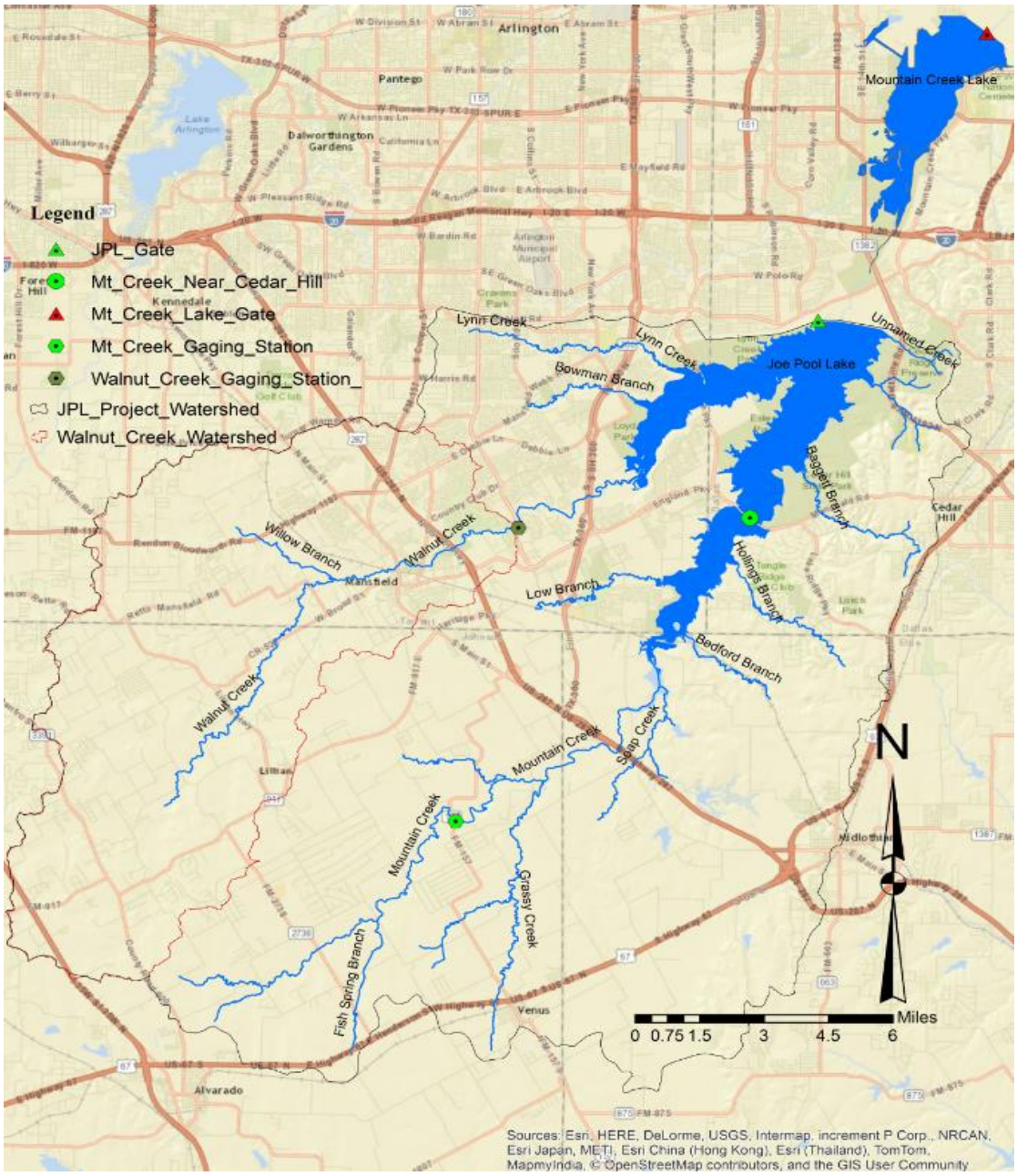

Figure 4-1 Location of the USGS streamflow gaging stations on WC near Mansfield, and on MC near Venus, and near Grand Prairie. A discontinued USGS gaging stations is located near Cedar Hill, now within JPL outflow points from JPL and MCL are also shown

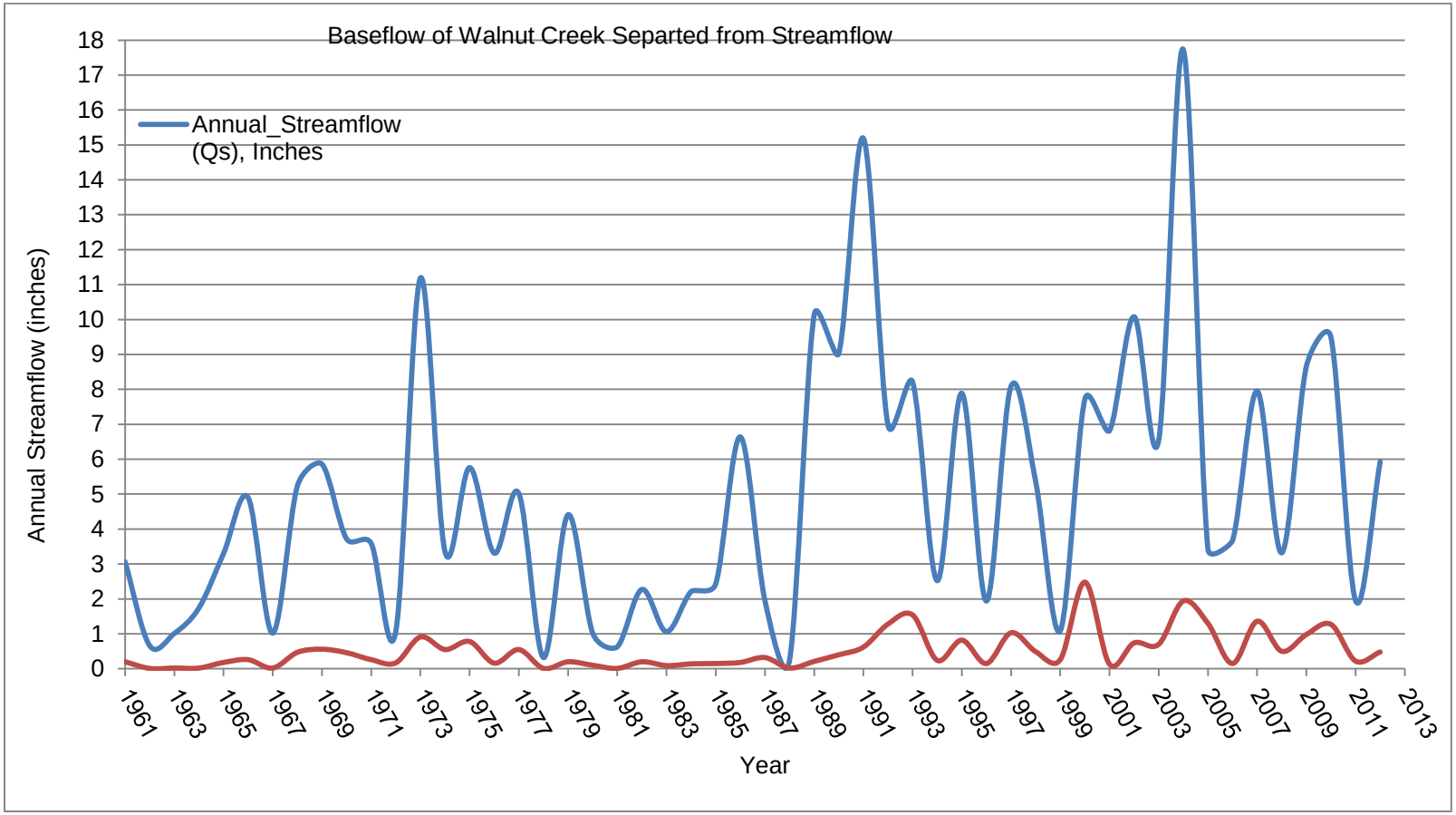

Figure 4-2 Total WC streamflow superimposed over the separated baseflow of WC gaging station near Mansfield Texas (USGS 08049700)

4.5 Results of Streamflow Analysis

Table 4-1 lists the average annual precipitation, the total average annual flow through the WC stream gage, and the average annual baseflow through the gage as calculated by PART; the ratio of calculated average annual baseflow to total average annual streamflow, the ratio of total average annual streamflow to total average annual precipitation, and the ratio of calculated average annual baseflow to average annual precipitation for the years 1961 through 2012 are also listed in Table 4-1. Figure 4-2 shows a plot of total annual flow and calculated baseflow vs. time for the 1961–2012 period, and Figure 4-5 shows a plot of the ratios of total flow and calculated baseflow to precipitation for the same time period. Figure 4-4 shows a plot of the ratio of baseflow to streamflow vs. time. The feature of Figures 4-2, 4-4, and 4-5 that most deserves notice is a change beginning in 1987, i.e., shortly after dam completion, and during the initial filling of the lake. The average value of annual precipitation for the pre-lake period (1961-1986) was 32.25 inches per year; the corresponding figure for the post-impoundment period (1987-2012) was 35.37 inches per year, an increase of about 9.6 percent. The precipitation trend of the catchment is given in Figure 4-3. Between the same two periods, however, the average annual total flow through the WC gage more than doubled, from less than 1,283,000 CFD to more than 2,700,000 CFD, and the estimated annual baseflow increased by a factor of more than 2.5, from less than 227,695 CFD to over 595,500 CFD. Thus, it appears certain that some characteristic of the gage or of the WC system upstream of the gage must have coincided with the impoundment of JPL. The simulations of groundwater flow showed that the altitude and configuration of the water table, and the exit flows from the groundwater regime were significantly altered by the creation of JPL. It is possible, though unlikely, that these changes might account for the observed increase in average baseflow of WC. However, it seems doubtful that any of the simulated changes in the groundwater regime could account for the observed increase in total streamflow through the gage. It therefore seems probable that the increase in total flow resulted from the diversion of a component of direct runoff, e.g., the discharge of a newly-constructed storm sewer system, into WC or one of its tributaries, although no record of such an event was located in this research. If something of this kind had occurred, however, the estimated increase in baseflow could simply be an artifact of the baseflow separation calculation.

Table 4-1 Streamflow, Baseflow, and Precipitation of Walnut Creek Gage Catchment

Parameters	Pre-lake (1961-1986)	Post-lake (1988-2012)
Average Annual Precipitation (in)	32.25	35.37
Total Av. Annual Streamflow ($feet^3$)	468,320,134	958,717,363
Total Av. Annual Baseflow ($feet^3$)	83,108,559	212,093,856
Total Av. Annual Walnut Creek Catchment Precipitation($feet^3$)	4,705,289,188	5,147,918,119
Ratio of Average of [Baseflow(Qb)/Precipitation(P)]	0.0167	0.0412
Ratio of Average [Streamflow (Qs)/Precipitation (P)]	0.0939	0.1808
Ratio of Average [Baseflo(Qb)/Streamflow(Qs)]	0.1718	0.2304

The baseflow value of WC gage station, evaluated by using PART program is shown in Table 4-2. The value is expressed in inches per year for the WC gage; the total watershed area drained through gaging station USGS 08049700 is 62.8 square miles. The pre-lake baseflow is about 0.6 inches per year, and it is increased to 1.5 in/year during the post-lake era. The average is about 1.1 in/year. This increase is perhaps related to the increased flow of the WC gage after JPL impoundment. In the same time the streamflow is increased by 4 in/year.

Figure 4-4 shows the slight increase in both the streamflow and baseflow during the post-lake area (1989 and beyond). The summary of baseflow data, streamflow, and their trend from pre-lake to the post-lake era is given in Table 4-2.

Table 4-2 Recorded Streamflow, Calculated Baseflow by PART, and Resulting Direct Runoff at the Walnut Creek Gage

Modeling Conditions	Baseflow (in/year)	Streamflow (in/year)	Direct Runoff (in/year)
Pre-lake (1961-1987)	0.5687	3.163	2.595
Post-lake (1989-2012)	1.55	7.027	5.477
Average (1961-1987 and 1988-2012)	1.059	5.095	4.036

4.6 Conclusions

The WC gage has a long term streamflow data and the result of streamflow analysis at this station is used to obtain the streamflow per unit area of JPL catchment. The baseflow separated from the data collected in this station is used to calculate the equivalent baseflow of the entire JPL basin and used to calibrate the MODFLOW model by comparing the calculated river output from the shallow aquifer in the pre-lake and post-lake JPL model.

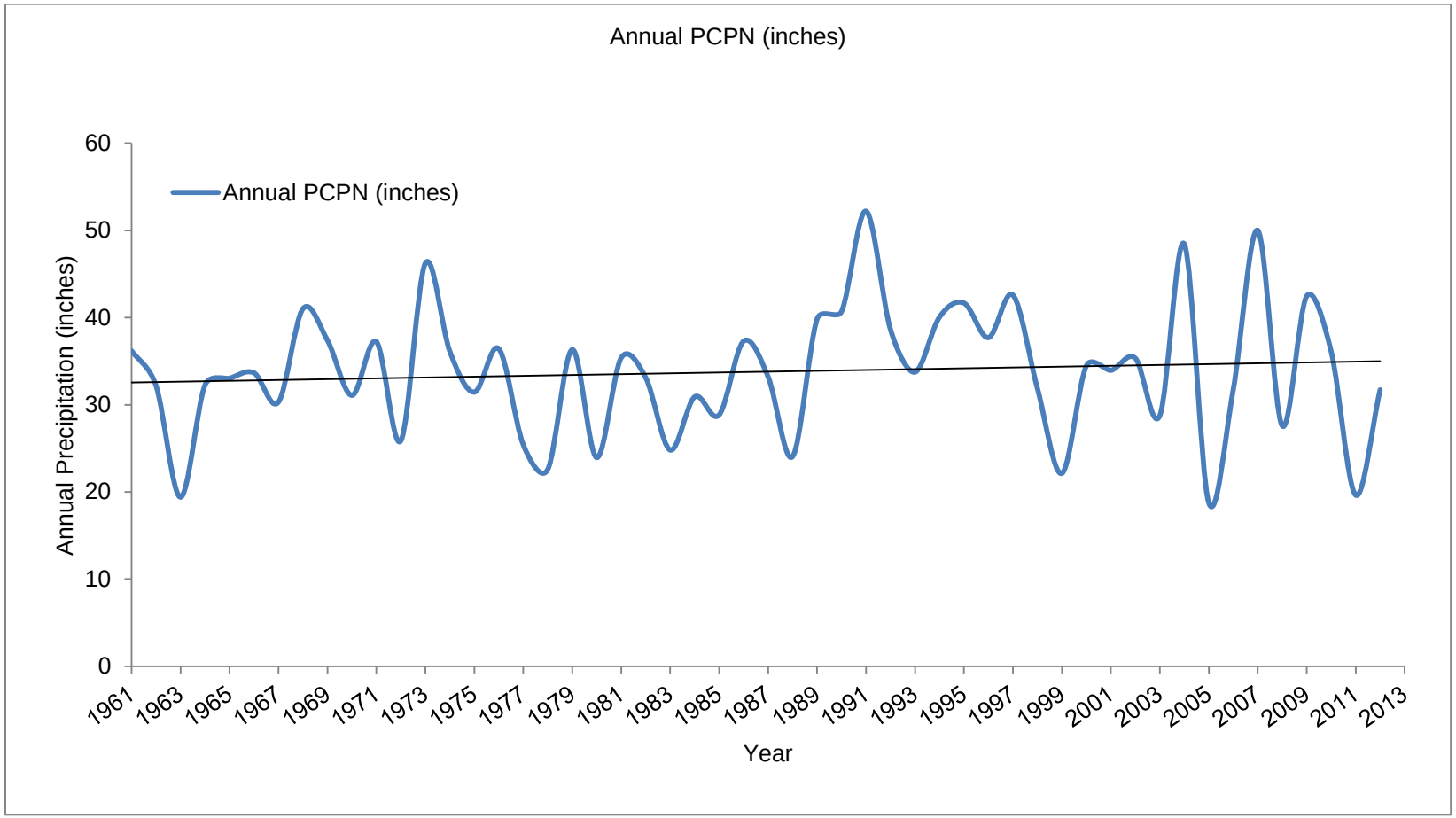

Figure 4-3 Precipitation (PCPN) trend of JPL catchment

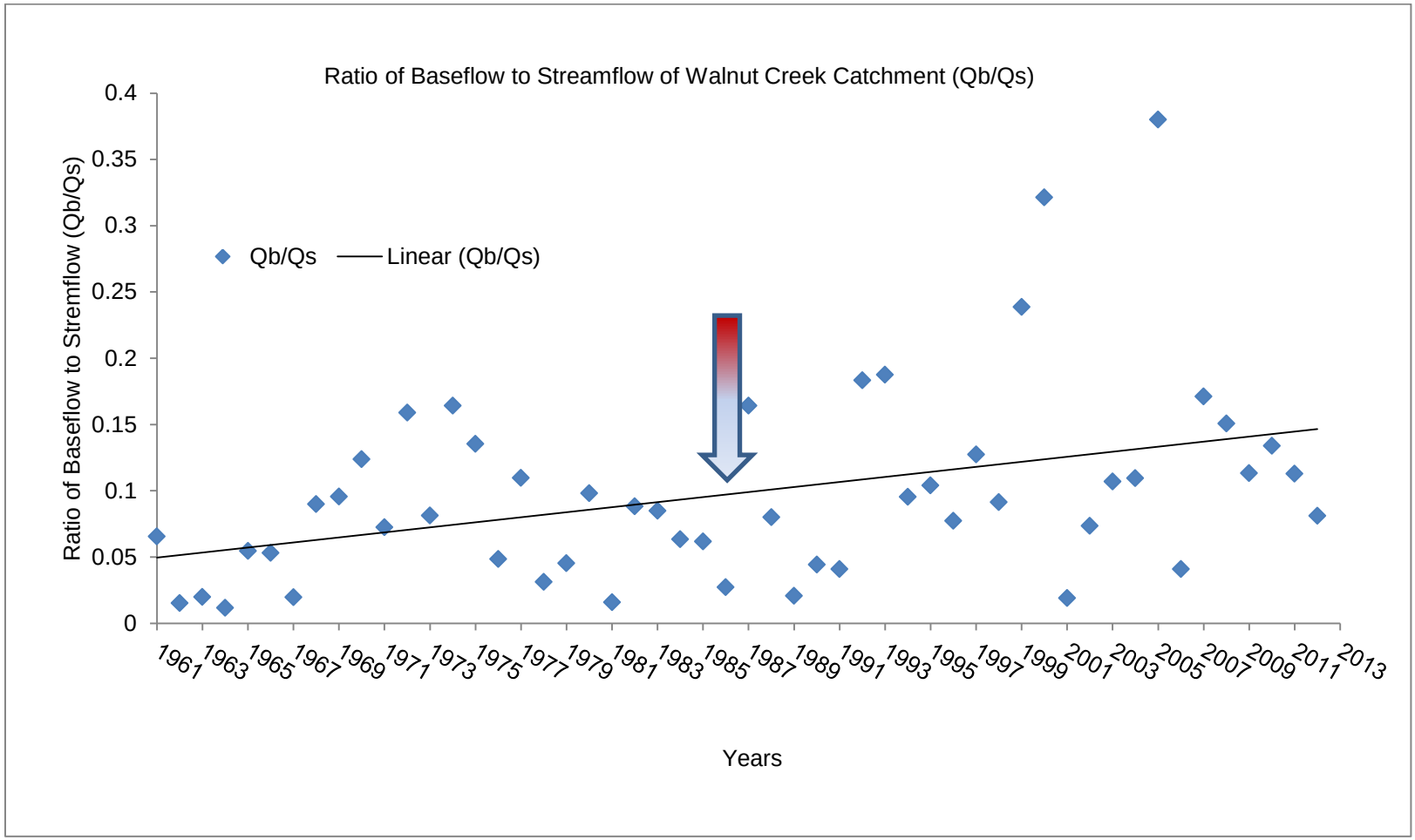

Figure 4-4 The ratio of baseflow to the streamflow

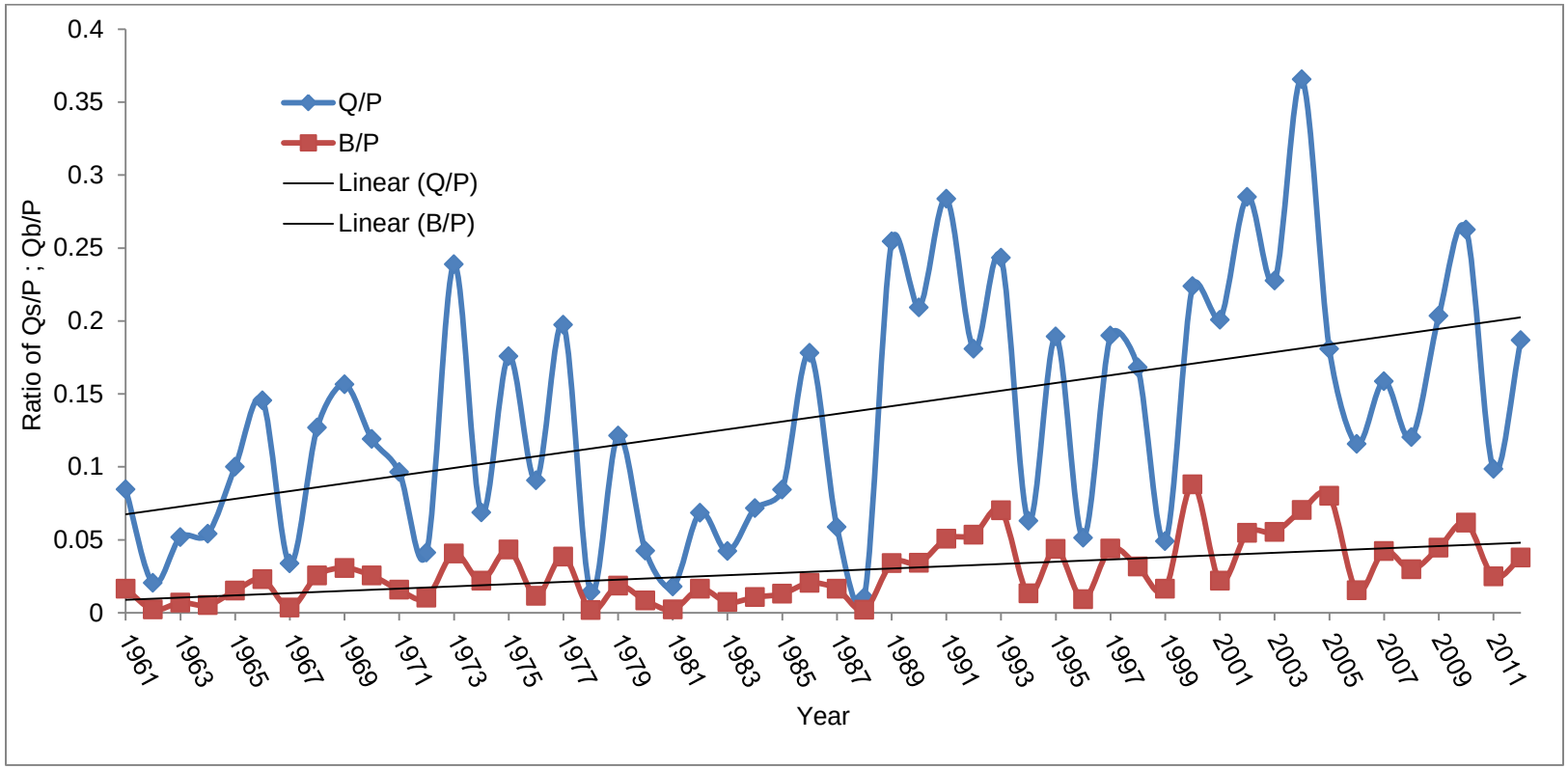

Figure 4-5 The ratio of baseflow (Qb) with precipitation (P) and ratio of streamflow (Qs) with precipitation (P) as a function of time (T) at Walnut Creek gage

Chapter 5

Simulation of Groundwater Flow

5.1 Introduction

This chapter deals with the development of a groundwater simulation model for the JPL catchment. As discussed previously, simulation of the groundwater segment of the flow regime was carried out using USGS MODFLOW-2005 software. Interpretation of the results was carried out with the help of the ZONEBUDGET postprocessor (Harbaugh, 1990). A system diagram depicting the overall hydrologic system (groundwater and surface water) in the JPL catchment under present-day (post-lake conditions) is first presented in this chapter. Finally, the calibration procedure used during model development is also discussed.

5.2 Conceptual Representation of the Overall Hydrologic System in the JPL Catchment

Figure 5-1 is a schematic diagram illustrating the major components of the present-day hydrologic regime in the JPL catchment, and the role of the alluvial groundwater system within it. The system as shown in Figure 5-1 served as the conceptual basis for analysis of the 2010 hydrologic regime and, except for the references to JPL itself, for the 1981 hydrologic regime as well.

The rectangles in Figure 5-1 represent the major elements of the flow regime, i.e, (1) the shallow aquifer itself, (2) the underlying bedrock aquifer and deeper aquifers, (3) the surface stream system, and (4) JPL. The arrows in Figure 5-1 represent flow paths linking the surface elements to the aquifer, to each other, and to the atmosphere (designated by the symbol A in Figure 5-1. Figure 5-1 shows only the major components of the overall hydrologic system, and reflects the various assumptions underlying the analyses.

The input sustaining the flow system is represented on Figure 5-1 by arrows (a) and (b), which together with the population-based water as discussed in Sections 3.6 and 3.7, account for the total applied water. Arrow (a) refers to precipitation on land surfaces and to that fraction of the water supplied through public distribution systems which ultimately reaches the land surface; the latter component was estimated on the basis of population, per capita use, fractions of distributed water typically used outdoors,

and incorporated vs. unincorporated political jurisdiction. Incorporated areas were assumed to be equipped with sanitary sewers; unincorporated areas were assumed to be without sanitary waste water collection systems. Arrow (b) represents precipitation on water surfaces. Arrow (c) represents direct runoff of applied water to the stream system or to the lake. The discharge arrows terminating in the atmosphere (A) on Figure 5-1 represent the part of the annual total applied water which is discharged from the soil and vadose zone by ET, from the streams and lake by evaporation, or directly from the alluvial groundwater by ET from the capillary fringe above the water table, as discussed in greater detail below. Recharge, arrow (d) on Figure 5-1, includes the precipitation and applied municipal water which eventually reaches the water table.

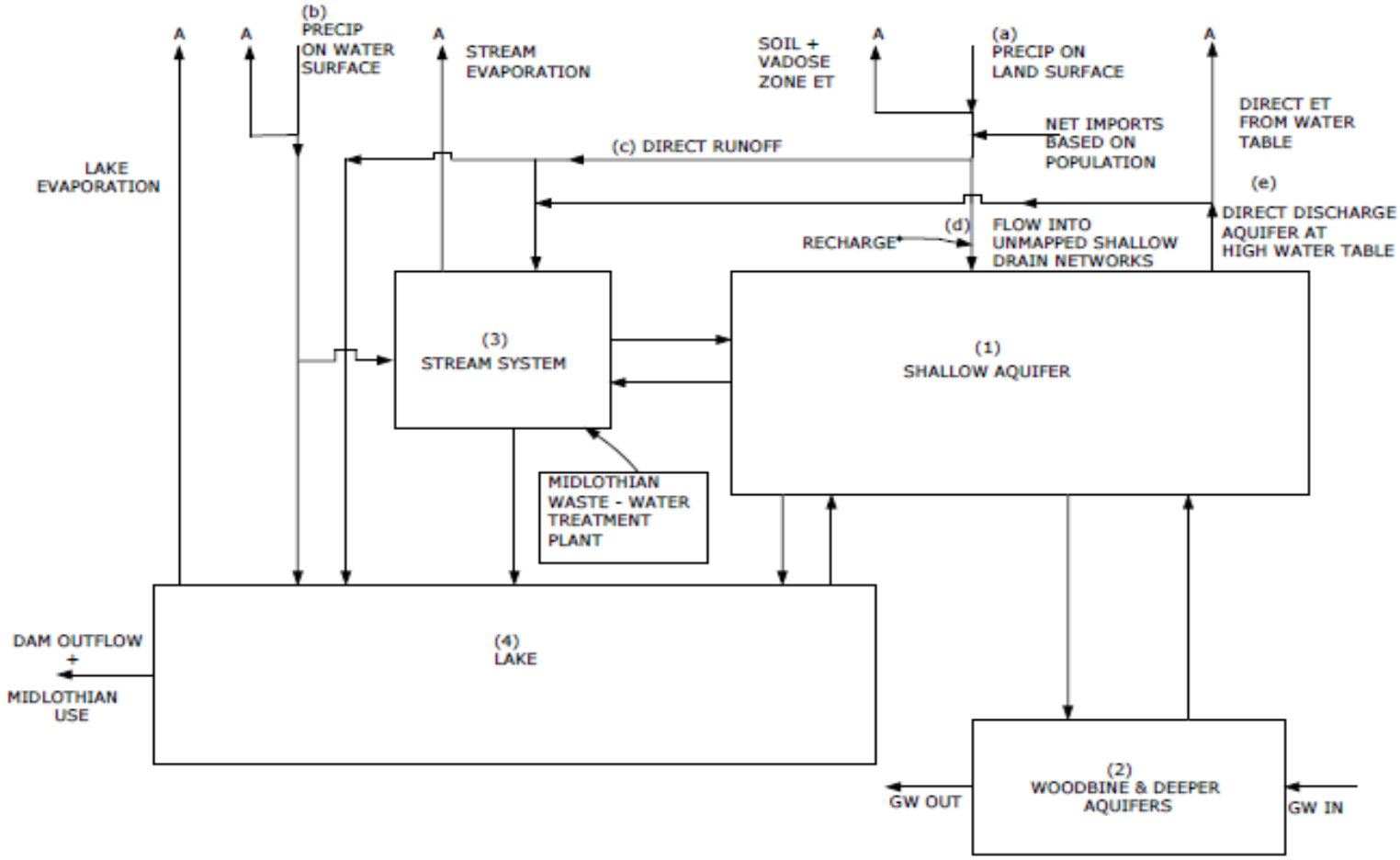

Figure 5-1 The schematic diagram illustrating the major components of the present-day hydrologic regime in the JPL catchment, and the role of the alluvial groundwater system within it

Arrow (e) on Figure 5-1 represents two processes which discharge water directly from the alluvial aquifer at times and in locations where the water table is close to land surface. The first is that noted above, direct ET from the water table or capillary fringe, which is assumed to be zero if the water table is more than a certain depth below land surface, and increases as the water table rises above that depth, eventually reaching a maximum value when the water table reaches land surface. This process is represented in simulation by a function relating ET discharge to the depth of the water table below land surface. Commonly, the function is assumed to be linear, although this linearity is recognized to be an approximation.

The second process represented by arrow (e) in Figure 5-1 is groundwater flow into unmapped or unrecognized shallow drainage features or drainage networks, which again is assumed to be zero when the water table is below the bottom elevation of the deepest such feature, and to increase as the water table rises above that depth, again reaching a maximum as the water table reaches the land surface. Treatment of such minor features individually in simulation is generally impractical, but their cumulative effect on a given model cell can be represented by using a function relating the total drainage discharge from that cell to the depth of the water table below land surface. Whereas the direct ET process leads to direct discharge from the aquifer to the atmosphere, the distributed shallow drainages process described here leads to direct discharge from the aquifer to the stream system, which is assumed to collect the net outflow of the shallow drainage features. However, the functional similarities between these two processes often makes it difficult to distinguish between their effects in the field, or to represent them independently in simulation; and it is probably true that in many cases, where the intention is to represent one or the other in simulation, both are actually being simulated, albeit inadvertently and imperfectly.

In any case, it appears that both may be significant processes in the JPL catchment area, both at present and in its condition prior to lake construction. For the purposes of the present research, it was decided that the best approach would be to represent their combined effect in simulation, and to assess that effect, to the extent possible, through the analysis of model results. It is for this reason that a single arrow, (e), is used to represent the combined process in Figure 5-1; this arrow is then shown as dividing into two discharge arrows, one leading to the atmosphere and one to the stream network. As discussed in

a subsequent section, the Evapotranspiration “Package” (EVT), or set of subroutines incorporated in the USGS MODFLOW software to represent ET, was used in this research to represent the combined process represented in Figure 5-1.

Several additional pathways of inflow to and outflow from the alluvial aquifer are shown in Figure 5-1, through the arrows between the element representing that aquifer and the elements representing the stream system, the Woodbine Aquifer, and the lake, respectively. Because a shallow groundwater divide is assumed to coincide with the surface water divide surrounding the JPL catchment, no regional groundwater inflow is shown directly entering the alluvial aquifer in Figure 5-1. Also, because pre-impoundment investigations (USACE, 1991) indicate generally low-permeability materials in the vicinity of the JPL dam, downgradient groundwater outflow from the alluvial aquifer is assumed to be negligible. However, regional inflow and outflow of groundwater does occur in the Woodbine Aquifer and deeper aquifers, and vertical interconnection between the Woodbine Aquifer and the alluvium is represented in Figure 5-1, and in the simulations.

The Mountain Creek Regional Waste Water Treatment Plant (MCRWS) is in operation since 2005 and treats wastewater released from cities such as Midlothian, Cedar hill, Venus, and Alvarado. As discussed earlier the treated effluent from the plat is 1.6 MGP. So, for the post-lake model this effluent must be included in describing overall conceptual model of the hydrologic system.

Similarly, the overall conceptual model of the hydrologic system for the pre-lake era is bit simpler than the post-lake conditions. So, as discussed in the previous sections and beginning of this section, by removing the MCRWS, lake evaporation, lake itself, and all the arrows directed toward and away from the lake will visualize the overall conceptual model of the hydrologic system during the pre-lake era.

5.3 Review of MODFLOW Program

The U.S. Geological Survey (USGS) three-dimensional finite-difference groundwater flow model (MODFLOW) is probably the most popular flow simulation code in use today, both in the USA and throughout the world (McDonald and Harbaugh, 1988; Harbaugh, 2005). As originally developed, MODFLOW was a FORTRAN batch program for simultaneous solution of a set of algebraic finite-

difference equations, which collectively simulate the partial differential equation (PDE) of groundwater flow. It is a well-documented public domain program that utilizes finite-difference methods. The PDE of groundwater flow is approximated as a set of algebraic finite-difference equations which are solved simultaneously as a set, normally by iteration. MODFLOW consists of modules – subroutines or groups of subroutines which address tasks necessary in the numerical solution process and are called by the main program in combinations and sequences according to information provided by the user. In the modular structure, similar program functions are grouped together, and specific computational and hydrologic options are constructed independently allowing new options to be added without changing the existing options. The various groundwater flow processes in MODFLOW are divided into “Packages” or parts of the program dealing with a single aspect of simulation. For example, the Well Package (WEL), and the River Package (RIV), simulate the effects of wells or the effects of rivers, respectively, whereas the Strongly Implicit Procedure (SIP) Package implements a particular numerical procedure to solve the system of simultaneous finite-difference equations. The number and variety of packages in MODFLOW are such that all of the packages will never be used during any single simulation exercise.

Numerous finite-difference groundwater flow models preceded MODFLOW in common usage. These models were initially two-dimensional codes (Pinder, 1970; Prickett and Lonnquist, 1971; Trescott, 1975; Trescott and others, 1976), evolving subsequently into three-dimensional codes (e.g., Trescott, 1975; Trescott and Larson, 1976). The original MODFLOW model as described in the 1988 documentation (McDonald and Harbaugh, 1988) has been revised and updated several times. The updated versions such as MODFLOW-1996 (Harbaugh and McDonald, 1996), MODFLOW-2000 (Harbaugh and others, 2000), MODFLOW-2005 (Harbaugh, 2005) are well documented by the USGS. Besides these public–domain versions, some proprietary models which incorporate the basic MODFLOW structure are also available. These popular proprietary models include: Groundwater Vista, Visual MODFLOW Flex (VMOD Flex), MODHMS-Surfact, MODFLOW GUI, Groundwater Modeling Systems (GMS), PMWIN, etc. In simpler terms, MODFLOW may be considered a program that takes input data describing a groundwater situation and calculates head values as output. Groundwater flows and other terms of interest are developed from the calculated heads.

The MODFLOW program since the original development has been enhanced by the addition of numerous packages. These packages address, for example, the relation between stream and aquifers (Miller, 1988; Prudic, 1989; Swain and Wexler, 1996; Jobson and Harbaugh, 1999; Prudic and others, 2004; Niswonger and Prudic, 2005), or provide new numerical solution techniques such as the Preconditioned Conjugate-Gradient (PCG) Package (Kuiper, 1987; Hill, 1990), or address such effects as subsidence (Leak and Prudic, 1991) or lake and groundwater interaction (Cheng and Anderson, 1993; Council, 1998; Merritt and Konikow, 2000). The development of extensive software associated with MODFLOW and intended for use in conjunction with it has prompted introduction of the concept and terminology of "process" to describe various aspects of the full simulation procedure. Thus, the solution of the flow equation itself is considered the Groundwater Flow (GWF) process, whereas closely associated but separate software addressing such issues as parameter estimation, solute transport, groundwater management, or so on are grouped as separate processes (e,g., Hill and others, 2000; Ahlfeld and others, 2005).

5.4 Partial Difference Equation (PDE) of Groundwater Flow in MODFLOW

The groundwater flow equation (Rushton and Redshaw, 1997; McDonald and Harbaugh, 1988; Harbaugh, 2005) as used in the MODFLOW program is a partial differential equation (PDE) that describes the three-dimensional movement of groundwater of constant density through porous earth material (Harbaugh, 2005). The flow equation (Figure 5-1) is given by:

$$\frac{\partial}{\partial x}\left(Kxx\frac{\partial h}{\partial x}\right)+\frac{\partial}{\partial y}\left(Kyy\frac{\partial h}{\partial y}\right)+\frac{\partial}{\partial z}\left(Kzz\frac{\partial h}{\partial z}\right)+W=Ss\frac{\partial h}{\partial t}, \quad \text{(5-1)}$$

where K_{xx}, K_{yy}, and K_{zz} are hydraulic conductivities parallel to the x, y, and z coordinate axes, respectively, which are assumed parallel to the major axes of hydraulic conductivity (LT^{-1}); h is the hydraulic head (L); W is the volumetric flux per unit volume representing sources and/or sinks of water (where W<0 implies groundwater outflow and W>0 implies groundwater inflow), (T^{-1}); S_s is the specific storage of the porous aquifer material (L^{-1}); T is time (T). The variables S_s, K_{xx}, $K_{yy,}$ and K_{zz} are functions of space (S_s= S_s(x, y, z), K_{xx}= K(x, y, z), etc.); W may be a function of space and time, i.e., W = W(x, y, z, t). For a homogeneous isotropic medium K_{xx} = K_{yy} = K_{zz}.

In Equation 5-1, the first, second, and third terms on the left side represent the differences between inflow and outflow of water in the x, y, and z directions, respectively, per unit volume of aquifer material. The fourth term on the left side represents the net flow to or from fluid sources and sinks, per unit volume of aquifer material; and the term on right represents the rate at which water is accumulating in storage, per unit volume of aquifer material. Basically, Equation 5-1 is obtained by combining flow terms, as expressed through Darcy's law, with the equation of groundwater storage, using the continuity equation. This model implies the conservation of mass, and the assumption that the compressibility of water can be neglected except insofar as it contributes to aquifer storage. A solution of Equation 5-1 is an array of head values, i.e., a distribution of head values in space and time, such that the derivatives of head, when substituted into Equation 5-1, satisfy the equation. A solution might be represented, for example, by a set of hydrographs of h vs. t, each representing the time variation of head at a particular point (x, y, z) in space, or by a set of maps, each representing head at a particular horizon (z) and time (t), or so on. In rare cases, a solution maybe represented as a mathematical function, h = h(x, y, z, t). In addition to satisfying the PDE itself, a solution must satisfy boundary and initial conditions characterizing the problem.

Equation 5-1 can be derived by considering the flow through an infinitesimal cube (Figure 5-2) of volume, $\mathrm{V} = \mathrm{dx} * \mathrm{dy} * \mathrm{dz}$. The net changes in flow along the x, y, and z directions are summed together with the net flow from sources and sinks in the volume element, and the result is equated to the rate of accumulation of water in storage in the element (Harbaugh and McDonald, 1996; Freeze and Cherry, 1979; Harbaugh, 2005; Bennett, 1989; Anderson and Woessner, 1992; Fitts, 2002). See Appendix A for a detailed derivation of the groundwater flow Equation, 5-1. The solution of this equation (Pinder and Leon, 1982) through finite-difference approximation is discussed in Appendix B.

The steady state condition of the above equation corresponds to situations in which both accumulation of water in storage and release of water from storage are negligible, so that the storage term on the right side of Equation 5-1 can be set to 0, i.e.,

$$\frac{\partial}{\partial \mathrm{x}}\left(\mathrm{Kxx}\frac{\partial \mathrm{h}}{\partial \mathrm{x}}\right) + \frac{\partial}{\partial \mathrm{y}}\left(\mathrm{Kyy}\frac{\partial \mathrm{h}}{\partial \mathrm{y}}\right) + \frac{\partial}{\partial \mathrm{z}}\left(\mathrm{Kzz}\frac{\partial \mathrm{h}}{\partial \mathrm{z}}\right) + \mathrm{W} = 0 \quad \text{(5-2)}$$

Hydrologic systems in nature tend toward equilibrium, but human intervention may perturb this equilibrium; however, nature will generally try to adjust towards a new equilibrium state following any such perturbation. In the present research, two steady-state simulations were undertaken. One corresponding to pre-lake (1981) conditions and the other corresponding to present-day or post-impoundment conditions (2010), termed as “post-lake” for brevity in subsequent sections.

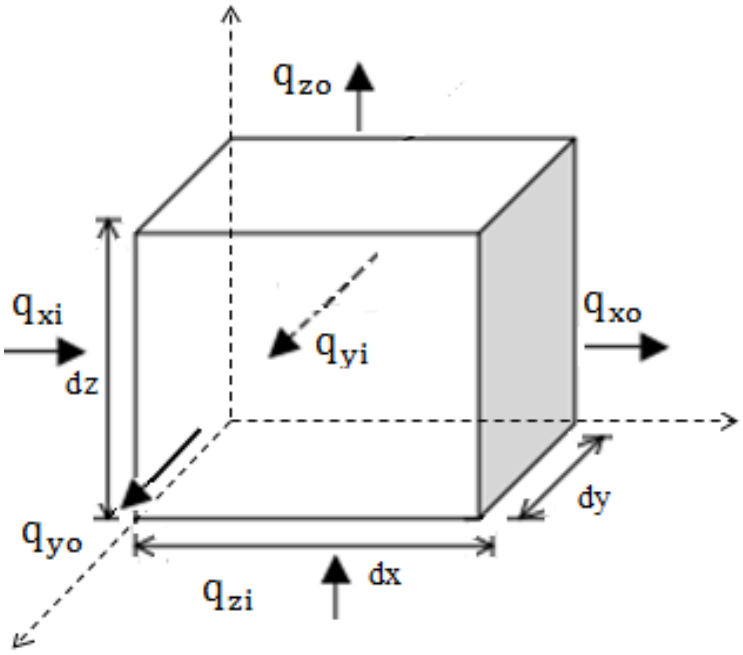

Figure 5-2 Diagram showing three-dimensional groundwater flow in an infinitesimally small cube, a representative elementary volume (REV)

5.5 Local and Regional Examples of MODFLOW Case Studies

The MODFLOW program has been widely used in Texas and elsewhere for investigations involving groundwater flow problems (Council, 1997; Yager and Metz, 2004; Stanton and others, 2010; Kuniansky and Hamrick, 1998; Feinstein and others, 2010; Barker and Braun, 2000).

Barker and Braun (2000) used MODFLOW and the associated particle tracking software MODPATH (Pollock, 1989) to study groundwater flow and the effects of contaminant remediation at the NWIRP and adjacent areas. The study involved definition of aquifer properties, water budget

computations, major flow path delineations, and detailed simulations of remedial operations at the site. Calibrated values of hydraulic conductivity ranged from 0.75 to 7.5 feet/day, and averaged about 4 feet/day. Calibrated specific yield values ranged from 0.005 to 0.15, and averaged about 0.08; infiltration rates ranging from 0 to 2.5 inches per year, distributed aerially on the basis of ground cover, were used in simulation; and a porosity of 0.15 was used in particle-tracking calculations to predict the time required to remove contaminant from the shallow aquifer.

Tetra Tech Nus, Inc. (2004) carried out remedial studies on affected properties of the NWIRP using MODFLOW 1996 to simulate flow in the vicinity of the NWIRP and the Naval Air Station (NASD), Dallas. The report provides guidance for the application and demonstration of Monitored Natural Attenuation (MNA) at affected properties of the NASD. MODFLOW simulation was used to calculate heads, and the head distribution was used to calculate flows. This procedure was followed by transport simulation using MODPATH and RT3D to calculate contaminant concentrations. The simulated results showed that a significant portion of contaminant was degrading; the vicinity of the plume area was geochemically reducing. However, both the concentration time graph and the modeling results indicated that some pollutant may remain above permitted concentration levels beyond 2017.

Kuniansky and Hamrick (1998) studied the Paluxy Aquifer near the Landfills of US Air Force Plant 4 located at Fort Worth, Texas. They used MODFLOW simulation and applied the output of MODFLOW in MODPATH calculations to track contaminant movement. The groundwater of the surficial terrace alluvial aquifer had been contaminated and volatile organic compounds were detected in fractures of the Goodland-Walnut confining unit that separates the alluvial aquifer from the underlying Paluxy Aquifer. The simulation and particle-tracking were successfully utilized to determine the optimal recovery well locations to achieve full contaminant capture.

TWDB has pioneered the application of groundwater availability models, and has prepared groundwater availability models for both major and minor aquifer systems. The state of Texas has identified 16 major groundwater districts, 13 major aquifers, 32 minor aquifers, and 23 major river basins. For many of these, groundwater availability models have been developed using the MODFLOW code. A model of the NTWGAM has been developed (Bene and others, 2004, Kelly and others, 2014) and used to

simulate the long term response of the aquifer under record drought conditions and under average annual recharge.

The well-known Edwards Limestone Aquifer of Texas has been studied extensively using groundwater simulation approach. Johnson and others (2005) utilized MODFLOW and MODPATH to study rates and directions of flow in the Panther Springs Creek Basin, comparing the simulation results with those of field tracer tests. Whereas the groundwater velocity was severely underestimated in the simulations, valuable insights were gained regarding aquifer behavior. Scanlon and others (2001) studied the Barton Spring segment of the Edwards Aquifer to estimate water availability, water levels, and spring flow in response to the 2001 drought and increased pumping. Sun and others (2005) used MODFLOW-DCM, which provides a dual conductivity approach, to simulate groundwater flow in the Barton Springs area of the Edwards Aquifer. Lindgren and others (2011) used MODFLOW (Harbaugh and others, 2000) and MODPATH (Pollock, 1994) to simulate flow and calculate pathlines of water particles in the Balcones Fault Zone area of the Edwards Aquifer. The results provided insights regarding the recharge sources for a public supply well in San Antonio. Feinstein and others (2010) utilized MODFLOW in a study of the groundwater resources of the Lake Michigan Basin. The simulations represented long term changes in the groundwater system between 1864 and 2005 in response to increasing groundwater withdrawal. The results identify the sources of water with major pumping centers, illustrated the groundwater system dynamics, and provided a measure of groundwater availability. Lambert and others (2011) used MODFLOW to study groundwater/surface water interaction near the Uinta River in Utah, with particular reference to potential streamflow depletion that might result from future excess groundwater withdrawal. The results showed that by the 10th year of withdrawal at the simulated rates, 89% of the simulated well discharge is derived from streamflow depletion, 10% from outside the budget zone, and 1% from storage.

Stanton and others (2010) utilized MODFLOW to study changes in stream baseflow due to pumping and due to changes in irrigated area in the Elkhorn and Loup River Basins, Nebraska. Optimization was used to estimate the minimum reduction in pumpage that would be required to maintain various levels of baseflow.

GIS application is now routinely coupled with MODFLOW software. The output files or results from MODFLOW are compatible as input to GIS and vice versa. Various researchers (e.g., Ajami and others, 2012; Ajami and Maddock, 2009; Bernardand others, 2005; Bernard and Steward, 2006) have demonstrated a strong link and dynamic applications of GIS and MODFLOW for groundwater modeling. ArcMap 10 has an add-in tool called “MODFLOW Analyst” which enables MODFLOW simulation in the ArcMap environment. ArcHydro Groundwater (Maidment, 2002; Strassberg and others, 2011) is in wide use in the hydrologic community for the analysis and visualization of geohydrologic data, and together with ArcMap has been refined to the point that coupling with MODFLOW simulation is straightforward. Pinder (2003) in his book “Groundwater Modeling Using GIS” discussed the coupling of GIS with MODFLOW for flow modeling, and for the flow simulation phase of transport modeling. In this context, he compared finite-difference simulation with finite-element simulation using an example in Tucson, Arizona.

The MODFLOW software is in widespread use around the globe, as well as in the United States. Dong and others, (2011) used MODFLOW in Zhuhai City, China to simulate groundwater-seawater interaction in a coastal region in response to sea level variation; he also used the Fourier sine transform method to interpret water-table fluctuations induced by sea-level changes. Mirlas (2009) used MODFLOW to solve the irrigation drainage problems in the Jahir irrigated fields of Israel. Malik and others (2012) applied MODFLOW groundwater simulation to locate groundwater recharge areas and to complete a water balance study in the Haryana district of India. Van Lanen and Van Weered (1994) used MODFLOW to simulate the groundwater discharge in the Dutch Chalk Plateau of the Netherlands and to determine its impact on streamflow. The study also focused on the impact of changes in groundwater recharge caused by land-use or climate change on groundwater head and baseflow. Ahmed and Umar (2009) modeled the groundwater flow in the Yamuna-Krishni interstream area of the Central Ganga Plain of India simulating the behavior of the flow system and evaluated the water balance using both steady-state and transient analysis. Torres-Gonzalez and others (2002) studied the alluvial aquifer in the valley of the Rio Grande de Manati of Puerto Rico to estimate the capacity of the alluvial aquifer system to attenuate bacteria and viruses, and to estimate the travel time of groundwater from the Rio Grande de Manati to a potential

production well. In his study, groundwater flow and groundwater-surface water interaction, were simulated using MODFLOW-96; MT3DMS was used for contaminant transport simulation.

Lampayan and others (2001) developed a three-dimensional groundwater flow model using MODFLOW to study the salinity change and water table variation in the Lachlan Catchment of New South Wales, Australia. Luo and Sophocleous (2011) used two-way coupling of the MODFLOW-96 and SWAT200 models to simulate the unsaturated-saturated flow interactions in the Hetao Irrigation District of Inner Mongolia, China. They developed an integrated surface water-vadose zone groundwater simulation system that provided an improved understanding of the land-based hydrologic cycle. Their aim was to provide a means for evaluating the impacts of land-use, irrigation development, and climate change on both surface and groundwater resources. Takounjou and others (2009) used MODFLOW to model groundwater flow in a shallow unconfined aquifer of the upper part of the Anga River watershed of Yaunde, Cameroon. The results indicated that surface topography was the dominant factor controlling groundwater flow in the Anga River area. Hernandez and others (2011) used MODFLOW to study the Calera Aquifer of Zacatecas, Mexico. In their study, estimated recharge rates were based on land-use type, and verified through model calibration. Hamer and others (2007) used MODFLOW in conjunction with rainfall-runoff simulation and water balance analysis to estimate the water balance of a small alluvial aquifer in southern Zimbabwe. Memon and Memon (2006) used MODFLOW to simulate water table fluctuation during five years of pumping of groundwater from an unconfined aquifer in the Sindh Province of Pakistan. Xu and others (2011) adapted the MODFLOW model coupled with ArcInfo GIS to simulate the efficiency of water saving options in irrigation districts of the upper part of the Yellow River Basin of North China. Flugel and Micht (1995) coupled GIS with MOFLOW to simulate the hydrodynamics of an alluvial aquifer of the River Sieg in Germany. The raster output data of GIS was overlaid into MODFLOW and MT3D to detect conceptual errors in the model and to input simulated infiltration from the rivers into MODFLOW.

MODFLOW is a public domain software. The code has been modified frequently by the USGS, for example MODFLOW-1996 (Harbaugh and McDonald, 1996), MODFLOW-2000 (Harbaugh and others, 2000), and MODFLOW-2005 (Harbaugh, 2005). Various secondary software, known as proprietary

software, are developed and they are commercially available (MODFLOW Vista, Visual MODFLOW Flex (VMOD Flex), MODHMS-Surfact, Groundwater Modeling System (GMS), PMWIN, FARM Process, Groundwater Management (GWM), UCODE (Harbaugh, 2010), MT3DMS, and MODFLOW+PHREEQC). ESRI has also developed a geo-database for the MODFLOW model as an add-in tool.

5.6 Relevance of MODFLOW Research to Further Scientific Investigations

The results of a MODFLOW simulation (i.e., an array of head values in space and time) can be used to calculate flows in various parts of the simulated groundwater regime, or to estimate discharge into rivers, wells, lakes or any surface feature. ZONEBUDGET (Harbaugh, 1990) is a MODFLOW post-processing program which provides a convenient approach to such calculations, in that it uses MODFLOW output to generate water budgets for user-defined subregions of the modeled area. Similarly, post processing programs such as 3-D particle tracking (MODPATH) developed by Pollock (1994 and 2012), and MODFLOW-compatible transport codes such as MT3DMS developed by Zheng (1990), Zheng and others (2001), Zheng and Wang (1999), Zhang and others (2010), and Zheng (2010) can be used in contaminant transport and particle transport studies. These models utilize the output of the MODFLOW model, reducing the need for transport model database preparation. The relevance of the proposed research at the JPL catchment to further scientific investigations will be achieved through three goals. First, the techniques developed in this investigation can be useful in investigations of the hydrologic effects of land-use change in other areas of North Texas. Second, the models developed in this research will provide the flow simulation capability required for future development of a solute transport model to investigate pollutant movement in the shallow groundwater regime around JPL. Third, the results of this investigation will provide insights on lake-groundwater interaction applicable to other lakes in North Texas.

5.7 General Model Characteristics and Simulation Approach

As discussed in Chapter 1, the immediate goals of simulation were to define the distributions and rates of recharge to/and discharge from the groundwater regime, and to estimate the directions and rates

of groundwater flow throughout the system, both under present conditions and prior to lake impoundment. Two steady-state finite-difference simulations of the groundwater flow regime in the alluvium were undertaken, corresponding to present-day and pre-lake conditions, respectively. The simulated area covered the JPL catchment, as shown in Figure 1-1. The division of the project area into rectangular cells, as shown in Figure 3-1 and as used as the basis for processing and interpreting GIS information (Sections 3-2 and 3.3 to 3.7), was also used as the horizontal discretization scheme in simulation. In terms of vertical discretization, the models consisted of two layers: an upper layer, designated Layer 1, represented the alluvial aquifer, and contained all the cells for which numerical solution of the flow equation was carried out; a lower layer, designated Layer 2, represented the Woodbine Aquifer. All hydraulic characteristics of the lower layer were considered fixed and constant in the simulation process, so that Layer 2 functioned in simulation only as a fixed-condition boundary layer for the actively-simulated upper layer. The fixed heads of the lower layer were taken from NTW-GAM (Bene and others, 2004; 2007; Kelly and others, 2014). As noted in Sections 5.2, 5.3, and 5.4, simulation was carried out using the MODFLOW software developed by USGS, and the results were interpreted with the help of related post-processing software, particularly the USGS program ZONEBUDGET (Harbaugh, 1990). GIS technology was used extensively to facilitate model input and to assist the interpretation of simulation results.

In both the present-day and pre-lake simulations, the model boundary followed the topographic divides defining the present catchment of JPL, and the results were taken to represent average annual conditions. Actual inflows and outflows for the simulation representing present conditions (also referred to as the post-lake or present-day simulation) were developed from data collected in the year 2010; those for the simulations representing pre-lake condition (also referred to as the 1981 simulation) were developed from data collected during the year 1981, or applicable to that year. Taking the model boundaries along the topographic divides defining the JPL catchment introduced the assumption that a groundwater divide exists also along this boundary, and has not migrated in response to construction of the lake or other changes in hydrologic controls.

The EFS was represented in simulation using the Quasi-Three-Dimensional (Quasi-3D) approach (Harbaugh, 2005, Pg.5-8). In this method, it is assumed that the EFS makes no significant contribution to

the horizontal hydraulic conductivity of either Layer 1 or Layer 2, and that its only effect is to reduce the total vertical hydraulic conductivity between those layers. Thus, wherever the EFS is present, the equivalent vertical hydraulic conductance of the interval between Layers 1 and 2 in that cell is reduced to reflect the low vertical hydraulic conductivity of the EFS.

Because the goal of simulation in this research was defining and understanding of the system, calibration and application of the model were essentially a single and virtually continuous exercise. The data on hydraulic head, or water level above datum, applicable to either the 1981 or 2010 simulation, are extremely sparse and generally of poor quality. The difficulties arising from these conditions, and the steps taken in calibration to compensate for them, are discussed in some detail in Section 5.8.

5.7.1 General Characterization and Discretization

The horizontal discretization of the finite-difference mesh follows the pattern used for the collection and processing of data, as shown in Figure 3-1, and incorporates 11,270 square (1,000 feet. x 1,000 feet.) cells in 98 columns and 115 rows. Of these 11,270 cells, 4,777 fall outside the JPL watershed boundary. These cells are treated as inactive and take no part in the simulation. The remaining 6,493 cells lie on or within the JPL watershed boundary and are designated as active cells to take full part in the simulations. The vertical discretization includes two layers, the upper layer representing the shallow aquifer, and the lower the Woodbine Aquifer, as shown in Figure 5-3. However, the hydraulic characteristics and the hydraulic heads of the Woodbine Aquifer are well known based on extensive prior work and simulation of that aquifer. The model cells in this layer are therefore all treated as specified-head cells in the simulations reported here. These cells retain assigned head values throughout the iteration process, consistent with published data on the Woodbine water level. Thus, the cells of the lower layer (Layer 2) serve only as boundary cells (or boundary conditions) for the solution process in the upper layer, supplying flow to or from the upper layer in response to the difference between the calculated heads of the upper layer (Layer 1) and the fixed heads of the lower layer.

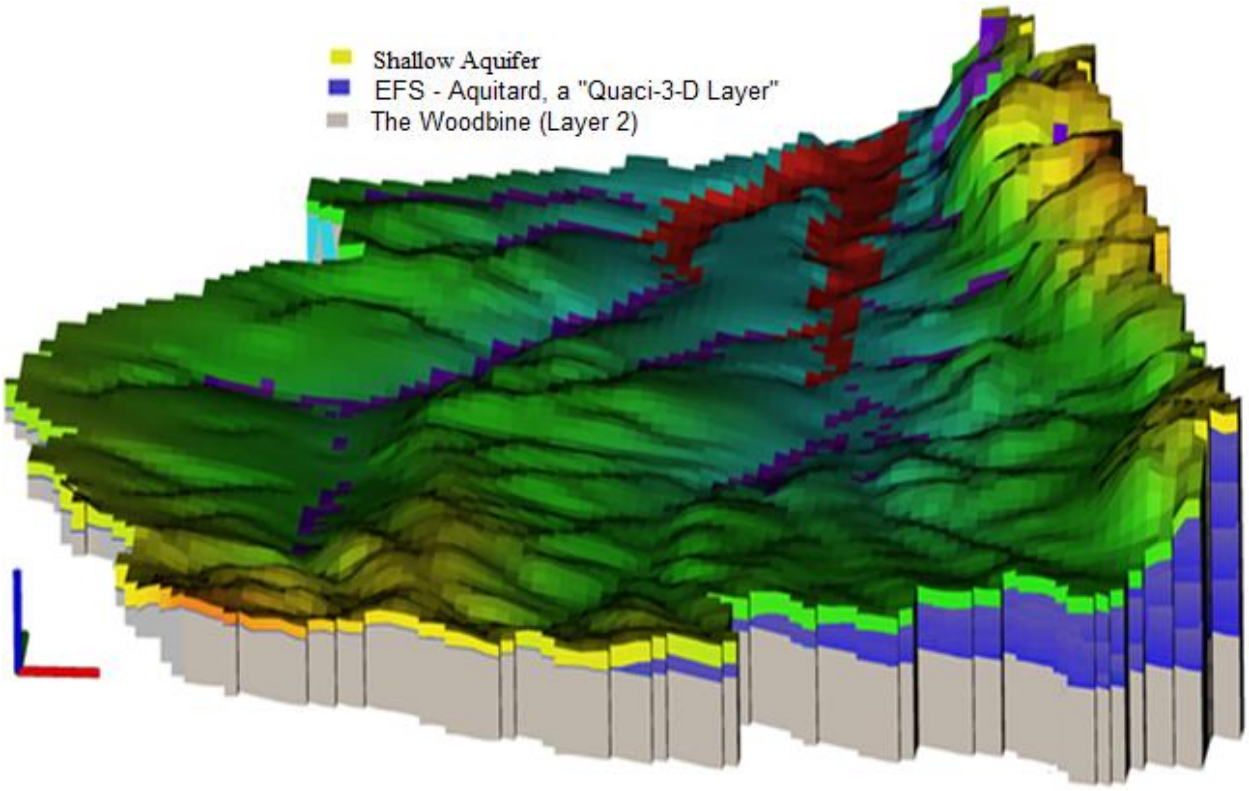

Figure 5-3 The vertical discretization of the JPL model; (Diagram is not to the Scale)

Two steady-state simulations were carried out, the first representing the condition of the flow regime in 2010, by the post lake time it was assumed to be in equilibrium with the present lake elevations (522 feet msl) , and the second representing the condition of the flow regime in 1981, prior to construction of JPL dam. The model as used in first case is variously referred to in this document as the present-day model, the post-lake model or the 2010 model; the model as used in the second case is referred to as the pre-lake or 1981 model, the latter term indicating that the precipitation, ET, and population data were collected in or are applicable to 1981.

5.7.2 Model Boundary Conditions

The version of MODFLOW used in the simulations solves the partial differential equation for three-dimensional groundwater flow under steady-state conditions (Equation 5-2), which differs from the general equation for transient conditions only in that the time derivative of head is always zero. This

assumption implies that accumulation or release of water in aquifer storage does not occur, so that terms involving storage do not appear in the equation. A no-flow boundary condition, assumed applicable to both the pre-lake and present-day simulations, exists around the outer perimeter of the model, i.e., following the topographic divide enclosing the JPL catchment, and following a line across the northern boundary of the study area, immediately north of the JPL dam. The condition on the topographic divide introduces the assumption that a groundwater divide coincides with the surface water divide surrounding the catchment, and remains undisturbed by hydrologic change within the catchment. The condition on the northern boundary is based on the findings of the USACE pre-impoundment investigations, which showed material of low permeability in this area (see Table 2-1). As discussed above, the second layer of the model is in effect a boundary layer for the solution of the upper layer, since all heads in the second layer are specified and unchanging. Other features which may be considered boundary conditions in a formal sense are embedded in the solution process as source-sink terms in the simulated equations (Equations 5-1 and 5-2). Examples include recharge, the lake itself, represented as a head-dependent boundary through the MODFLOW-GHB Package, the perennial reaches of streams, represented as head-dependent boundaries through the MODFLOW River (RIV) Package, and near-surface discharge processes, represented through the MOFFLOW Evapotranspiration Package (EVT). The Woodbine Group strata is the lower boundary of the model and in effect represents an approximation to the full bedrock sequence below the shallow aquifer, in that there is no simulated flow between the Woodbine Aquifer and deeper aquifers.

5.7.3 Representation of Land Surface

One of the first steps in model development was to impose a representation of the land surface elevation on the model mesh of Figure 3-1. This assumption is required for estimating an average land surface elevation for each 1,000 feet x 1,000 feet cell of the mesh. The actual topography of the project area varies on a much finer scale than this, and is available as a GIS file through USGS Digital Elevation Model (DEM) data. An average land surface elevation for each cell, weighted by the areas of the individual land parcels making up that cell, was calculated using GIS tools. The result can be visualized

as a stepwise assembly of flat planes, each 1,000 feet x 1,000 feet in area, and each having an elevation which is an area-weighted average of the actual topographic elevation in the area it represents. Land surface elevations enter the simulation process in several ways, and the fact that the model is characterized by these flat-plane areas, therefore affects the simulation in several ways.

5.7.4 Representation of the Base of the Shallow Aquifer

Information on the base of the alluvium was compiled from lithological logs of wells in the records of the Texas Water Development Board (TWDB), the logs of test borings for road construction, bridge construction, and overhead water tank construction as obtained from the cities, and the JPL dam construction records obtained from the USACE. Significant numbers of test boring logs were also obtained from the Texas Department of Transportation (TxDOT) and used for both the delineation of the depth of the shallow alluvium, and for water table information in model calibration.

However, preliminary versions of the JPL model in which the thickness of the upper layer of the model was fixed, and was based exclusively on information derived from the well logs, gave poor agreement with field data regarding both flow and water level. Model-calculated groundwater discharge into streams failed to agree even approximately with estimates derived from baseflow analyses of WC gage records, and model-calculated water levels were incompatible with the topography of the catchment. Increasing the thickness of the upper layer gave improved agreement in both cases. These results supported the interpretation that the shallow aquifer is not limited to the alluvium alone, but rather include a zone of fractured and weathered consolidated rock below the bedrock surface. New base elevations of Layer 1, corresponding to the revised aquifer thickness concept, were therefore adopted, and were retained through all later phases of model development; Figure 5-4 gives an approximate representation of the resulting base elevation of Layer 1, as represented in the simulations. It should be kept in mind that the base elevations in the model, like the land surface elevations discussed above, each apply uniformly over the area of a model cell, and that the thickness of flow in cell (i,j) of Layer 1, in the final unconfined form of the model, is calculated as H(i,j) – BOT(i,j), where H(i,j) is the model-calculated water level in the cell, and BOT(i,j) is the elevation of the base of Layer 1 in that cell. In actual simulation practice these

elevations make a step wise flat surface of 1,000 feet x 1,000 feet cells.

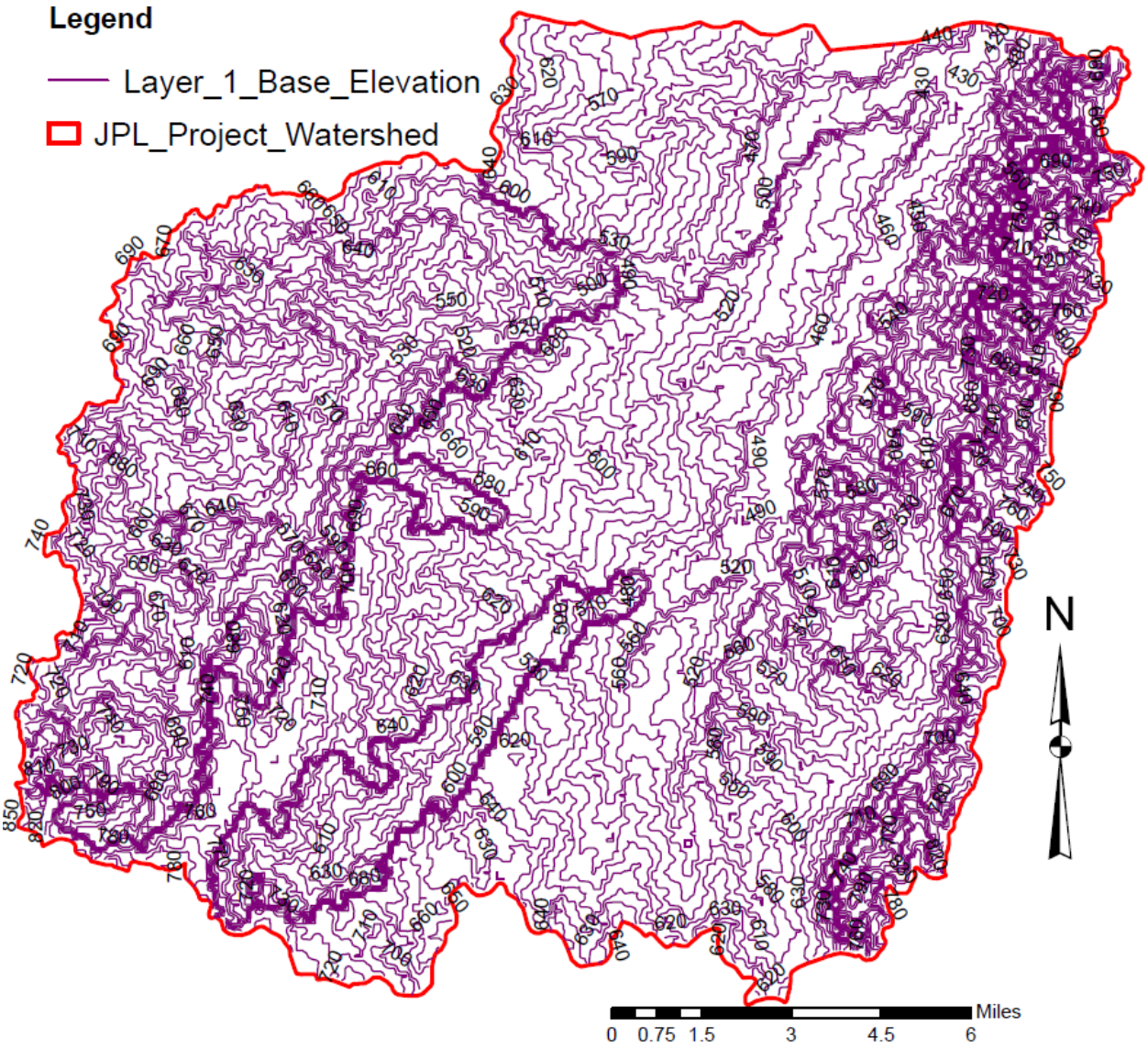

Figure 5-4 An approximate representation of the Layer 1 base elevation of the shallow groundwater aquifer of JPL groundwater simulation

5.7.5 Simulation of Near-surface Discharge Processes

The processes of (1) direct evapotranspiraton from the water table (or from the capillary fringe above the water table) and (2) discharge of groundwater into networks of unmapped shallow drains or ditches, from which it then flows into the stream system, have been discussed in Section 5.1 (Figure 5-1).

These two processes are functionally similar, in that each operates only when the water table is within a few feet of land surface, and the total discharge provided by each increases as the water table rises, reaching a maximum as the water table reaches land surface. For the purposes of this research, the MODFLOW Evapotranspiration (EVT) Package was used to simulate the joint effect of these two processes, as discussed in Section 5.1. This assumption represents a limitation of the simulation techniques used in this study; that limitation was accepted in recognition of the fact that the field data needed to utilize the greater resolving power of a more sophisticated simulation technique were not available, and could not be acquired within the time and funding constraints of the project. Thus, in evaluating the results of the MODFLOW EVT Package as used in this study, it should be kept in mind that the calculated ET outflow from the aquifer (or from any zone within it) represents the sum of two components. One of these is a small part of the total ET outflow, whereas the other represents a contribution to the total discharge from JPL itself, in that all drainage in the stream system (including unmapped drainage) ultimately reaches the lake.

5.7.6 Simulation of Unconfined Conditions

Simulations were carried out for both the present-day condition, including the lake, and for the pre-lake condition. The shallow aquifer is unconfined, except in the areas directly underlying the lake. This implies that in the pre-lake simulations, and in all areas of the present-day simulations except those covered by the lake itself, the upper surface of the model (i.e., the upper surface of the flow regime in Layer 1) should be the water table. Thus, the upper surface of the flow system is undetermined until the solution process is complete, i.e., until water table elevations are known throughout the system. Initial or trial values for water table elevation must therefore be specified in order to begin the iterative solution process. In both the pre-lake and present day simulations, the land surface elevations, approximated as discussed above in each model cell, were taken as the initial values for the top of the flow regime in all areas of Layer 1, except beneath the lake itself in the present-day simulations. Ideally, during the iteration process, in each cell should then be taken as [H(i,j) – BOT(i,j)], where now H(i,j) refers to the water table

elevation in cell (i,j) as calculated in the current step of the iteration, and again BOT(i,j) refers to the elevation of the bottom of that cell.

MODFLOW offers an unconfined or water-table option which implements this approach to the issues arising in simulating a model layer where unconfined conditions prevail. In the simplest form of this option, starting water table elevations in iterations after the first are set equal to the final calculated values from the preceding iteration. However, using this approach can lead to numerical oscillations or other problems in the solution process (McDonald and Harbaugh, 1988), and these problems, in fact, proved to be the case in the JPL model. To circumvent these difficulties, a “manual iteration” approach was ultimately used in the solution of both the pre-lake (1981) and the present day versions (2010) of the JPL model. In this approach, an initial simulation (or series of simulations) was first undertaken in which the top elevation of the flow regime in cell of Layer 1 was assumed to remain fixed at a value equal to the elevation of land surface in that cell. After a satisfactory solution for this condition had been obtained, a new series of simulations was undertaken. In the first simulation of this new series, the top elevation of the flow regime in each cell of Layer 1 was held constant at the water level value determined for that cell in the final solution of the preceding series. In subsequent simulations of this new series, the top elevation of the flow regime (and hence the thickness of flow) was again held constant in all cells, but now always, in each cell, at the final water level calculated for that cell in the preceding simulation of the series. In effect this procedure mimicked that of the MODFLOW unconfined option, except that the change to a new thickness of flow occurred at the end of a full solution, rather than at the end of an individual iteration within a solution, and incorporated the water table determined in the preceding solution, rather than that at the end of the preceding iteration. Thus, the simulations in this research involved first, a fixed-thickness series which was then followed by a variable flow-thickness series.

In the present-day model, after a number of simulations in the new series, the calculated water table elevations obtained in successive steps of the process ceased changing, indicating that the “manual iteration” process had converged, and that the thickness of the flow regime was now correctly represented as H(i,j) – BOT(i,j) in all cells. Unfortunately, this process did not happen in the case of the pre-lake model, indicating that for the pre-lake condition, the numerical problems continued. The

simulated result for the pre-lake model is therefore an approximation, obtained through the assumption of a fixed aquifer thickness, given at all cells by the expression LSD(i,j) – BOT(i,j), where LSD(i,j) is the average land surface elevation (the top elevation) in cell (i,j) of Layer 1. The hydrologic conditions in the catchment prior to lake construction would probably have favored a water table very close to land surface, so the approximation is probably satisfactory.

5.7.7 Representation of JPL in Simulation

Using the lake bathymetry map (Lake Products LLC, 2003.), a map of lake-bottom elevation was generated. The lake was then represented in the present-day model by imposing a head-dependent boundary on the lake bottom surface, using the MODFLOW General Head Boundary (GHB) Package, and taking as the source head as the mean conservation pool level of the JPL. The mean conservation pool level of JPL is 522 feet msl. The lakebed material was assumed to be 10 feet in thickness and to have a hydraulic conductivity of 0.25 feet/day. The conductance term of the GHB package in each cell thus represented the conductance of a square block of lakebed material, 1,000 feet on each side, and 10 feet thick. The effect of this boundary condition was to hold the water level in cells beneath the lake very close to the mean lake level, throughout the present-day simulations, the water level in these cells never fell below the top of the cell, and the issue of thickness of the flow regime did not arise in the area beneath the lake.

The top of Layer 1 in the area beneath the lake was always the lake bottom, and the thickness of flow was always the difference in elevation between the lake bottom and the bottom of Layer 1. In the pre-lake (1981) simulations, the GHB boundary condition was removed, and the elevation of land surface prior to lake construction in the area now occupied by the lake was taken as the starting value of the upper surface elevation of Layer 1. The bathymetry map of the JPL is as illustrated in Figure 5-5. There are 305 cells inside the lake represented as GHB cells. The selections of the GHB cells were based on the standard assumption that if the area represented by the cell was equal to or more than 50% occupied by the lake, the cell was considered a lake cell and modeled as GHB.

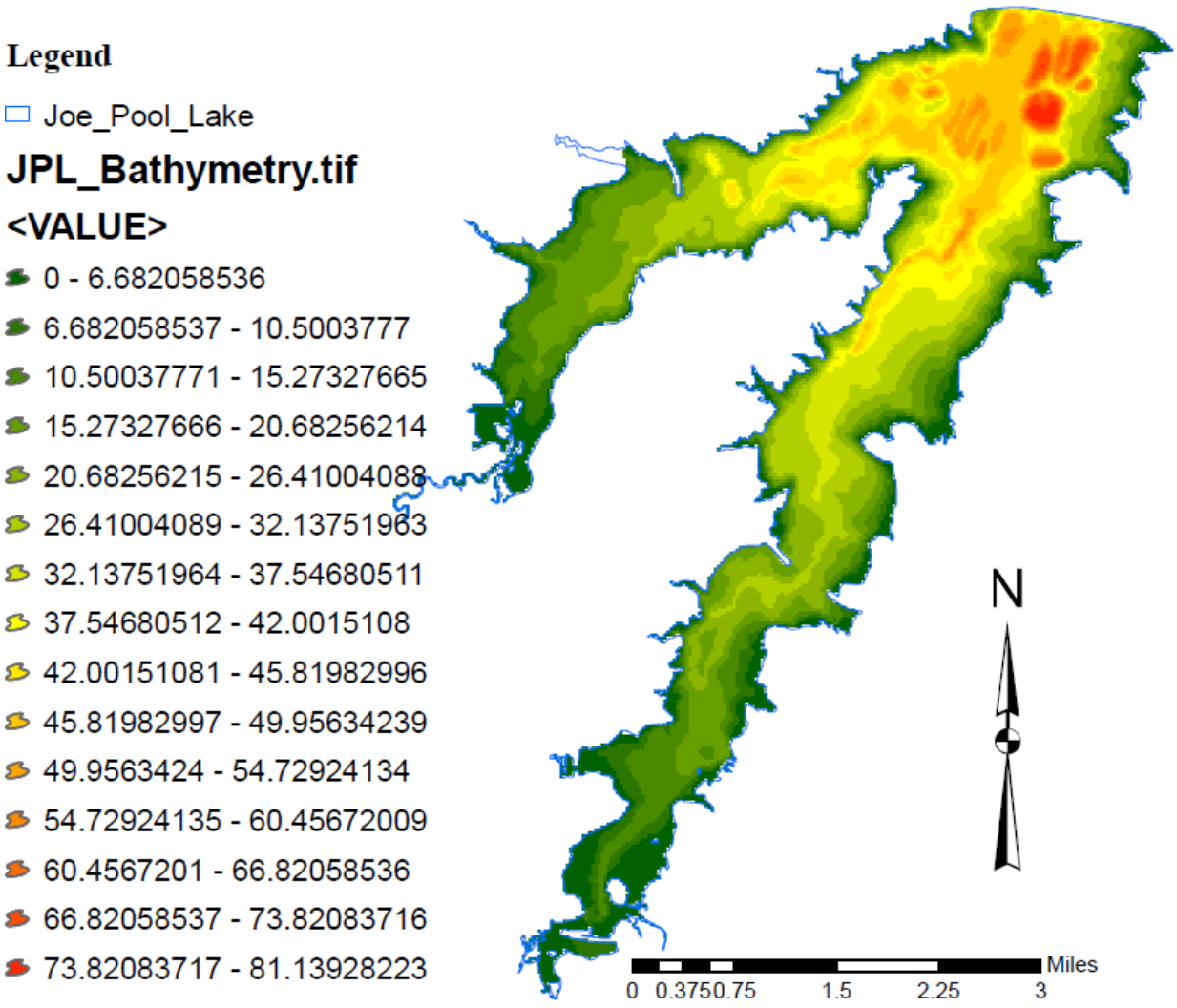

Figure 5-5 The JPL bathymetric map as represented on the model

5.7.8 Representation of Flow between the Shallow Aquifer and Stream System

Flow between the shallow aquifer and perennial reaches of the stream system was simulated using the MOFLOW River (RIV) Package, with the stream conductance at each cell crossed by a perennial stream reach estimated initially as KLW/b, where K represents the hydraulic conductivity of the streambed material taken as 0.25 feet/day, L the length of the stream reach within the cell, W the stream width, and b the thickness of the streambed material. The streambed conductance values were varied in calibration in recognition of the fact that the factor K/b in this term is generally unknown. In this process,

the difference between the net model-calculated flow into the stream system upstream of the WC gage was compared to the baseflow of WC as estimated from the analyses of the gage records. Increasing the stream conductance made little difference in the results; decreasing it increased the difference between model-calculated inflow and estimated baseflow. These results suggest that the hydraulic characteristics of the aquifer itself, rather the streambed conductance, were primarily responsible for controlling the flow between the aquifer and the stream system. The detailed description about the concept of conductance and mathematical procedure to estimate its value and equivalent conductance in a model cell, river cell, lake cells, and half-way between the cells during the development of the finite-difference approximations using the concept of conductance in series and conductance in parallel arrangement is given in Appendix B (see Figures B-1 and B-2).

5.7.9 Representation of Bedrock Aquitards Separating the Shallow Aquifer (Layer1) and the Woodbine Aquifer (Layer 2)

As noted previously, the quasi-three-dimensional (quasi-3D) approach was used to simulate the effects of low-permeability bedrock separating the shallow aquifer from the Woodbine Aquifer (Harbaugh, 2005, Pg.5-8). In this approach, the vertical hydraulic conductance of the material separating the two aquifers is reduced where the EFS is present, but no change is made in horizontal conductance, in effect introducing the assumption that the lower-permeability rock has a significant influence on vertical flow, but very little effect on horizontal flow. In the western part of the JPL model area, i.e., the area in which the EFS is missing, the equivalent vertical conductance of the interval separating the two aquifers was calculated simply as a harmonic mean of that aquifer and taking the lower half of the shallow aquifer and that for the upper half of the Woodbine Aquifer. In the central part of the study area, where the EFS overlies the Woodbine Group strata, the equivalent vertical conductance was progressively reduced toward the southeast, in proportion to the increasing thickness of the EFS. In the eastern part of the study area, the interval separating the two aquifers includes both the full thickness of the EFS and a small but southeastward-increasing thickness of the Austin Chalk. In theory, an additional term should have been included in the calculation to account for the effect of the Austin Chalk in this area. However, trial

calculation showed that the effect would be negligible in comparison to the effect of the EFS; thus, the vertical conductance in this area was left constant at the value corresponding to the full thickness of the EFS.

5.8 Model Calibration

Model calibration task was constrained by the lack of available data on water levels in the shallow aquifer. Data on the hydraulic head, or water level elevation above datum are extremely sparse and generally of poor quality, both for the present-day and the pre-lake condition. Most wells in the project area are open either only to bedrock aquifers, or to both bedrock aquifers and the alluvium. In either case, the recorded water level in the well reflects primarily the water level(s) in the bedrock zones, which is typically lower than the bottom elevation of the alluvium itself, and cannot be taken as an indication of the water level in the shallow aquifer. The records of the Texas Water Development Board (TWDB) has a list of only 17 water wells in the in the project area opened to the alluvium alone. For each of these only one water level is provided, in most cases they were made at the time of completion by the driller; moreover, there is considerable uncertainty in each case regarding the elevation of the measuring point. A limited amount of shallow water level data is available from records of test borings made prior to the construction of roads, bridges or buildings in the project area. However, a confidence in these measurements is often limited by incomplete information on measuring point elevation, or by uncertainty as to whether the water encountered in the hole actually represents the water table, or a very local “perched” zone of saturation above the water table. Piezometers installed in connection with the construction of JPL itself generally provide a continuous and very reliable water table measurements, but are concentrated in the immediate vicinity (area) of the lake itself, and are therefore of limited use for overall model calibration. These piezometer observations (data) are highly influenced by the normal pool elevation of the lake. No synoptic water table measurements made essentially at one time, and covering the full model area, are available.

Given these limitations, and lacking the resources for an extensive program of test drilling or other field investigation, it was decided to supplement the calibration process by checking each calculated head array of the initial or fixed-thickness simulation process, to verify that (1) the model-calculated

outflow from the aquifer to the stream system, per unit land surface area, was of the same order as the average baseflow per unit land surface area, as calculated for the WC gage catchment using PART; and (2) the computed water level array constituted a “subdued image of the topography”, i.e., the calculated head array followed the expected relation to the topographic surface. Hubbert (1940), in his classic paper “Theory of Groundwater Motion” showed that in a region characterized by gaining streams, the water table should be a subdued image of the topography. Hubbert’s analysis also showed that groundwater levels in the vicinity of near-surface discharge features (such as streams and springs) in an unconfined aquifer, must increase with depth below land surface, and must be higher than the land surface elevation at the discharge feature, or outflow to the stream system is impossible. Haitjema and Mitchell-Bruker (2005) analyzed the conditions under which the water table can be expected to represent a subdued image of the topography, and point out that low permeability and anisotropy favor the condition. Barker and Braun (2000) confirm that the water table immediately north of the JPL study area is in fact a subdued image of the topography. It follows that for a calculated head array to represent a solution applicable to the groundwater system in the JPL catchment, most of the calculated water levels should fall between land surface and the base of the shallow aquifer, but at least some, in the vicinity of perennial stream reaches or the lake itself, should be above land surface. In addition, the fact that local dry conditions are often reported in the shallow aquifer implies that at least some calculated water levels can be expected to fall below the base of the aquifer in a reasonable solution.

Based on these considerations, each completed model run of the fixed-thickness series was first tested to determine whether the model-calculated flow from the aquifer into the stream system, per unit land surface area, was of the same order as the baseflow per unit land surface area as calculated for the WC gage using PART. If the agreement was not satisfactory, the recharge distribution used for the run was modified and a new run was made. In all cases, the initial recharge distribution was taken as the applicable (pre-impoundment or present-day) distribution of net applied water (see Sections 3.6 and 3.7 in Chapter 3). Successive changes in recharge were made by multiplying each term in the prior recharge distribution by a common factor, so as to preserve the relative magnitudes of the applied water

distribution by changing the total recharge value. This means the MODFLOW model calculated river outflow must be comparable with the observed JPL baseflow value.

If or when a satisfactory flow comparison was achieved, a second test was applied (in this case directly to the calculated head array) to determine the combined fraction of the calculated water levels falling either above land surface or below the base of the aquifer. Simulations for which this fraction exceeded 0.25 were rejected. Those data for which the combined fraction fell within the 0.0 to 0.25 range were retained.

The calibration exercise involved comparing the measured water levels in shallow boreholes, each an exploratory hole drilled in connection with construction of a building, road, bridge, or the JPL dam itself, with calculated water levels at the corresponding locations. For the pre-lake simulations 22 such wells were available, whereas for the present-day simulations, 14 were available. Hydraulic conductivity values were modified within the range of field test results reported from the investigations at NASD, NWIRP and the proposed SSC area. No effort was made to reduce the residual (observed minus calculated water level) at a single observation point through adjustment of the hydraulic conductivity (see Figure 5-6) or recharge in the cell containing that point; rather, adjustments were made on an aerial basis to reduce the mean residual of all observations to a value as near zero as possible. The runs that gave acceptable residual values were subjected to a final series of tests, in which all values of horizontal hydraulic conductivity and all values of recharge were multiplied by a common factor, a new simulation was carried out, new residuals were calculated, the factor was changed, and the process repeated. This procedure was done to offset the tendency, common among steady state problems, for solutions having similar ratios of conductivity to flow to produce equivalent calibrations. The optimal fixed-thickness solution was taken as that yielding the mean residual value closest to zero.

The optimal “fixed flow-thickness” solution was then subjected to the manual iteration procedure described in Section 5.7.6 to determine the effect of variable flow-thickness on the result. For the post–lake condition, this procedure was followed until the manual iteration had converged to a variable flow-thickness result. The head array representing this result was then subjected to the three calibration tests described above (baseflow-matching, expected relation of heads to topography, and calibration head-

matching) and adjusted as necessary until an optimum solution corresponding to the variable thickness or unconfined condition had been obtained. At that point, the procedure of multiplication of conductivities and recharge by a common factor, as described above for the fixed flow-thickness simulation, was repeated and the optimal solution was taken as that yielding a mean residual closest to zero. As discussed in Section 5.7.6, the convergence was not achieved for the pre-lake case and the results for that case are therefore an approximation based on the fixed thickness simulation.

Figure.5-6 shows the hydraulic conductivity of the shallow aquifer used in the optimum run of the MODFLOW model for the pre-lake and post-lake conditions. As described earlier in this section the hydraulic conductivity was never changed to fit the model nor changed in areas of interest. As shown in Figure 5-6, the horizontal hydraulic conductivity of shallow aquifer in Layer 1, ranged from 3.0 to 9.39 feet/day.

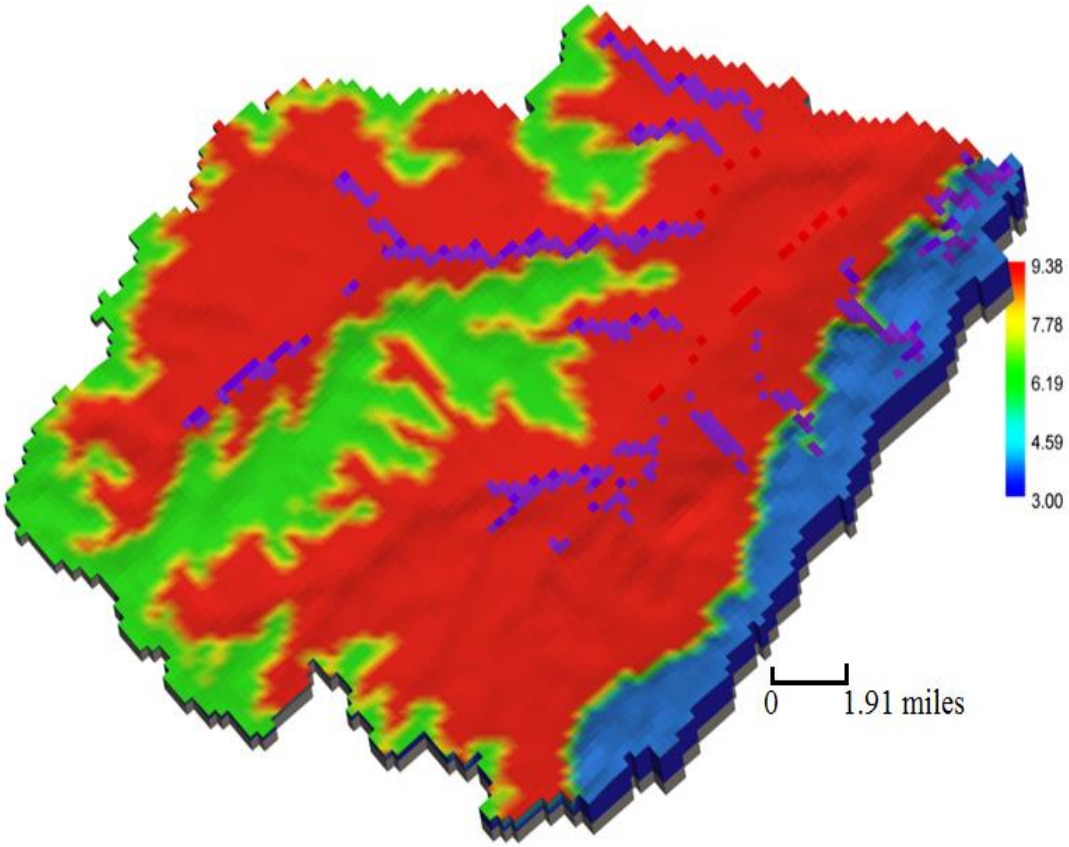

Figure 5-6 The horizontal hydraulic conductivity of shallow aquifer used in optimum simulations in pre-lake and post-lake conditions

Chapter 6

Results and Discussion

6.1 Introduction

The results of the finite-difference groundwater flow simulations and their implications for changes in the hydrology of the JPL catchment are summarized in this chapter. The results of the simulations include calculated water levels and calculated distributions of groundwater flow. Groundwater flow values are summarized as integrated totals in the output of each simulation, but internal flows between individual areas of the mesh can also be calculated by using the ZONEBUDGET post-processor, as discussed in Chapter 5. Data for the year 1981 were used to represent pre-lake conditions in the MODFLOW simulations, whereas data for the year 2010 were used to represent post-lake conditions.

Contours of calculated water level for the post-lake simulation are shown in Figure 6-1, whereas contours of calculated water level for the pre-lake simulation are shown in Figure 6-2. Figure 6-3 shows contours of the difference in calculated water level between these two simulations. Integrated or model-wide flow values for the two simulations are summarized in Table 6-1; Table 6-2 summarizes the vertical exchange of flow from the Woodbine Aquifer and the shallow aquifer in the pre-lake and post-lake conditions. Table 6-3 compares the saturated volumes of the shallow aquifer, as calculated from the results of these two simulations, and also compares the number of cells, in each simulation, for which outflow through near-surface discharge processes was calculated.

A number of calculations relating to the results of the two simulations were made using the ZONEBUDGET postprocessor. Tables 6-4 and 6-5 and Figures 6-5 through 6-8 refer to the results of these ZONEBUDGET calculations. Figure 6-4 shows a map of the zones defined in the shallow aquifer. Tables summarizing the flows between individual zones are presented in Tables S-1 and S-2 in the Supplemental Section. Table 6-4 shows inflow and outflow between each zone and the external source/sink mechanisms as calculated by the pre-lake model. Similarly, Table 6-5 shows inflow and outflow between each zone and external source/sink mechanisms as calculated by the post-lake model.

Subsequent to the discussion of model results, generalized hydrologic budgets for the JPL catchment are presented for the pre-lake and post-lake conditions. These general budgets are based on

field data, **not** on simulation results. Pre-lake period (1981, see Table 6-6) field data consists of precipitation, NLDAS ET, and runoff based on extrapolation of the WC gage results over the full JPL catchment area. For the post-lake (2010, see Table 6-7) budget, the data consists of precipitation, NLDAS ET, population-based water use, estimated runoff based on JPL gated flow, reported flow through the MCRWS treatment plant (which was assumed to represent imported water), lake evaporation (see Figure C-7 in Appendix C), and Midlothian withdrawal from the JPL. These budgets are included to illustrate both the strength and weakness in overall hydrologic data in the catchment. They are intended to show overall hydrologic implications rather than those focused on groundwater alone.

Subsequent to the discussions of model results, generalized hydrologic budgets (groundwater and surface water) for the JPL catchment are presented for the pre-lake and post-lake conditions. These general budgets are approximate; the pre-lake budget is based on 1981 data, whereas the post-lake is again based on 2010 data. They are intended to show overall hydrologic implications rather than those focused on groundwater alone. The results of the simulations were used as general guidelines in developing and interpreting these general budgets.

6.2 Head Distribution Results of Pre-lake and Post-lake Models

The final calculated heads as given in the model output are shown in Figures 6.1 and 6.2 for the post-lake and pre-lake conditions, respectively. As discussed in Chapter 5, and following Hubbert (1940) and Haitjema and Mitchell-Bruker (2005), some of the calculated heads are expected to be above the land-surface, whereas some are expected to be below the bottom of the simulated layer; and this case was in fact true in both final simulated head distributions. However, in constructing Figures 6-1 and 6-2, only heads falling within the saturated thickness of the aquifer were contoured. Both of these head distributions represent subdued images of the topography, although near the lake area the topography itself varies between the two cases. The area of the lake in Figure 6-1 appears as the Mountain Creek-Walnut Creek valley in the pre-lake water table; for both pre-lake and present day conditions, the water level elevations in that area indicate groundwater discharge; i.e., the lake in the present-day results and the stream valley in the 1981 result, function as groundwater discharge features.

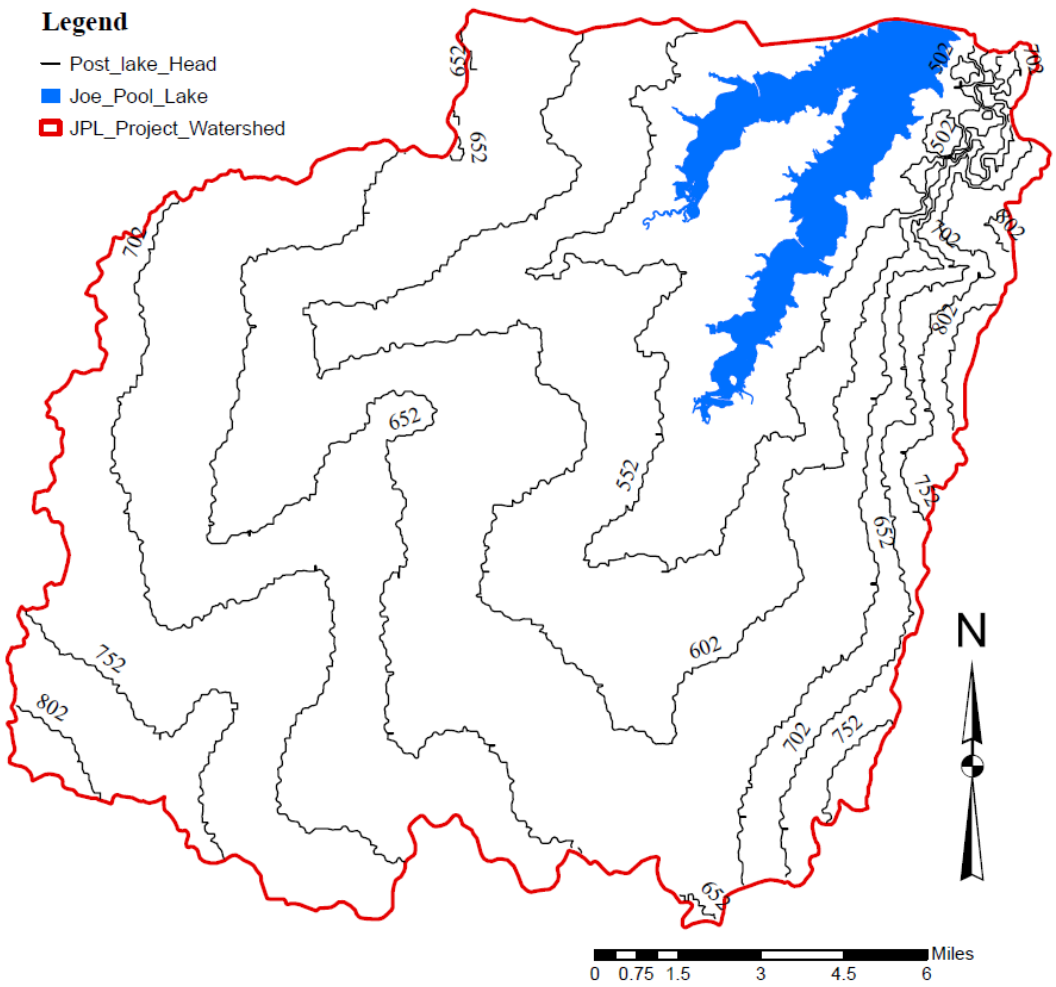

Figure 6-1 Simulated post-lake head distribution of shallow aquifer in JPL catchment

Figure 6-3 shows contours of the change in water level between pre-impoundment and present-day conditions. Note that although the differences are positive (present-day heads are greater than the pre-impoundment heads) close to the lake, several other areas show negative change (present day water levels are lower than the pre-impoundment levels). The overall results in terms of water levels is suggested by Table 6-3, which compares the volume of saturated aquifer as calculated from the simulated water table elevations and the number of cells in each case from which near surface discharge processes are operative.

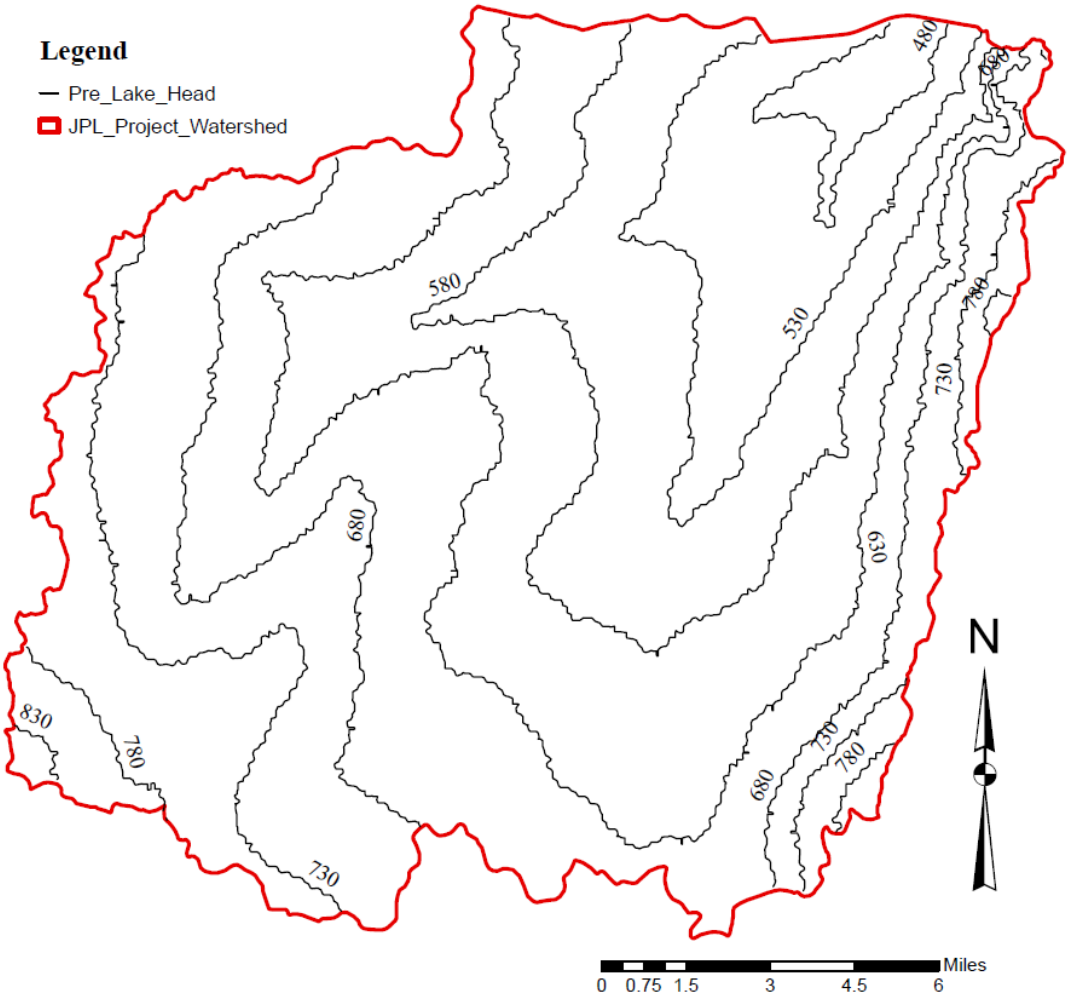

Figure 6-2 Simulated pre-lake head distribution of shallow aquifer in JPL catchment

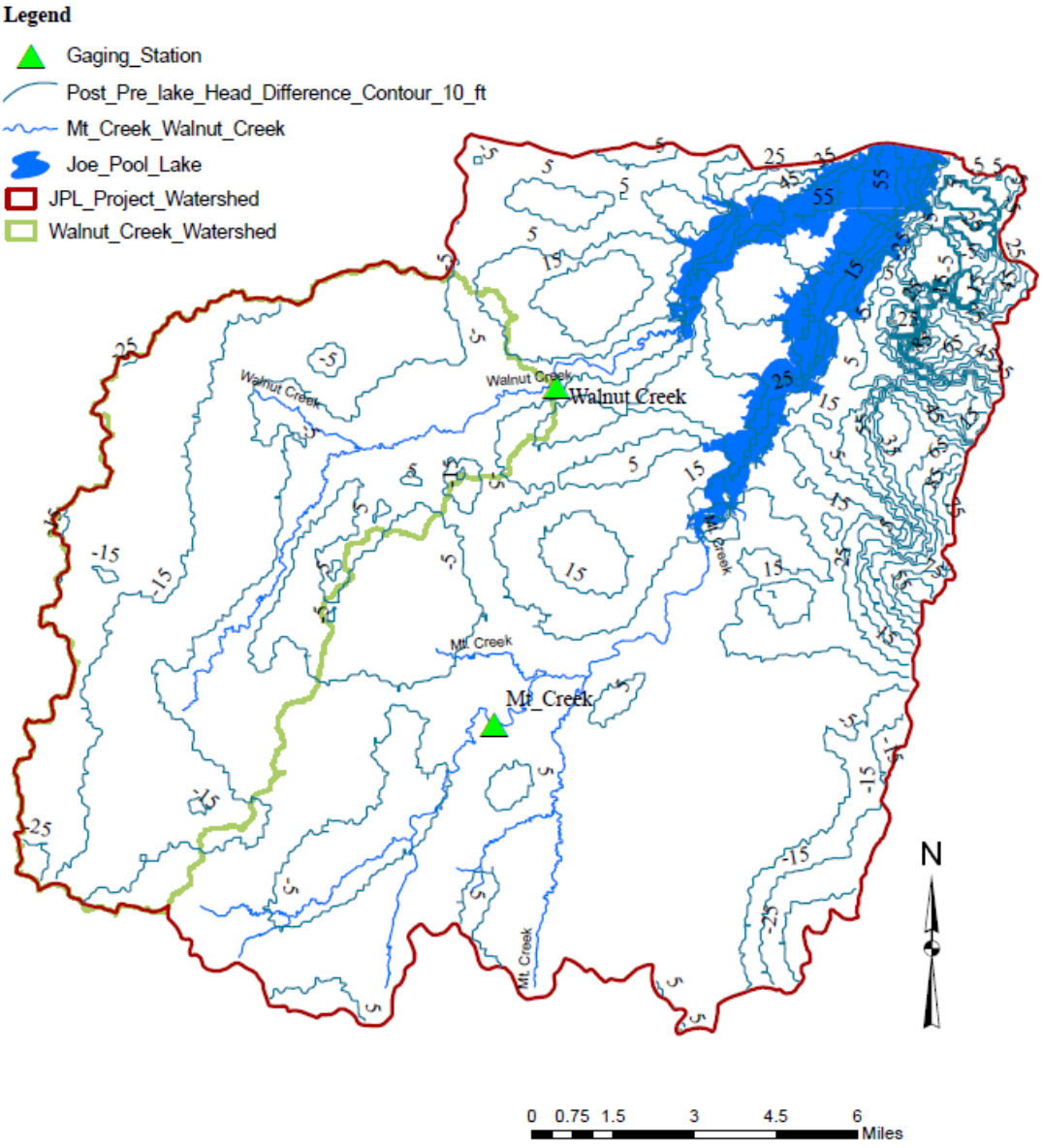

Figure 6-3 The head difference between the post-lake and pre-lake conditions of shallow aquifer

The primary mechanisms for discharge of water from the aquifer in both the pre-lake and post-lake simulations are (1) near-surface discharge processes, and (2) discharge into the stream system. The near-surface discharge processes, again, include flow from the aquifer into unmapped small drainage features, and direct ET loss from the water table. Together, they discharge approximately 1.70xE+06 CFD during the pre-lake period, and about 2.30 x E+06 CFD during the post-lake period. Discharge to the

perennial reaches of streams accounts for about 2.7xE+06 CFD in the pre-lake period and about 1.5xE+06 CFD in the post-lake period. In contrast, direct discharge to the lake accounts for only about 0.2xE+06 CFD in the present day model results (see Table 6-1). The GW head contours in Figure 6-1 show that relatively stable water level of the lake acts as a significant boundary condition in the shallow aquifer. This stability of JPL is in some contrast to conditions in other lakes in the area which have shown significant fluctuations in recent years. It is possible that this difference reflects the relatively limited use of JPL for water supply, in comparison to other lakes.

Overall, Figures 6-1, 6-2, and 6-3 indicate a significance hydrologic change in the vicinity of JPL and beyond. However, isolation of the hydrologic effect of JPL alone is complicated by the fact that the precipitation in 1981, which is characteristics of the pre-lake era (1979 to 1986) is more than 20% lower, than that for 2010, which in turn is closely representative of post-lake period. The catchment recharge determined through model calculation for the pre-lake period was approximately 4.28xE+06 CFD, whereas that obtained for the post-lake period was approximately 4.503xE+06 CFD, an increase of about 5%, compared to an increase of about 22% in precipitation. Thus, the difference in precipitation is much larger than the estimated difference in recharge, and uncertainties persist regarding the relative influences of precipitation and of the lake.

Table 6-1 The Groundwater Budget of the Pre-lake and Post-lake Final Simulations

Modeling Conditions	Flow between the Shallow Groundwater Aquifer and the Woodbine Aquifer (CHD)		Flow between Shallow Groundwater Aquifer and Perennial Stream Reaches (RIV)		Near-surface Discharge Processes	Recharge (RCH)	Flow between Shallow Groundwater Aquifer and Lake	
	Woodbine Aquifer to Shallow Aquifer, CFD	Shallow Aquifer to Woodbine Aquifer, CFD	Rivers to Shallow Aquifer, CFD	Shallow Aquifer to Rivers, CFD	Shallow Aquifer to Near-surface Flows (Gullies, Ditches, and Direct ET from Water Table), CFD	Surface Recharge, CFD	Lake to Shallow Aquifer, CFD	Shallow Aquifer to Lake, CFD
Pre-lake (1981)	1,518	872,741	1,014,360	2,712,121	1,710,803	4,281,327	-	-
Post-lake (2010)	1,355	753,383	320,194	1,543,257	2,347,695	4,503,152	201,50	199,568

6.3 Flow Distribution between JPL and the Shallow Groundwater Aquifer

Table 6-1 summarizes the model-wide groundwater budgets as calculated in the post-lake and pre-lake simulations. In each case, the largest inflow term is recharge which is 5% higher for the post-lake than for the pre-lake. In the pre-lake period, outflows were provided by near-surface discharge and downward flow into the Woodbine Aquifer. The total inflow was 5,297,205 CFD of which 4,281,327 CFD was recharge and 1,014,360 CFD was seepage. Discharge from the aquifer was provided by seepage into the river (40%), near-surface discharge processes (32%), the flow into the river reaches (51%) and discharge into the Woodbine Aquifer (16%). For the post-lake, the input was 4,844,851 CFD of which 4,503,152 was recharge. Of this inflow, approximately 50% was discharged by near-surface processes, approximately 31% was discharged by flow into perennial stream reaches, approximately 15% was discharged by downward seepage to the Woodbine Aquifer, and approximately 4% was discharged to the lake. The largest outflows are provided by direct a discharge from the aquifer to rivers, and by near-surface discharge processes, which reflect the increase in average water level. The downward flow to the Woodbine Aquifer is similar for the two cases.

The presence of the lake has raised the base level of the creeks from range of 470-500 feet msl to the present normal pool level of about 522 feet msl. The increased depth of surface water on the unconsolidated alluvium might lead one to assume that the flow under post-lake conditions would be primarily from the lake into the groundwater, but the simulation results do not support this conclusion. A calculation of the flow distribution can be made using ZONEBUDGET, the previously-discussed post-processor to MODFLOW. Figure 6-4 shows the subdivision of the shallow aquifer into 16 zones for use in the ZONEBUDGET calculations of this research. Zones 1-10 are directly below the bottom of the lake; Zones 14 and 12 together surround the lake; Zones 11, and 13 are zones in the shallow aquifer above the Woodbine Group strata and Austin Chalk subcrop areas, respectively. Note that the EFS subcrops beneath Zones 1-10, 15, 12, 14, and 16. Zone 16 is the dam cell zone. The Woodbine Aquifer, Layer 2, is represented as Zone 0 in MODFLOW. The arrows in Figures 6-5 and 6-6 represent inflow or outflow from the individual zones in CFD. ZONEBUDGET calculates the flow between adjacent zones, and between

each zone and various external source or sink mechanisms (Harbaugh, 1990). As discussed in Chapter 5, flow between the shallow aquifer and the lake was represented in the post-lake simulation by the MODFLOW GHB Package. In effect, ZONEBUDGET applies this package to individual zones in turn, calculating flow between each zone and the lake. The results of the ZONEBUDGET calculation are summarized in Tables 6-4, 6-5, S-1, and S-2 and visualized in Figures 6-5 and 6.6. Table 6-5 shows the results for the post-lake condition and indicates that the net flow between the lake and the aquifer is predominantly directed into the lake.

Figures 6-5 and 6-6 illustrate the exchange of horizontal flow between various zones of the shallow aquifer. In using Figure 6-6, it should be kept in mind that the arrows directed towards the lake actually refer to horizontal flow into the area of Layer 1 beneath the bottom of lake, rather than to flow into the lake itself. Flow reaching Layer 1 cells beneath the lake may then be directed either upward toward the lake or downward into the Woodbine Aquifer.

The size of zone and number of cells that has common boundary with each other will play a big role in the amount of inflow it will receive from other zones and amount of outflow it will release to the neighboring zones. Obviously, Figure 6-4 shows that Zone 15 is the biggest zone and Zone 16 is the smallest zone. All other zones are intermediate in size and their sizes range between them. Some zones have more than two common border neighbor zones, but Zones 11, 13, and 16 have only two common border zones. In this way, Zone 12 has highest number of common border neighboring zones which connects almost all the zones and is a most social zone.

Looking at the Figures 6-5 and 6-6 and tables 6-6 and 6-7, it can be confirmed that in both pre-lake and post-lake conditions Zone 11 received a highest inflow from the shallow aquifer of Zone 15. This figure is the highest of the inflow among the 16 zones of post-lake and pre-lake model. Similarly, Zone 11 delivered a highest outflow to Zone 12 in both the pre-lake and post-lake conditions than any other zones. However, these values were slightly lower in post-lake condition. In general, Zones 1 through 10 have lower flow rate exchange during post-lake condition than the pre-lake, probably due to the constant water

level of JPL used in general head boundary package (GHB). Obviously, post-lake condition has more inflow towards the lake zones (Zones 1-10) than pre-lake condition.

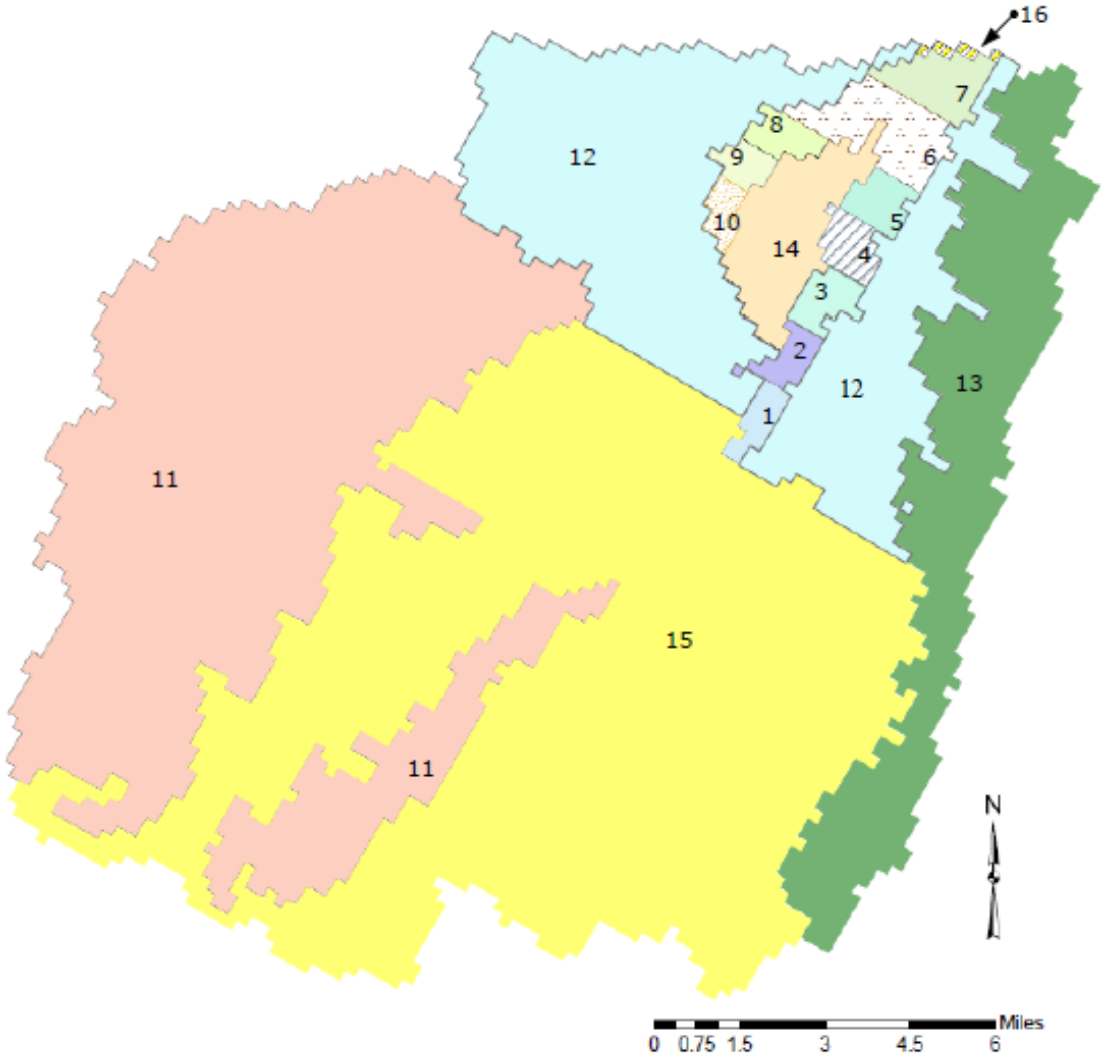

Figure 6-4 The shallow groundwater aquifer zones in JPL model

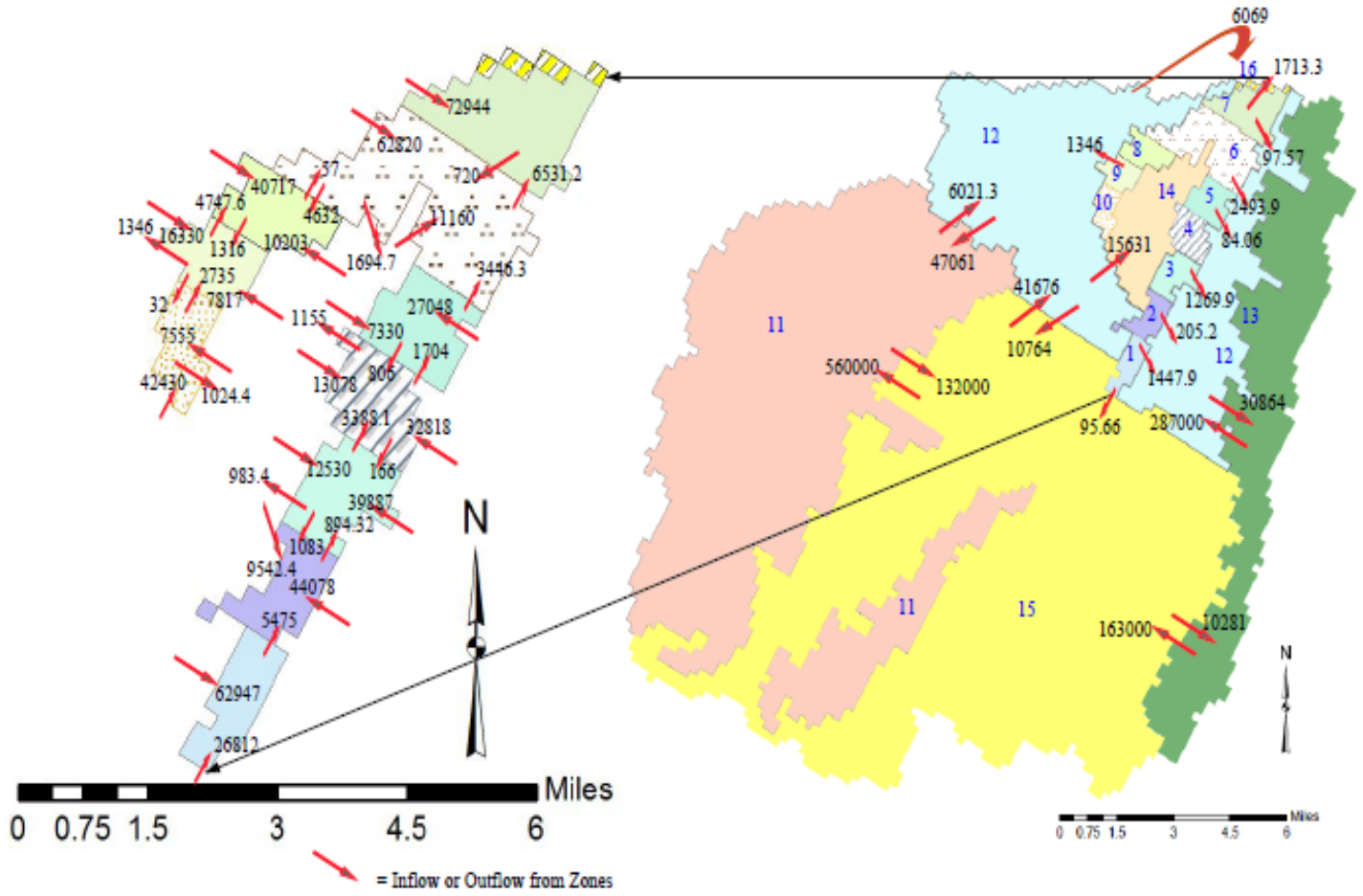

Figure 6-5 The distribution of horizontal flow between zones in the shallow groundwater aquifer under pre-lake conditions.

The figures with arrows represent the inflow and outflow from the individual zones in cubic feet per day (CFD);

figures in blue print represent the shallow aquifer zone number

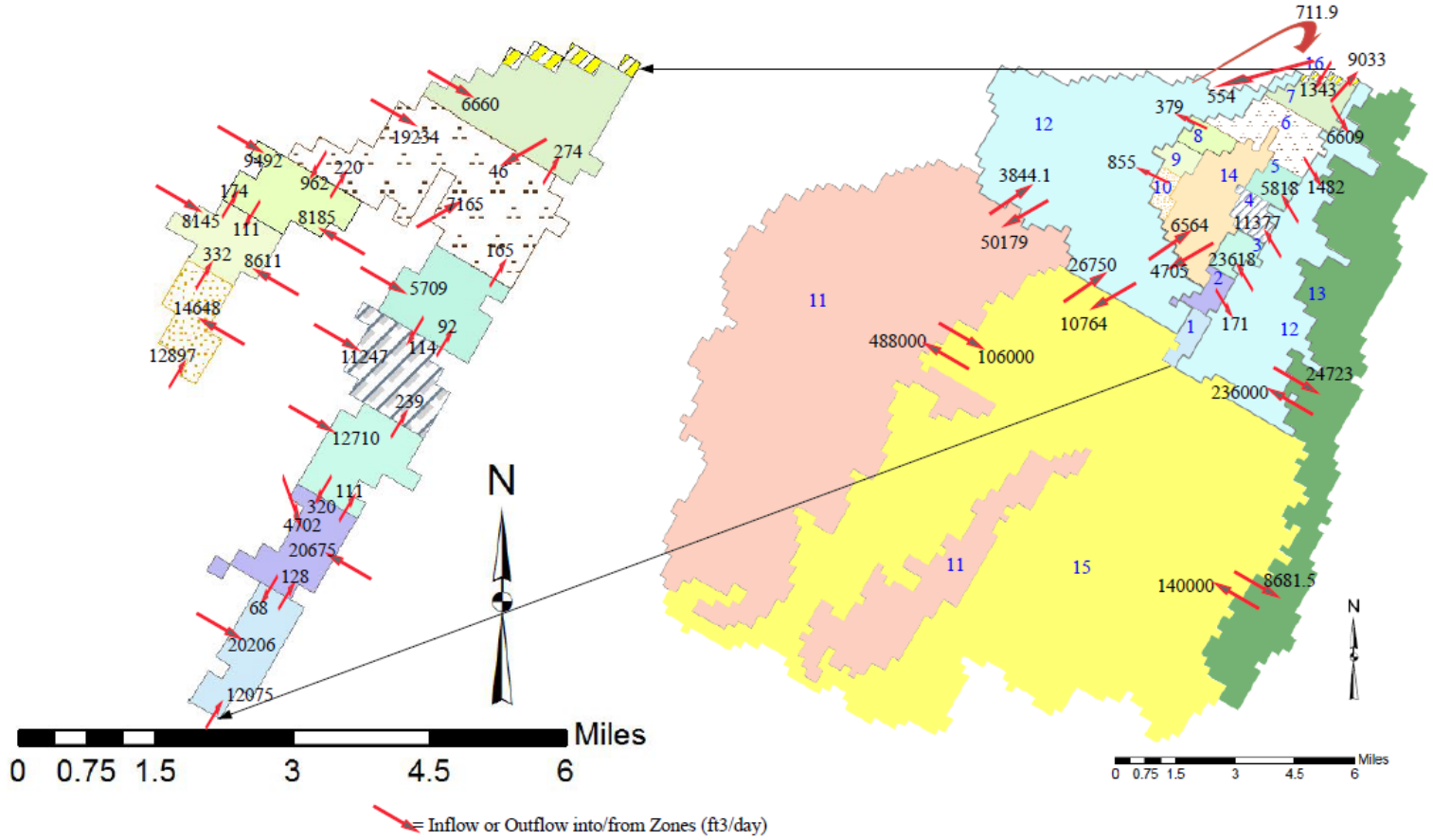

Figure 6-6 The distribution of horizontal flow between zones in the shallow groundwater aquifer under post-lake conditions.

The figures with arrow represent the inflow and outflow from the individual zones in cubic feet per day (CFD);

figures in blue print represent the shallow aquifer zone number

6.4 Distribution of Flow Into and Out from the Woodbine Group Strata

The Woodbine Group strata is a minor aquifer in North Central Texas; it outcrops in the Western portion of the JPL watershed. The outcrop area covers the entire WC sub-watershed and also extends along the terraces and thalweg of MCL. Stratigraphically, the Woodbine group strata lies below the EFS, a low-permeability aquitard composed of Upper Cretaceous clay (see Figures 1-2 and 1-3 and Table 1-2). The subcrop area of the Woodbine Group strata is an important recharge zone for the subcrop and downdip portions of the Woodbine Group strata itself, and for deeper aquifers as well. Knowledge of the groundwater flow regime of the Woodbine Aquifer is very important for understanding all aspects of JPL catchment hydrology. Fortunately, as discussed in Chapter 2, the hydrology of the Woodbine Aquifer is reasonably well known, and is summarized in the NTW-GAM reports (2004, 2007, and 2014); and for this reason, the Woodbine Aquifer was not treated as an active model layer in the JPL simulations. Instead, all cells of the second model layer, which represents the Woodbine Aquifer, were designated as constant-head cells, with the specified heads set at the levels indicated on Figure 4-29, page 4-53 and in Figure 4-30, page 4-54 by Bene and others, (2004). Kelly and others (2014) have refined the older version of the NTW-GAM (Bene and others, 2004, 2007) and illustrated the water level estimate of the Woodbine Aquifer for the years 1990 and 2010 in Figure 4.3.38, Page No. 4.3-94 with finer grid than the 2004 model, but still lower resolution grid than the model developed in this research. The water level of the Woodbine Aquifer from predevelopment to 1950 and predevelopment to 2010 is also given in Figure 4.3.39, page 4.3-95. Mace and others, (1994) have presented an excellent result of water level of the Woodbine Aquifer in the study area and in north-central Texas. ZONEBUDGET allows areas or layers made up of constant-head cells to be designated as zones, and calculates flows into and out of those zones exactly as it does for zones made up of active model cells. In the ZONEBUDGET analyses made in this research, the second layer of both JPL models was designated as zone 0, and both the total vertical flow into and out of the Woodbine Aquifer over the full JPL catchment, and the individual flows between the Woodbine Aquifer and each zone of Layer 1, were calculated, for both pre-lake and post-lake conditions.

Table 6-2 MODFLOW Model Inflow and Outflow to the Woodbine Group strata from Shallow Groundwater Aquifer

Flow Direction	Pre-lake Model	Post-lake Model
Flow from the Woodbine Aquifer to the Shallow Groundwater Aquifer, CFD	1,518	1,355
Flow from the Shallow Groundwater Aquifer to the Woodbine Aquifer, CFD	872,741	753,383

The results for total flow into and out of the Woodbine Aquifer are given in Table 6-2. Table 2 is a simplified version of the Table 1. The results for flows between the Woodbine Aquifer and individual shallow groundwater zones of Layer 1 are shown in Figure(s) 6-7 and 6-8. Very little upward vertical flow is calculated out of the Woodbine Aquifer under either pre-lake or post-lake conditions, whereas a downward flow of 872,741 CFD occurs into the Woodbine Aquifer from the shallow aquifer under pre-lake conditions, and a downward flow of 750,625 CFD occurs under post-lake conditions.

In ZONEBUDGET calculations the shallow aquifer above the Woodbine subcrop area is represented by Zone 11. The results show that during post-lake conditions, the flow from the shallow aquifer into the Woodbine Aquifer is 2.8 x E+04 CFD within the subcrop area, whereas the upward flow into the shallow aquifer is only a 390 CFD. However, for the pre-lake conditions the downward flow is 3.19 x E+05 CFD, but the upward flow is absent. Although the upward flow of 390 CFD is observed during the post lake conditions we can conclude that in both the pre-lake and post-lake conditions, the flow is directed predominantly downward into the Woodbine Aquifer (see Figures 6-7 and 6-8).

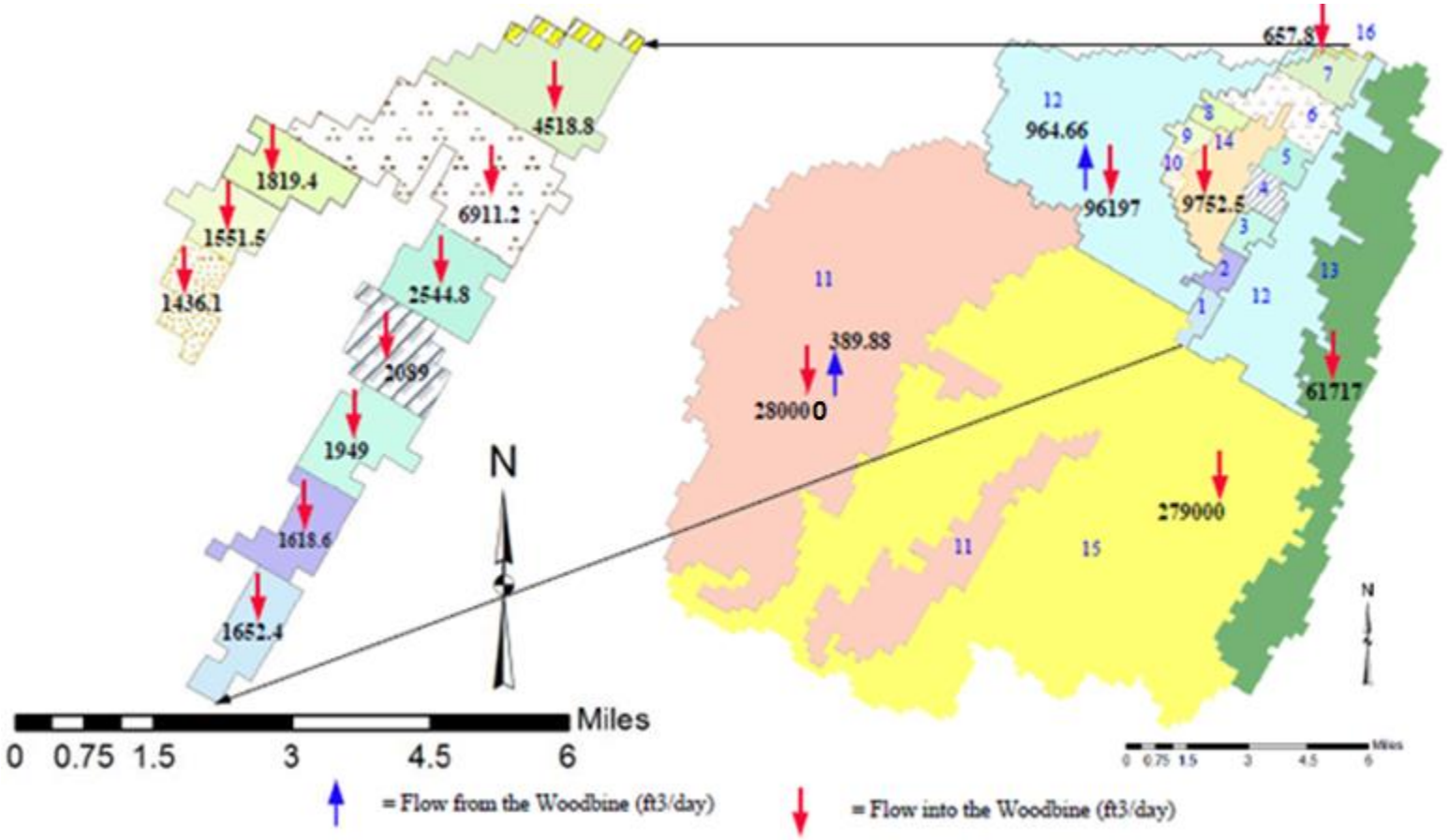

Figure 6-7 Distribution of vertical flow between the Woodbine Aquifer and the shallow groundwater aquifer under post-lake conditions. The figures with arrow represent the flows from shallow aquifer into the Woodbine Aquifer and vice versa in cubic feet per day (CFD); figures in blue print represent the shallow aquifer zone number

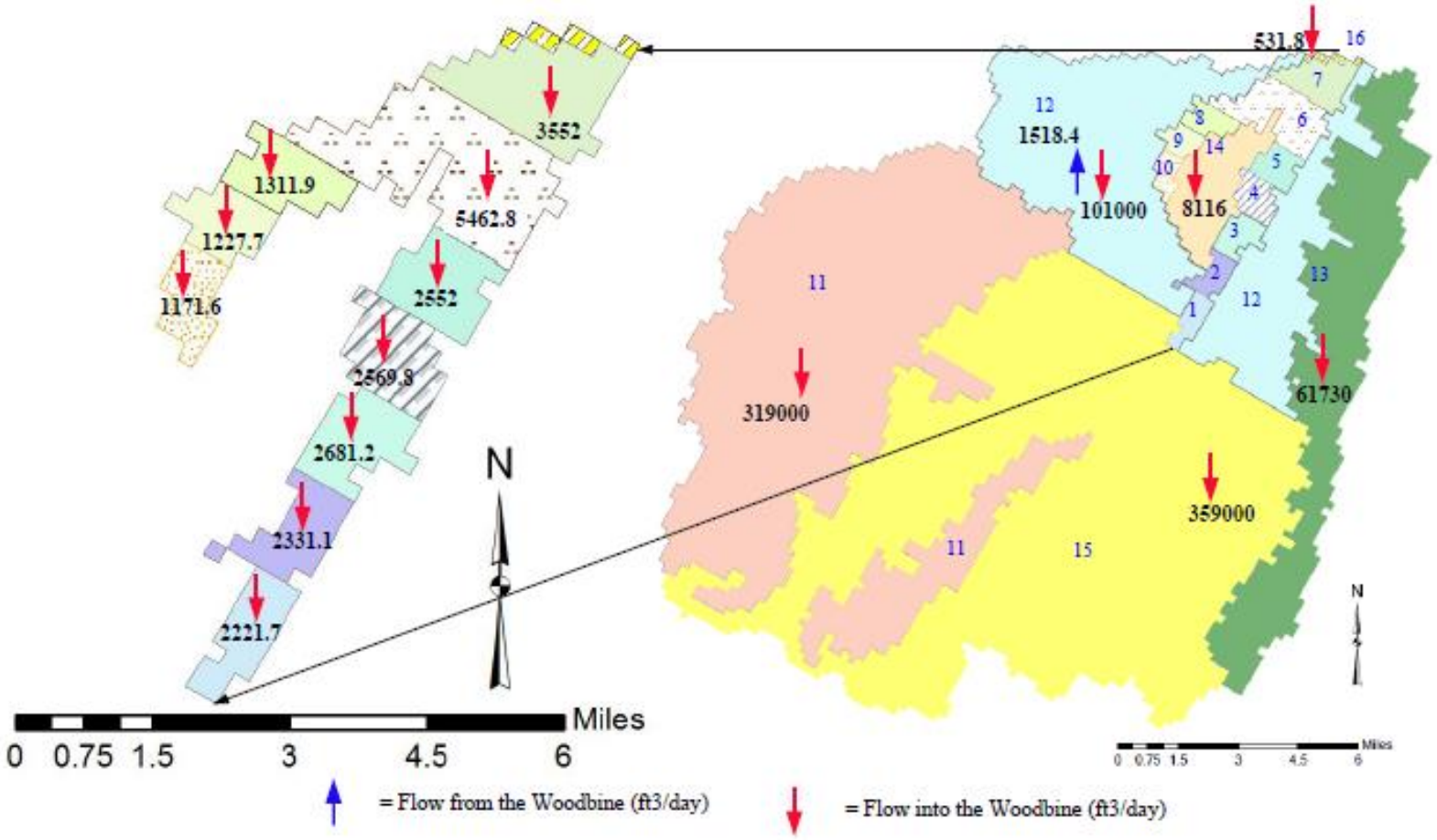

Figure 6-8 Distribution of vertical flow between the Woodbine Aquifer and the shallow groundwater aquifer under pre-lake conditions.

The figures with arrow represent the flow from shallow aquifer into the Woodbine Aquifer and vice versa in cubic feet per day (CFD); figures in blue print represent the shallow aquifer zone number

6.5 Saturated Thickness and Groundwater Volume in Pre-lake and Post-lake JPL

The volume of saturated material below the water table in the shallow aquifer within the JPL catchment was calculated by taking the difference of the calculated head and the Layer 1 bottom elevation. Also, the number of cells with head H(i,j) higher than the cutoff elevation for near-surface discharge processes has been evaluated. This number is higher for the post-lake conditions (Table 6-3) than the pre-lake conditions. For the estimation of the groundwater volume inside the saturated shallow aquifer porosity factor is required and, for the present purpose the porosity value was used as 0.18. As evident from the result of Table 6-3, the groundwater volume is higher by 4% in present conditions than the pre-lake conditions. These calculations indicate that even though some areas show a decrease in water level in the post-lake period relative to that in the pre-lake period, the overall or average result of the changes in water level illustrated in Figure 6-3 has been a raising of the water table closer to land surface. It should be bear in mind that the increase in groundwater volume is related to the increase in recharge (2%) and the presence of lake rather than the urbanization until now. This increase in groundwater volume due to change in the saturated thickness is given below:

Table 6-3 The Estimated Groundwater Volume in Shallow Aquifer as Calculated in Pre-lake and Post-lake Simulations

Modeling Conditions	Saturated Volume (feet^3)	Number of Heads H(i,j) Higher than ET cut-off Elevation
Pre-lake (1981)	37,553,404,649	1,750
Post-lake (2010)	39,213,765,163	1,861

6.6 Comparison of Groundwater Budget for Pre-lake and Post-lake Model

For understanding the change in groundwater regime/system from the pre-lake (1981) to post-lake (2010), a comparative study of the calculated budget of groundwater from different systems may be sufficient. However, other measures such as the hydraulic head and the sub-regional flow of groundwater in two model scenarios can be useful.

The results of the post-lake and pre-lake budget (Table 6-1) show that the groundwater flow into the river from the aquifers is decreased during post-lake because the total length of river in post-lake era is decreased due to the replacement of the Layer 1 cells on the JPL location by 305 GHB cells, that covers considerable portions of rive cell along the WC an MC valleys. This decrease must be compensated by the flow from aquifers into the river. However, the near-surface process is increased during post-lake era. Probably this change is due to the increased surface recharge as revealed by the model (Table 6-3) and increased water table near the JPL in post-lake condition (Figure 6-1). So, during the calibration processes the baseflow per unit area of JPL catchment during the post-lake conditions was weighted by the lake output and the near surface discharge.

6.7 Results of ZONEBUDGET Program

The results of MODFLOW ZONEBUDGET post-processer program are tabulated in Tables S-1, S-2, 6-4 and 6-5. The sub-regional flow from one zone to another and from different sources and sink inside these zones are illustrated on Figures 6-5, 6-6, 6-7 and 6-8. Figures 6-5 and 6-8 and Tables 6-4 and S-2 refer to the pre-lake (1981) conditions and Figures 6-6 and 6-7 and Tables S-1 and 6-5 refer the post-lake (2010) conditions. Tables 6-4 and 6-5 are the zone-wide flow related to the sources or sinks. Note that in all Figures 6-5 through 6-8, the number in front of arrow head represents the flow reaching from the corresponding zone to the zone it is pointing.

Tables S-1 and S-2 are input and output matrix of different zones in post-lake model and pre-lake models, respectively. The figures in each cell along the row in these tables represent the flow from the zone belonged to that row, and being reached into the zone corresponding to the zone belonged to the column of that cell. The total inflow and outflow pertaining to each zone is given along the diagonal of the table in red print. Together with the flow from each zone and flow from or into sources and sinks corresponding to each zone given in Tables 6-4 and 6-5 add up to this total input and output presented along the diagonal of Tables S-1 and S-2.

Obviously, the pre-lake zones do not have general head boundary used to represent lake cells. So, as discussed earlier in the introduction section of this chapter, there is no and sink source features

related to general head boundary in pre-lake conditions. Similarly, no other inks and sources terms except the general head boundary are present in post-lake conditions under the 305 lake cells, which are modeled as GHB cells.

Looking at the Tables 6-4 and 6-5, it will be clear that there is some change in recharge, near surface discharge processes, flow exchange between the river and shallow aquifer, and flow exchange between the shallow aquifer and lake of different zones between the pre-lake and post lake conditions. Because the Zones 1 to 10 have different stress regime at the pre-lake and post-lake conditions, it will be inconvenient to compare the zone-wide flow in two situations separately. Comparing the inflow and outflow in collective may be intelligent. Collectively, the inflow and outflow in post-lake conditions from Zone 1 to 10 due to external stress are 19,670 CFD and 199,569 CFD, respectively. Similarly, in pre-lake condition the collective inflow and outflow from Zones 1 to 10 due to external stress are 180,027 CFD and 696,688 CFD, respectively. As described above, the change in stress patterns from pre-lake to post-lake has caused a large difference in stress related flow of Zones 1 to 10.

The distribution of flow due to external stresses such as recharge (RCH), river (RIV), lake (GHB), and near surface discharge process (EVT) during the pre-lake and post-lake condition at different zones of MODFLOW ZONEBUDGET program looks interesting. In pre-lake condition, Zone 11 received a highest recharge, highest groundwater outflow from shallow aquifer to river, and highest near surface discharge process than the Zones 12, 13, 14, 15, and 16. In pre-lake condition, the recharge and groundwater outflow was 25% higher than post-lake condition of Zone 11 and the near surface discharge process was 3% higher than the post-lake condition of Zone 11. Whereas, in post-lake condition, Zone 15 received the highest recharge, highest groundwater flow from shallow aquifer to river, and highest near surface discharge processes than among the Zones 11, 12, 13, 14, and 16. Quantitatively recharge, groundwater outflow from shallow aquifer to river, and near surface discharge process were higher by 17%, 4%, and 52% , respectively than the Zone 15 of pre-lake condition. The remaining Zones 12, 14, 13 and 16 have some intermediate variations of their zonal flow due to external stresses.

Table 6-4 Flow Between each Zone and External Sources or Sinks as Calculated for the Pre-lake Model.

Flow Unit CFD

Zones	Zone-wide Groundwater Inflow From Rivers into Shallow Aquifer, CFD	Zone-wide Surface Recharge, CFD	Zone-wide Groundwater Outflow from Shallow Aquifer into River, CFD	Zone-wide Outflow from Shallow Aquifer due to Near-surface Discharge Processes, CFD
1	1,706	8,211	88,341	2,094
2	14,000	8,602	71,326	8,022
3	2,091	10,166	51,255	5,075
4	0	10,557	48,620	6,434
5	5,616	10,550	37,733	7,623
6	15,072	29,798	82,946	19,307
7	12,311	14,918	95,147	12,787
8	4,283	9,127	68,700	2,325
9	9,606	7,096	37,198	349
10	61	6,256	50,042	1,364
11	35,369	1,580,000	938,000	831,000
12	367,000	535,000	495,000	97,604
13	206,000	414,000	135,000	13,182
14	0	66,842	0	0
15	5,5949	1,560,000	226,000	702,000
16	0	2,003	994	936

Table 6-5 Flow Between each Zone and External Sources or Sinks as Calculated for the Post-lake Model.

Flow Unit CFD

Zones	Zone-wide Groundwater Inflow from Rivers into Shallow Aquifer, CFD	Zone-wide Groundwater Inflow from Lake into Shallow Aquifer, CFD	Zone-wide Surface Recharges, CFD	Zone-wide Groundwater Outflow from Shallow Aquifer into River, CFD	Zone-wide Outflow from Shallow Aquifer due to Near-surface Discharge Processes, CFD	Zone-wide Groundwater Outflow from Shallow Aquifer into the Lake, CFD
1	0	0	0	0	0	30,569
2	0	0	0	0	0	23,856
3	0	0	0	0	0	33,931
4	0	0	0	0	0	20,797
5	0	62	0	0	0	8,858
6	0	3,705	0	0	0	20,906
7	0	15,903	0	0	0	3,974
8	0	0	0	0	0	16,283
9	0	0	0	0	0	15,473
10	0	0	0	0	0	24,922
11	47,413	0	1,190,000	576,000	808,000	0
12	145,000	0	821,000	601,000	321,000	0
13	98,214	0	678,000	131,000	240,000	0
14	0	0	115,000	0	33,909	0
15	29,368	0	1,830,000	236,000	1,070,000	0
16	0	481	4,478	0	12,148	0

6.7 Comparison of Overall Hydrologic Budget

The preceding sections have dealt with groundwater budget issues, particularly as those can be approached through the MODFLOW post-processor ZONEBUDGET. However, the hydrologic changes that have affected the catchment between 1981 and 2010 clearly involve more than groundwater issues. For these reasons it is of interest to construct overall water budgets (surface water as well as groundwater) for the catchment for both time period. These budgets have been based on field data rather than on simulation results, although the simulation results have provided useful guidance. The system diagram of Figure 5-1 has also been followed in developing these budgets. The data used, in generating pre-lake and post-lake budget has been briefly discussed in Section 6.1.

The most serious difficulty on this task is the lack of data on ET, at a sufficiently detailed scale/higher resolution for the local scale. Areal estimates of ET are available for the years since1979 through NLDAS; the estimates, particularly for the earlier years, apply at a regional scale with a low resolution ET value, but have been used here as the best available information.

Table 6-6 presents the overall hydrologic balance for the pre-lake era (1981), and Table 6-7 presents the results for the post-lake era (2010). Reliable and budget specific data for the water balance estimation is lacking in the area. Subject to the available data, the calculated water budgets are presented below:

6.7.1 Pre-lake Budget

In the pre-impoundment budget the only component of inflow is precipitation. Some input due to human activities (e.g., leakage from utilities, outdoor water use, etc.,) was clearly present, but was considered too small in comparison with precipitation to be included. The output components include ET and runoff. Some direct evaporation from open water surfaces must also have occurred, but is excluded because the total area of open water surface was very limited in the pre-lake era. Total runoff per unit land surface was based on the WC gage results, which were assumed to be approximately representative of the entire catchment when multiplied by the area ratio of 3.67. Groundwater outflow from the catchment was assumed to be approximately zero, given the low permeabilities (Table 2-1) determined

by USACE (1991) and the groundwater divides following the topographic divides defining the catchment were assumed to remain in place. Thus, both groundwater inflow and groundwater outflow were assumed to be negligible relative to other terms in water balance.

Table 6-6 Estimated General Water Budget (Flow Unit is Cubic Feet per Year (CFY)) for the JPL Catchment, 1981

Year	NLDAS ET, CFY	Precipitation, CFY	Discharge, CFY	Total Inflow, CFY	Total Outflow, CFY	Inflow minus outflow, CFY
1981	1.62E+10	1.84E+10	3.29E+08	1.84E+10	1.65E+10	1.87E+09

6.7.2 Post-lake Budget

During the post-lake era the water budget is slightly different than the pre-lake era. The components of inflow for the post-lake water budgets are the precipitation (PCPN), the treated waste water effluent of the Mountain Creek Regional Wastewater System (MCRWS), and the population-based water input inside the catchment, calculated as discussed in Chapter 3, Sections 3.6 and 3.7; the outflow components are lake evaporation from JPL (see Figure C-7 in Appendix C), the gated flow from JPL, Midlothian withdrawal from JPL, and the total ET loss from the catchment. The Midlothian withdrawal figure is an average for the post-impoundment period, and the total ET loss includes the ET component of the near-surface groundwater discharge process discussed earlier, but also includes the much larger ET loss from the soil and vadose zone. Also, for the post-lake or JPL impoundment era, all runoff from the catchment eventually gets into the lake (including the distributed-discharge from minor unmapped drainage features), and contributes to the various discharge pathways from the lake. ET loss from the basin was prepared using NLDAS data (see Section 3.5.2). With regard to the treated water from MCRWS facility, the treated water was assumed to be imported to the catchment or pumped from deep bedrock aquifer within the catchment and so was considered to be imported.

Table 6-7 Estimated General Water Budget (Flow Unit is Cubic Feet per Year (CFY)) for the JPL Catchment, 2010

Year	MCRWS, CFY	PCPN, CFY	JPL Gated flow, CFY	Midlothian Pump, CFY	JPL Evaporation, CFY	Population-Based Water, CFY	NLDAS ET, CFY	Total inflow, CFY	Total outflow, CFY
2010	7.80E+07	2.26E+10	4.17E+09	2.478E+08	1.64E+09	1.16E+09	1.84E+10	2.38E+10	2.44E+10

6.8 Model Calibration

6.8.1 Pre-lake Model Fit

A total of 22 observations were available for the pre-lake water table of the shallow aquifer. Together with these 22 water table observations, the baseflow of the JPL catchment was also used as a reference flow to compare with the model calculated out flow from the shallow aquifer into the perennial reaches of the stream systems. Calibration followed the procedures outlined in Chapter 5, Section 5.8.

Contours of calculated head for the optimal pre-lake model are shown in Figure 6-2. Figure 6-9 is a plot of observed heads vs. model calculated heads for these 22 points. Prior to the model evaluations using the recorded water levels, the calculated head distributions were compared with the land surface data as discussed in Chapter 5, Section 5.8 and total simulated flow into the perennial reaches of streams was compared with baseflow data as obtained from the WC baseflow analyses, adjusted for the full area of the JPL catchment. The plot in Figure 6.9 is a linear best fit curve that shows fairly equal number of these observed pairs of points on both side of the 45 degree (symmetry) line.

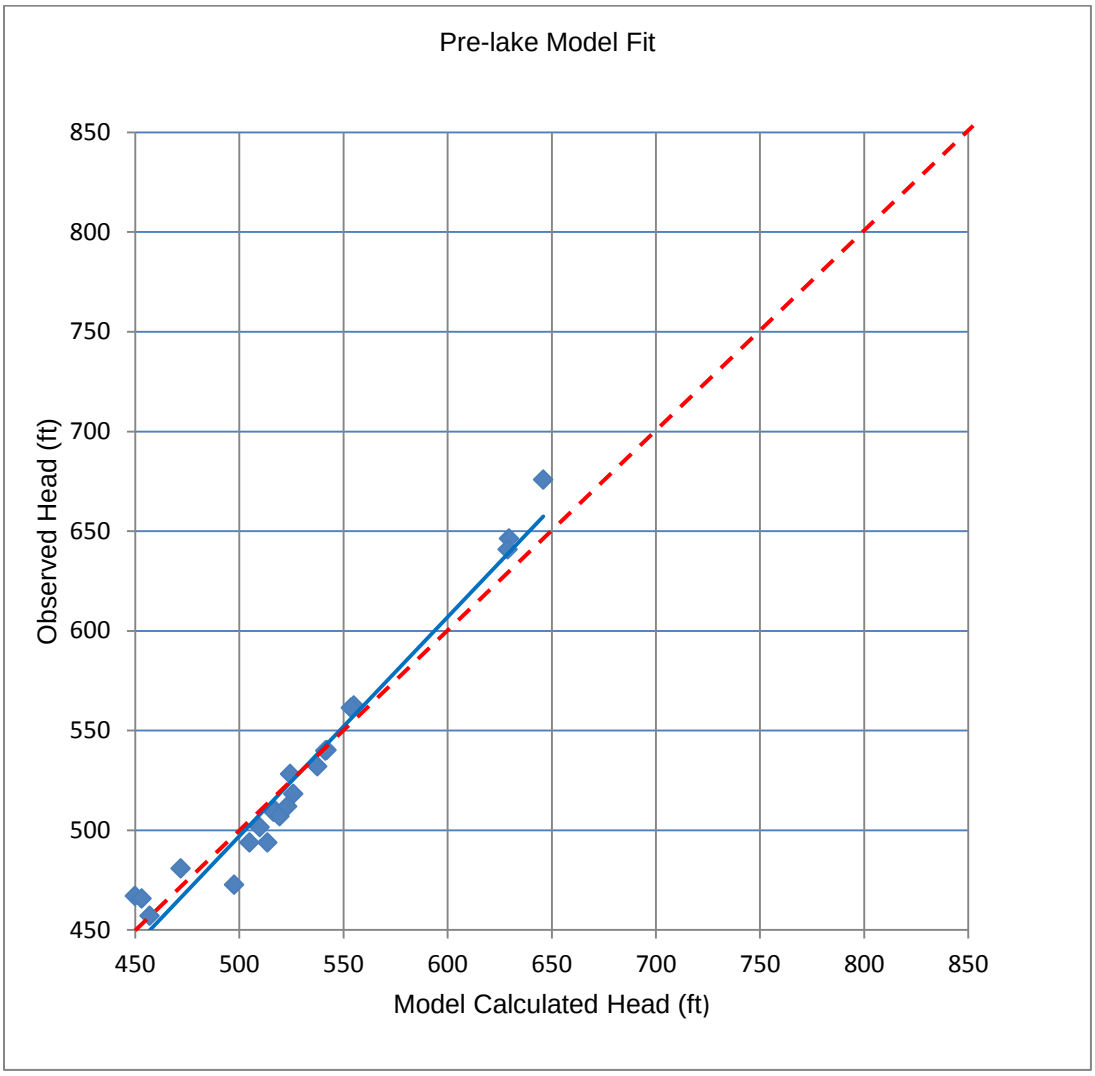

Figure 6-9 Pre-lake model fit of JPL project MODFLOW simulation

6.8.2 Post-lake Model Fit

Similarly, contours of calculated heads for the optimal post-lake model are given in Figure 6-1. A total of 14 observations were available for the post-lake water table of the shallow aquifer. These 14 observed water table records were used to calibrate the post-lake model. As discussed in Section 6.8.1, prior to the model evaluations using the recorded water levels, the calculated head distributions were compared with the land surface data as discussed in Chapter 5, Section 5.8; and total simulated flow into the perennial reaches of streams was compared with baseflow data as obtained from the WC baseflow

analyses, adjusted for the full area of the JPL catchment. Again, the plot in Figure 6-10 is a linear best fit curve of observed heads vs. calculated heads, which shows fairly equal number of these observed pairs of points on both side of the 45 degree (symmetry line) line.

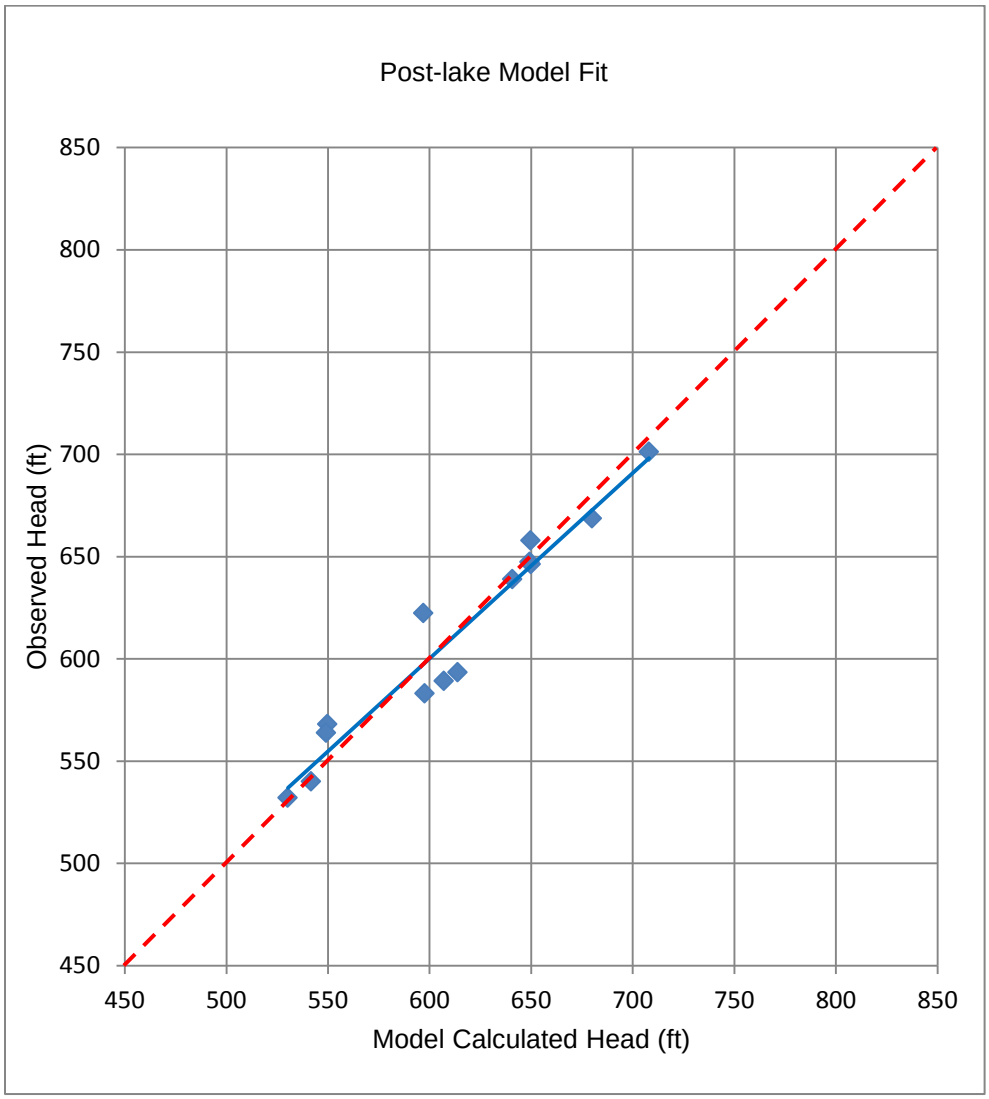

Figure 6-10 Post-lake model fit of JPL project MODFLOW simulation

6.9 Results of Land-use Analysis, Population Analysis, and Streamflow Analysis

Land-use has changed drastically during 20 years since the impoundment of JPL, mostly shrinking the vacant land into developed land such as housing or commercial facility. This change has somehow changed the surface water hydrology in the catchment. As shown in Figures 4-2 and 4-4 as well as Tables 4-1 and 4-2, the WC gage has changed both of its baseflow, streamflow, and precipitation, respectively. The land-use trend presented in Figures C-1 through C-4 has shown that there is a substantial decrease in vacant land-use and increased in developed land-use category such as residential and commercial. The population trend inside the WC watershed and JPL watershed is given in Figure 3-10. Similarly, the population trend of the 10 cities inside the catchment that share some area inside the watershed is given in Figure C-8, whereas the total population of each of four counties (Tarrant, Ellis, Dallas, and Johnson) that touch the JPL watershed is given in Figure C-9. These graphs visualize a steady state increase in population since 1970 to 2010. This increase in population has potential to impact the groundwater and surface water conditions inside the JPL catchment. However, the simulation results do not support the strong impact.

The land use change inside the WC watershed and JPL watershed is influenced by the population increase and urban expansion and growth. Tables 3-3 and 3-4 presented in Section 3.3.2 of Chapter 3 show that WC watershed has a decrease of vacant land from approximately 79% to 45%, whereas the residential land is increased from approximately 14% to 40 % from 1990 to 2010. In the same time period, JPL watershed has a decrease of vacant land from approximately 79% to 50% and increase in the residential land-use from approximately 8% to 25%. The land-use trend of the JPL project area is shown in Figures 3-5 through 3-9. Tables 3-3 and 3-4 also highlight the actual change in each land-use category in each of the five year span.

A broad land-use category was created and analyzed to differentiate the land-use category that has hydrological influences as discussed in Section 3-3.2. Tables 3-5 and 3-6 and Figures 3-5 through 3-9 show that the lumped residential land-use category was increased from 15% to 25% in WC watershed and 9% to 25% in JPL watershed. The lumped land-use category, “Non Residential Land-use With Water Distribution and Wastewater Collection Systems” increased from 5% to 13% in WC watershed and 4% to

13% in JPL watershed. Another lumped land-use category, “Non Residential Land-use Without Water Distribution and Wastewater Collection Systems” has decreased the land-use from 80% to 47% in WC watershed and 87% to 63% in JPL watershed.

Obviously, the impact of urbanization is very minimal and the hydrological system inside the watershed is in equilibrium. A large scale impact is possible when entire unincorporated areas of the Johnson, Tarrant, and Ellis counties enclosed by the JPL watershed are developed and vacant land-use are converted into housing or commercial unit. These vacant lands are between the small cities like Venus, Alvarado, and Burleson and they are likely to expand or the migratory populations from the Fort Worth, Dallas, Mansfield, Arlington, and rural part of Texas may move into these areas.

Chapter 7

Conclusions and Further Studies

7.1 Introduction

The JPL catchment has undergone rapid development since the impoundment was completed. Extensive data on population and land-use is available for the catchment, and these factors are generally considered potential forcing mechanisms for hydrologic change. Although the present research was not intended for predictive purposes, the modeling results, combined with the land-use and population dynamics, suggest that the effect of development to date has been moderate, and probably less than that of an increase in precipitation since 1987. More extensive impacts may result as more of the unincorporated area of the catchment is replaced by new residential and commercial facilities. The present flow trend of WC gaging station indicates that flood frequency and magnitude will perhaps increase in the future, although this depends heavily on future precipitation trends. So climatic factors such as precipitation patterns and ET loss may pose some uncertainty on the prediction established from the development oriented factors such as land-use and populations among others.

7.2 Conclusions

7.2.1 Impact of JPL on the Groundwater Regime

The impacts of development on the groundwater regime to date are primarily limited to those associated with the lake itself. These impacts include the development of a groundwater mound beneath the lake (Figure 6-1) and minor changes in the groundwater budget of the catchment (Table 6-1). Impacts associated with the urbanization that has followed impoundment are more difficult to identify. In general, moreover, the problem of isolating the effect of either the lake itself or the subsequent urbanization is complicated by the fact that a significant increase in precipitation (Table 4-3) has occurred during the time since JPL impoundment. Thus, the hydrologic changes that a simulation approach attempts to duplicate are to some extent the result of a combination of causes, the strongest of which, in this case, is probably the precipitation change. The simulation approach used in this research involved, in part, adjustment of

the recharge value until observed conditions were matched, beginning, in every case with a starting value equal to the total rate of application of water to the vadose zone. In theory, the procedure should reach the correct recharge value regardless of the starting point, but in practice may not always work out. In any case, the value of recharge reached in this process is partially dependent on precipitation and an evapotranspiration, which may be influenced by precipitation.

7.2.2 Impact of Land-use Changes on Hydrology

Land-use change will always have an impact on the hydrology. The unused land in the catchment is decreasing and the residential and commercial area is increasing. As discussed in Chapter 3 Section 3.3.2 and Chapter 6 Section 6.9, the WC watershed has increased residential land-use from 14% to 40% while it has decreased the vacant land-use from 79% to 45% from 1990 to 2010. In the same time frame JPL watershed has increased residential land use from 8% to 24%, whereas the vacant land-use was decreased from approximately 79% to 59%. Obviously, WC watershed has higher rate of land-use rate than other part of JPL catchment. This change may directly affect the groundwater. The increased population increases the water use, and this in turn increases recharge. The study shows the impact is difficult to detect at present because the amount is relatively small compared to the precipitation, but the full impact will be visible once the entire unused land of the catchment is converted into residential or commercial area.

7.2.3 Impact of Population Dynamics and Indicator on WC Gage

Population change has increased water use in the catchment. This additional population-based water use is still small at present and during the pre-lake era this was assumed negligible; however, the consequences may be intensified as the ratio of residential to vacant land rises. At least some of the additional water requirement may come from wells within the catchment-tapping deeper aquifers or import from outside the catchment. This process will affect the deeper aquifers, which receive recharge through the shallow aquifer. Thus, any increase in withdrawal from the deeper aquifers will ultimately affect the entire system. A comprehensive model including deeper aquifer will ultimately be needed to predict the

impact of population induced recharge. Note that the increasing streamflow and baseflow data of the WC catchment (Figures 4-2 and 4-5) is indicative of the interaction of population dynamics and hydrology.

7.2.4 Model Improvement with Finite-Element Method of Simulation

MODFLOW finite-difference simulation calculates head at the centroid of the cell, and the hydraulic processes and parameters are simulated at the centroid of the cell. Greater resolution in simulating land surface elevation will be required in any area involving highly uneven topography or near a stream or other hydraulic feature where the topography changes rapidly. Because the present available topographic data from the USGS DEM has 10 meter resolution; a higher resolution grid as available through the finite-element method (Istok, 1989; Czarnecki and Waddell, 1984; Pinder and Gray, 1977) might be preferable to MODFLOW.

7.3 Further Studies

Improved simulation strategies to better isolate the effects of lake and urbanization from the effects of precipitation would clearly be useful. Further study may also be required to update the model as improved calibration data becomes available. Finally, the impact of urbanization frequently involved deterioration of the water quality; when that is the case, solute transport modeling is usually mandated; this study will allow the present model, or improved version of this model, to a solute transport model would therefore be required to address such issues.

7.3.1 Simulation with High Resolution Grids

The present simulation of the JPL has a grid resolution of 1,000 feet x1,000 feet. The NTW-GAM report (Bene and others, 2004) states that the model initially incorporated a grid size of 1 mile x 1 mile. Kelly and others (2014) refined this model to a grid size of 1,300 feet x 1,300 feet. The grid size used in this research has higher resolution; but based on the surface topography of the JPL catchment, a much finer grid will better serve the groundwater model. In addition, the MODFLOW model has a local grid refinement (LGR) capability (Mehl and Hill, 2005), which can be implemented in areas of interest such as

stream channel where the topography changes unevenly. This process requires finer scale data. NCTCOG has a topographic map of 1 meter resolution, which is better than the USGS DEM of 10 meters resolution, which is used in this study.

7.3.2 Particle Transport and Contaminant Transport Modeling

The scope of the present dissertation excluded the simulation of contaminant transport. Commonly, a contaminant transport model (e.g., MT3D, MT3DMS, etc.) uses the output of MODFLOW, and the present model setup can serve as a direct interface for a contaminant transport study in the catchment (Zheng, 1990; Zheng and others, 2001, Zheng and Wang, 1999, Zhang and others, 2010; Zheng , 2010). There are various contaminant sources such as a wastewater treatment plant, and a superfund site within the JPL catchment; a detailed study of contaminant transport around these sites may ultimately be needed to evaluate the threat of contamination to JPL reservoir, the Woodbine Aquifer, and other potential targets. JPL is an important source of drinking water to Midlothian City, and is also extensively used for recreation in the Dallas-Fort Worth Metroplex. The western side of the watershed, where WC flows, has subcrop of the Woodbine Aquifer which further downdips from the eastern margin of the WC Watershed below the EFS. Protecting this recharge zone of the Woodbine outcrop (the recharge zone of the Woodbine Aquifer) and enhancing clean water recharge from any surface water sources may be another step to protect the Woodbine and deeper aquifers. Although JPL watershed has only a small portion (Figure 1-2) of the Woodbine outcrop, this attempt can be an example to safeguard the integrity of our groundwater resources at least in this part of the catchment in North Central Texas.

7.3.3 A Combined Study of Shallow and Deeper Groundwater

This dissertation research is only focused on the shallow groundwater of the JPL. The Northern Trinity Woodbine Groundwater Availability Model (NTW-GAM) deals with the simulation of the deeper aquifers and outcrop portions of the Woodbine Aquifer and the Trinity Aquifers. However, a combined study of the JPL watershed including the shallow aquifers and deeper aquifers can be implemented. Such an integrated model of surface water, shallow groundwater, and deeper groundwater will provide a

broader view of the relations and connections of the shallow groundwater and deeper groundwater and lake and groundwater interactions.

7.3.4 Urban Water Use and Recharge Studies

The Dallas-Fort Worth Metroplex, including the cities within the JPL catchment are gaining population and thus, their potable water requirement is increasing, but the amount of available water is also shrinking due to increased drought in North Texas. An alternative and sustainable approach of conserving total available water may be helpful in this situation. To conserve the water in such situation, details of water loss and uses are required. A detailed study of the urban water use and enhanced recharge can be conducted so that local cities can start water conservation measures and conserve the resource. TWDB has already started the water loss accounting in government funded water project and supply agencies, private agencies, and any water supply company must comply this ordinance. A recent study in the City of Austin, Texas has shown a greater water recharge in urban setting than the rural setting (Garcia-Fresca, 2004; Garcia-Fresca and Sharp, 2005; Vazquez-Sune, 2003; Yang and others, 1999; Lerner, 1997(b); Grischek and others, 1996). Similar studies in the Dallas-Fort Worth Metroplex will provide answers to the water resource managers and cities in this region and will be able to plan, manage, and conserve the available water resource.

7.3.5 Further Study Using Improved Version of MODFLOW

The MODFLOW program has continuously evolved since its first debut. Many new packages have been added. Many newer and faster solver programs are solving the finite-difference equations. Moreover, newer and improved versions of MODFLOW, such as MODFLOW-NWT (Niswonger and others, 2011), MODFLOW-USG (Panday and others, 2013), and Graphical User Interface (GUI) (Winston, 2009; Harbaugh 2010) for these new and older models (MODFLOW 2005, MODFLOW 2000, MODFLOW 1996, etc.,) and post-processing and visualizations programs are already in the public domain. The model developed in this dissertation may be further improved with newer versions and

calibrated using calibration programs such as UCODE (Harbaugh, 2010), OPR-PPR (Tonkin and others, 2007), and SIM_ADJUST (Poeter and Hill, 2008).

Appendix A

A Derivation of Partial Differential Equation (PDE) of Groundwater Flow Equation in MODFLOW Program

The groundwater flow equation (Rushton and Redshaw, 1997; McDonald and Harbaugh, 1988; Harbaugh, 2005) used in MODFLOW program is a partial differential equation (PDE) that describes the three-dimensional movement of groundwater of constant density through porous earth material (Harbaugh, 2005). The flow equation is given by (Figure A-1):

$$\frac{\partial}{\partial x}\left(Kxx\frac{\partial h}{\partial x}\right)+\frac{\partial}{\partial y}\left(Kyy\frac{\partial h}{\partial y}\right)+\frac{\partial}{\partial z}\left(Kzz\frac{\partial h}{\partial z}\right)+W=Ss\frac{\partial h}{\partial t}\text{ ,}\qquad\text{A-1}$$

where K_{xx}, K_{yy}, and K_{zz} are hydraulic conductivities parallel to the x, y, and z coordinate axes, respectively, which are assumed parallel to the major axes of hydraulic conductivity (LT^{-1}); h is the hydraulic head (L); W is the volumetric flux per unit volume representing sources and/or sink of water (where W<0 implies groundwater outflow and W>0 implies groundwater inflow), (T^{-1}); S_s is the specific storage of the porous aquifer material (L^{-1}); T is time (T). The variables S_s, K_{xx}, $K_{yy,}$ and K_{zz} are a function of space (S_s= S_s(x, y, z), K_{xx}= K(x, y, z), etc.,); W may be a function of space and time, i.e., W = W(x, y, z, t). For a homogeneous anisotropic medium K_{xx} = K_{yy} = K_{zz}.

In Equation A-1, the first, second, and third terms on left side represent the differences between inflow and outflow of water in the x, y, and z as three direction of the rectangular coordinate system, respectively. These three directions in the rectangular coordinate system are later substituted by the row (i), column (j), layer (k) of the three-dimensional finite-difference flow model (MODFLOW). The fourth term on the left hand side of the equation represents the net flow to or from fluid sources and sinks, per unit volume of aquifer material, and the term on right represents the rate at which water is accumulating in storage, per unit volume of aquifer material. Basically, Equation A-1 is obtained by combining flow terms, as expressed through Darcy’s law, with the equation of groundwater storage, using the continuity equation. This model implies the conservation of mass, and the assumption that the compressibility of water can be neglected except insofar as it contributes to aquifer storage. A solution of Equation A-1 is an array of head values, i.e., a distribution of head values in space and time, such that the derivatives of head, when substituted into Equation A-1, satisfy the equation. A solution might be represented, for example, by a set of hydrographs of h vs. t, each representing the time variation of head at a particular point (x, y, z) in space, or by a set of maps, each representing head at a particular horizon (z) (Figures 6-1 and 6-2) and time (t) (Figure B-3), or so on. In rare cases, a solution maybe represented as a

mathematical function, h = h(x, y, z, t). In addition to satisfying the PDE itself, a solution must satisfy boundary and initial conditions characterizing the problem (see Section 5.7.2 in Chapter 5).

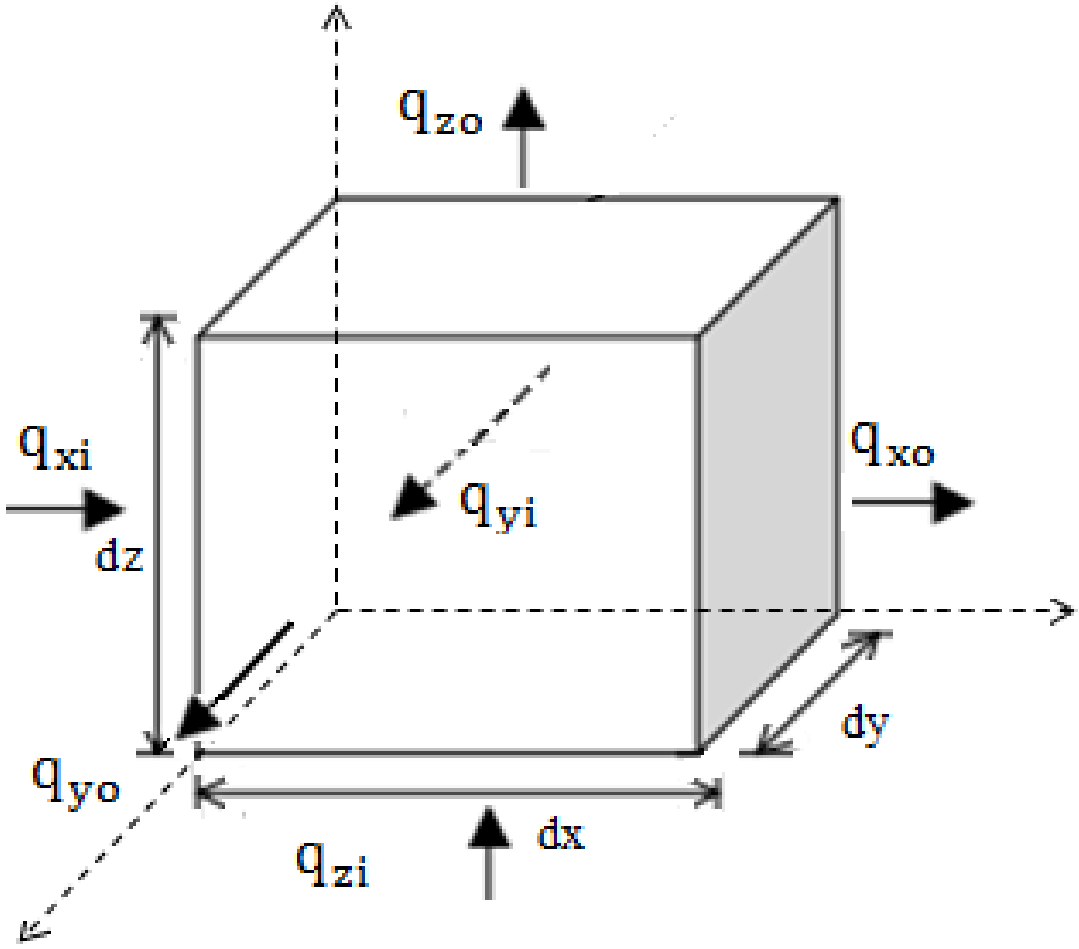

Figure A-1 Diagram showing three-dimensional groundwater flow in an infinitesimally small cube, a representative elementary volume (REV)

As noted above, Equation A-1 is derived by considering the flow through an infinitesimal cube (Figure A-1) of volume, $V = dx * dy * dz$. The net changes in flow along the x, y, and z directions are summed together with the net flow from sources and sinks in the volume element, and the result is equated to the rate of accumulation of water in storage in the element (Harbaugh and McDonald, 1996; Freeze and Cherry, 1979; Harbaugh, 2005; Bennett, 1989; Anderson and Woessner, 1992; Fitts, 2002).

In Figure A-1, let us consider the groundwater flow through the infinitesimal cube, where $q_{xi}, q_{yi}, \text{and } q_{zi}$ are input (specific discharge per unit area) in the x, y, and z directions and $q_{xo}, q_{yo}, \text{and } q_{zo}$ are outflow along the x, y, and z directions. $A_x = dy * dz$ = area of the input and output faces normal to the x-axis; $A_y = dx * dz$ = area of the input and output faces normal to the y-axis; $A_z = dx * dy$ = area of the input and output faces normal to the z-axis.

Input volume in the x-direction, $V_{in} = q_{xi}A_x = q_{xi}\,(dydz)$ and the output volume in the x-direction, $V_{out} = q_{xo}(dydz) = q_{xi}(dydz) + \frac{\partial q_x}{\partial x}\,dx(dydz) = (q_{xi} + \frac{\partial q_x}{\partial x}dx)dydz$.

For transient flow, using the continuity equation, it follows that "$V_{in} - V_{out}$ = Change in storage". Now, for the flow along the x-direction, using the continuity equation, Volume Inflow - Volume Outflow = Change in storage = $q_{xi}(dydz) - \left(q_{xi} + \frac{\partial q_x}{\partial x}dx\right)(dydz) = -\frac{\partial q_x}{\partial x}(dxdydz)$.

Similarly, for the y-direction and the z-direction, the net-flows (Inflow-Outflow) are $-\frac{\partial q_y}{\partial y}(dxdydz) \text{ and } -\frac{\partial q_z}{\partial z}(dxdydz)$, respectively. For the representative volume of the entire cube, the net flow from all three directions = $-\frac{\partial q_x}{\partial x}(dxdydz) - \frac{\partial q_y}{\partial y}(dxdydz) - \frac{\partial q_z}{\partial z}(dxdydz)$. For transient saturated flow, the total volume inflow – total volume outflow = rate of change in storage $= -\frac{\partial V}{\partial t}$. The minus sign indicates the outflow is greater than the inflow, but $-\frac{\partial V}{\partial t} = S_s V_T \left(\frac{\partial h}{\partial t}\right)$ and $V_T = dxdydz$.

Now combining the flow equations, we have:

$$-\left\{\frac{\partial q_x}{\partial x}(dxdydz) + \frac{\partial q_y}{\partial y}(dxdydz) + \frac{\partial q_z}{\partial z}(dxdydz)\right\} = S_s V_T \left(\frac{\partial h}{\partial t}\right)$$

or, $-\left(\frac{\partial q_x}{\partial x} + \frac{\partial q_y}{\partial y} + \frac{\partial q_z}{\partial z}\right)dxdydz = S_s\,(dxdydz)\left(\frac{\partial h}{\partial t}\right)$. This expression can be simplified to,

$$-\left(\frac{\partial q_x}{\partial x} + \frac{\partial q_y}{\partial y} + \frac{\partial q_z}{\partial z}\right) = S_s \left(\frac{\partial h}{\partial t}\right).$$

In vector notation, $\nabla \cdot \mathbf{q} = S_s \left(\frac{\partial h}{\partial t}\right)$. The flow into the cube along the principal direction of the axis is given by Darcy's Law. Thus, for the flows along the principle directions of axis x, y and z, these flow along those directions are expressed as $q_x = -K_{xx}\frac{\partial h}{\partial x}$, $q_y = -K_{yy}\frac{\partial h}{\partial y}$, and $q_z = -K_{zz}\frac{\partial h}{\partial z}$, respectively,

where, K_{xx}, K_{xyy}, and K_{zz} etc., are the directional hydraulic conductivities. By substituting these values, into above equation, we have

$$\frac{\partial}{\partial x}\left(Kxx\frac{\partial h}{\partial x}\right)+\frac{\partial}{\partial y}\left(Kyy\frac{\partial h}{\partial y}\right)+\frac{\partial}{\partial z}\left(Kzz\frac{\partial h}{\partial z}\right)=Ss\ \frac{\partial h}{\partial t}. \quad \text{A-1}$$

For steady state flow, $\frac{\partial h}{\partial t}=0$, there will be no storage in the aquifer and equation for steady state reduces to

$$\frac{\partial}{\partial x}\left(Kxx\frac{\partial h}{\partial x}\right)+\frac{\partial}{\partial y}\left(Kyy\frac{\partial h}{\partial y}\right)+\frac{\partial}{\partial z}\left(Kzz\frac{\partial h}{\partial z}\right)=0. \quad \text{A-2}$$

The results of MODFLOW simulation of JPL project for the years 1981 and 2010 are based on the steady-state solutions.

Appendix B

Three-Dimensional Finite-difference Approximation of Groundwater Flow in MODFLOW Program

Solving the groundwater flow equation by formal analytical means is generally not possible. Therefore, in practical applications of using MODFLOW, a finite-difference method –as signaled by approximation – is used. As implemented in MODFLOW, this method sets up a spatial mesh of N points or nodes, each at the center of a "block" or "cell", and replaces the partial differential equation with a set of N finite-difference algebraic equations, involving N unknown heads or potentials (Wang and Anderson, 1982; Celia and Williams, 1992) one at each node of the mesh for each specified time of problem simulation. The finite-difference equations must be solved simultaneously as a set, normally by iteration. Other methods, notably the finite-element approach, (Istok, 1989; Wang and Anderson, 1982; Lapidus and Pinder , 1982) exist, but the MODFLOW code utilizes the finite-difference (Pinder and Leon, 1982) method.

The cells and nodes in MODFLOW are designated by indices, i, j, and k, giving their position in the mesh. Figure B-1(a) shows six aquifer cells – i-1,j,k; i+1,j,k; i,j-1,k; i,j+1,k; i,j,k-1; i,j,k+1 surrounding a central cell - i,j,k - through which flow is occurring. Figure B-1(b) shows the flow in one direction from cell i,j-1,k into cell i,j,k. Figure B-1(c) shows the flow through the six faces of cell i,j,k. Using the continuity equation, the algebraic sum of all six groundwater flows and the flows from or into all sources and sinks within the cell is equal to the rate of change of water in storage within the cell.

$$\sum_{i}^{N} Q_i = Ss \frac{\Delta h}{\Delta t} \Delta V, \qquad \text{B-1}$$

where, Q_i = flow rate into the cell (L^3T^{-1}) including the sources and sinks; Δh = change in head in time Δt (LT^{-1}); S_S = specific storage (L^{-1}); ΔV = volume of cell (L^3).

The flow into the cell i,j,k from cell i,j-1,k {Figure B (b)}, and using Darcy's Law, is given as

$$q_{i,j-\frac{1}{2},k} = KR_{i,j-\frac{1}{2},k} \Delta c_i \Delta v_i \frac{h_{i,j-1,k} - h_{i,j,k}}{\Delta r_{j-\frac{1}{2}}}, \qquad \text{B-2}$$

Where, the negative sign of Darcy's Law has been dropped and flows into i,j,k are considered positive, whereas outflows are considered negative, and $h_{i,j,k}$ = head at nod i,j,k and $h_{i,j-1,k}$= head at node i,j-1,k; $q_{i,j-\frac{1}{2},k}$ = volumetric flow through the face between cells i,j,k and i,j-1,k; $KR_{i,j-\frac{1}{2},k}$ = hydraulic conductivity along the row between nodes i,j k and i,j-1,k; $\Delta c_i \Delta v_i$ = area of cell faces normal to the row direction; and $\Delta r_{j-\frac{1}{2}}$ = the distance between nodes i,j,k and i,j-1,k, The subscript $i, j\frac{1}{2}, k$, used in the above flow equation,

and subsequently in later equations, represents the region between nodes i,j,k and i,j-1,k, and not the halfway point between nodes.

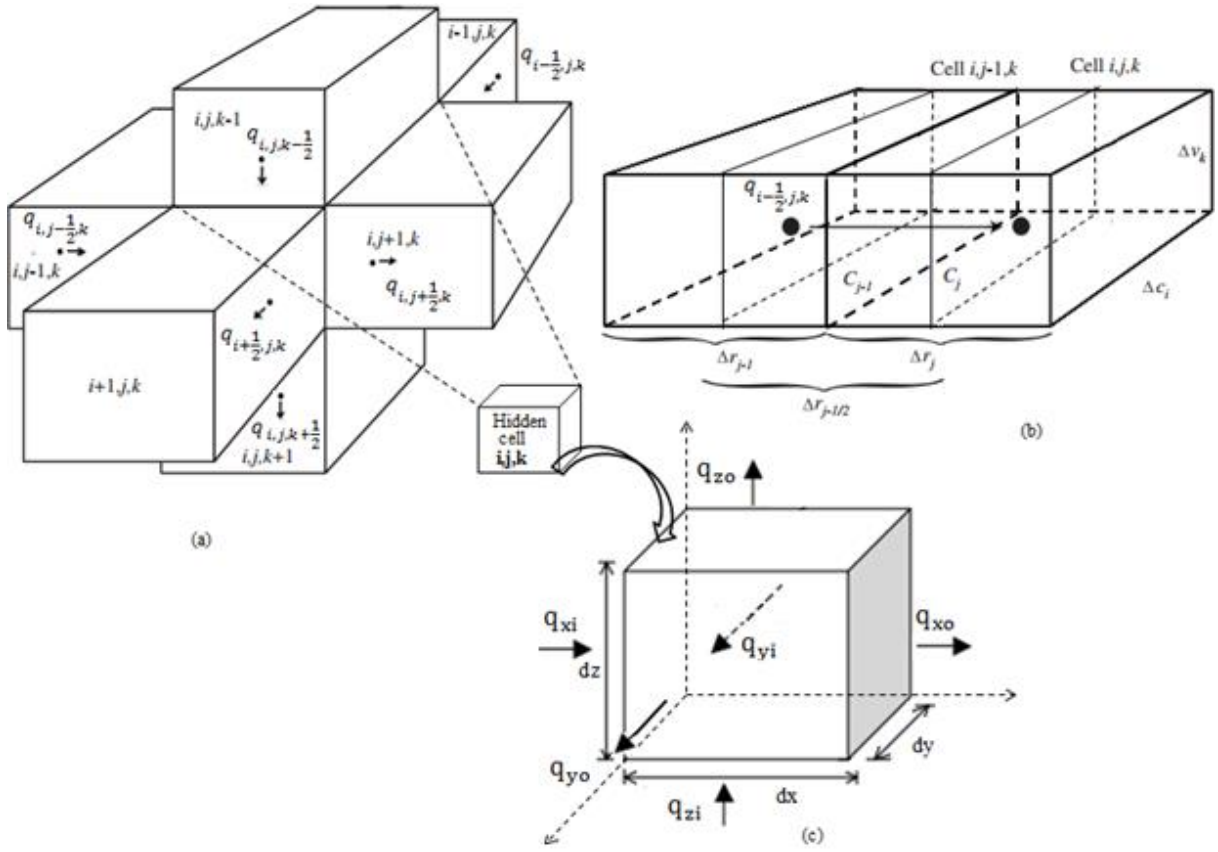

Figure B-1 Illustrating the conventions of cells used in finite-difference approximation of groundwater flow equation. Where, (a) three-dimensional representation of flow in MODFLOW simulation; the center of the cell i,j,k (hidden) is surrounded by six cells, (b) one dimensional groundwater flow into the cell i,j,k from an adjacent cell, and (c) the 3-D cube receiving flow from six adjacent cells

Let $\mathrm{CR}_{\mathrm{i,j-\frac{1}{2},k}} = \mathrm{KR}_{\mathrm{i,j-\frac{1}{2},k}} \Delta \mathrm{c_i} \Delta \mathrm{v_i} \frac{1}{\Delta \mathrm{r}_{\mathrm{j-\frac{1}{2}}}}$, where $\mathrm{CR}_{\mathrm{i,j-\frac{1}{2},k}}$= hydraulic conductance along the row i and layer k between nodes i,j,k and i,j-1,k. The “hydraulic conductance” or simply “conductance” is the product of hydraulic conductivity and cross-sectional area of flow divided by the length of the flow path. In MODFLOW the hydraulic conductivity of the entire region between the nodes is calculated as a harmonic

mean (Figure B-2) (Collins, 1961). This conductance is defined considering a prism of aquifer material and calculated for a particular direction. In the block-centered approach used in MODFLOW, and in an anisotropic medium, the conductances of the prisms in the three principal directions will generally vary. Internally, MODFLOW calculates and uses equivalent conductances in each direction (column, row, and vertical) for the intervals between nodes; these conductances are calculated as the conductances of two half-cells in series and are also known as “branch conductances”.

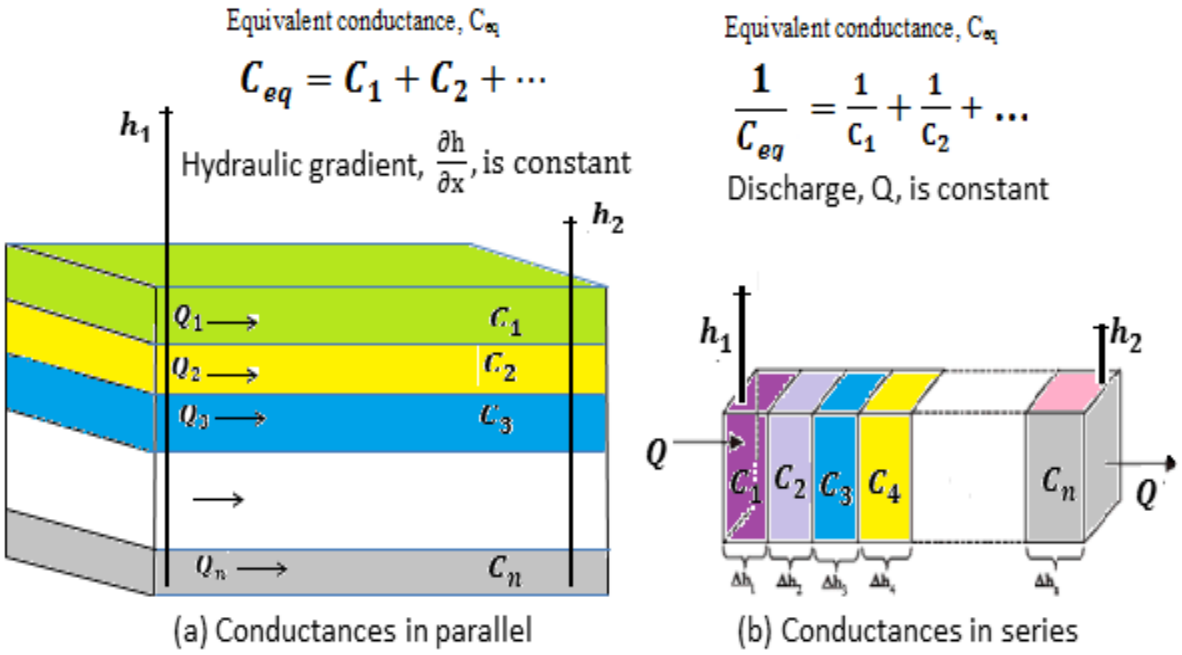

Figure B-2 Figures illustrating the concept of equivalent conductance and its mathematical calculation through the entire region between nodes using effective hydraulic conductivity, the cell dimensions, and flow distance. (a) Conductances in series and (b) conductances in parallel; Q, Q_1, Q_2, etc., are discharges; C, C_1, C_2, etc., are conductances; h_1, h_2, h_3,etc., are the head values; Δh is the difference in hydraulic heads values; (Harbaugh, 2005)

With this notation, the inflow into the cell i,j,k in row direction is given by

$$q_{i,j-\frac{1}{2},k} = CR_{i,j-\frac{1}{2},k}(h_{i,j-1,k} - h_{i,j,k}) \quad \text{B-3}$$

The inflow into the two faces of cells and outflow from three faces of cells in the finite-difference flow volume can be approximated with similar expressions. The outflow from the cell i,j,k in the row direction through the face between cells i,j,k and i,j+1,k is given by $q_{i,j+\frac{1}{2},k} = CR_{i,j+\frac{1}{2},k}(h_{i+1,j,k} - h_{i,j,k})$.

In the column direction, inflow into the block through the rear and outflow through the front face is given by $q_{i-\frac{1}{2},j,k} = CC_{i-\frac{1}{2},j,k}(h_{i-1,j,k} - h_{i,j,k})$ and $q_{i+\frac{1}{2},j,k} = CC_{i+\frac{1}{2},j,k}(h_{i+1,j,k} - h_{i,j,k})$, respectively.

Similarly, in vertical direction the inflow through the upper and outflow through bottom face of the cell is given by $q_{i,j,k-\frac{1}{2}} = CV_{i,j,k-\frac{1}{2}}(h_{i,j,k-1} - h_{i,j,k})$ and $q_{i,j,k+\frac{1}{2}} = CV_{i,j,k+\frac{1}{2}}(h_{i,j,k+1} - h_{i,j,k})$, respectively.

Sources and sinks represent flows which do not cross the cell faces, but rather represent flow between the groundwater and some external feature, where that flow happens within the boundaries of the cell. Examples include wells located in the volume of aquifer represented by the cell, or seepages into rivers from cell i,j,k. Two kinds of such source and sink terms are treated in MODFLOW (1) constant rate sources such as recharge, wells, and (2) head-dependent sources such as stream aquifer interaction, lake-aquifer interractions, drains, and ET. These entries are also known as stress terms on the MODFLOW and have to be counted properly to model the groundwater flow.

Suppose N constant sources affect a cell i,j,k: the volumetric flux of water into cell i,j,k per unit volume of aquifer from a single source, n, is designated $q_{i,j,k,n}$ and the total recharge from all N constant sources affecting cell i,j,k is $\sum_{n=1}^{N} q_{i,j,k,n}$. Similarly, for head dependent sources the volumetric flux of water into cell i,j,k per unit volume of aquifer from a single head-dependent source, m, is given by

$q_m = C_{i,j,k,m}(h_m - h_{i,j,k})$,……B-4

where, $C_{i,j,k,m}$ is a conductance associated with source m at node i,j,k; h_m is the head in the source (e.g., a stream); $h_{i,j,k}$ is the head in cell i,j,k. If a total of M head-dependent sources affect cell i,j,k, the total flux from all head dependent source = $\sum_{m=1}^{M} C_{i,j,k,m}(h_m - h_{i,j,k})$ ……B-5

Hence, the total volumetric flux into cell i,j,k from all sources is,

$W = \sum_{m=1}^{M} C_{i,j,k,m}(h_m - h_{i,j,k}) + \sum_{n=1}^{N} q_{i,j,k,n} = \sum_{n=1}^{N} q_{i,j,k,n} + \sum_{m=1}^{M} C_{i,j,k,m} h_m - \sum_{m=1}^{M} C_{i,j,k,m} h_{i,j,k}$……B-6

Let $Q_{i,j,k} = \sum_{n=1}^{N} q_{i,j,k,n} + \sum_{m=1}^{M} C_{i,j,k,m} h_m$ and $P_{i,j,k} h_{i,j,k} = -\sum_{m=1}^{M} C_{i,j,k,m} h_{i,j,k}$

Then, the total volumetric flux of water per unit volume entering the cell from all external sources and sinks will be

$$W_{i,j,k} = P_{i,j,k}\, h_{i,j,k} + Q_{i,j,k} \quad \text{B-7}$$

Applying the continuity equation to the cell i,j,k and considering the flow from six adjacent cells as well as the sources and sinks, the finite-difference approximation of the MODFLOW equation (Harbaugh and McDonald, 1996; Freeze and Cherry, 1979; Harbaugh, 2005; Anderson and Woessner, 1992; Fitts, 2002) (Figures B-1 and B-2) is given by

$$q_{i,j-\frac{1}{2},k} + q_{i,j+\frac{1}{2},k} + q_{i+\frac{1}{2},j,k} + q_{i-\frac{1}{2},j,k} + q_{i,j,k+\frac{1}{2}} + q_{i,j,k-\frac{1}{2}} + P_{i,j,k}\, h_{i,j,k} + Q_{i,j,k} = S_{S_{i,j,k}} \Delta c_i \Delta r_j v_k \frac{\Delta h_{i,j,k}}{\Delta t}, \quad \text{B-8}$$

where $\frac{\partial h_{i,j,k}}{\partial t} = \frac{\Delta h_{i,j,k}}{\Delta t}$ is the finite-difference approximation for the time derivative of head with respect to time (LT^{-1}), $S_{S_{i,j,k}}$ is the specific storage of cell i,j,k (L^{-1}), and $\Delta c_i \Delta r_j v_k$ is the volume of the cell i,j,k (L^3).

Now, substituting the values of terms $q_{i,j-\frac{1}{2},k}$ and $W_{i,j,k}$ into above equation, we have,

$$CR_{i,j-\frac{1}{2},k}\left(h_{i,j-1,k} - h_{i,j,k}\right) + CR_{i,j+\frac{1}{2},k}\left(h_{i,j+1,k} - h_{i,j,k}\right) + CC_{i-\frac{1}{2},j,k}\left(h_{i-1,j,k} - h_{i,j,k}\right) + CC_{i-\frac{1}{2},j,k}\left(h_{i-1,j,k} - h_{i,j,k}\right) +$$

$$CV_{i,j,k-\frac{1}{2}}\left(h_{i,j,k-1} - h_{i,j,k}\right) + CV_{i,j,k+\frac{1}{2}}\left(h_{i,j,k+1} - h_{i,j,k}\right) + P_{i,j,k} h_{i,j,k} + Q_{i,j,k} = S_{S_{i,j,k}} \Delta c_i \Delta r_j v_k \frac{\Delta h_{i,j,k}}{\Delta t} \quad \text{B-9}$$

In addition to the discretization of space provided by the finite-difference mesh, time must be discretized in a finite-difference approach. For this purpose, MODFLOW uses a backward-difference approach, i.e., an approach in which the flow terms are represented at the end of the period used to simulate the time derivative, rather than at the beginning of that period.(Figure B-3). The backward-difference approach is always numerically stable such that any errors introduced during any preceding time step of simulation will diminish progressively at succeeding times (McDonald and Harbaugh, 1888).

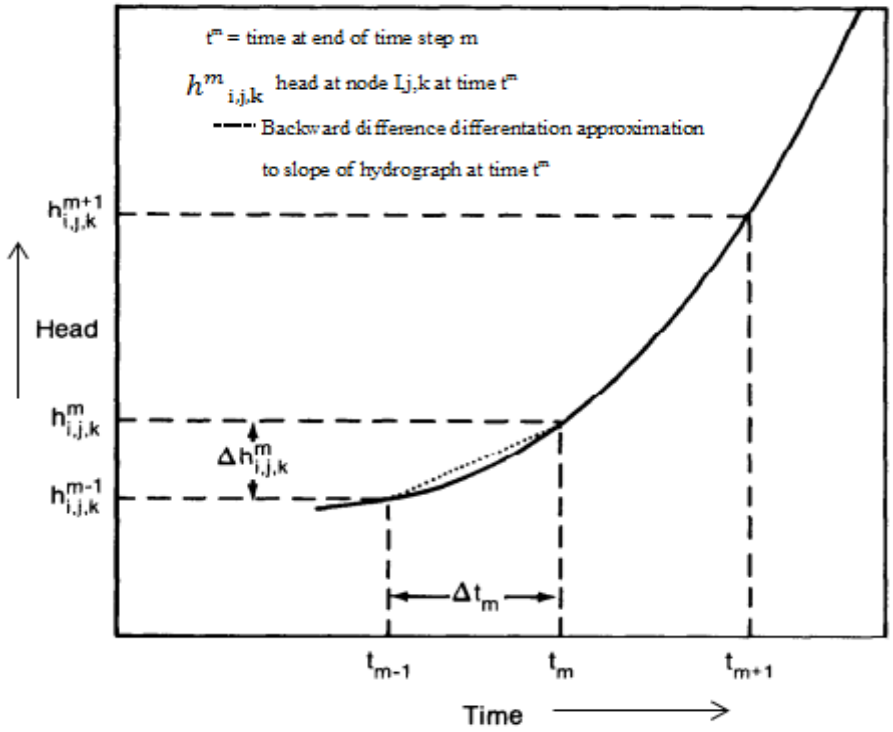

Figure B-3 Hydrograph for cell i,j,k used in backward-difference approach of finite-difference approximation (McDonald and Harbaugh,1988)

For finite-difference approximation, $\frac{\partial h_{i,j,k}}{\partial t} = \frac{\Delta h_{i,j,k}}{\Delta t} \cong \frac{h^m{}_{i,j,k} - h^{m-1}{}_{i,j,k}}{t^m - t^{m-1}}$,.....B-10

where, $h^m{}_{i,j,k}$ and $h^{m-1}{}_{i,j,k}$ are head values associated with times t^m and t^{m-1}, respectively, for the node i,j,k (Figure B-3) in the backward difference approach of the finite-difference approximation. Also, considering $h^{m-1}{}_{i,j,k}$ as the head at the beginning of time t^{m-1} at time step m-1, as known, and our aim is to determine the head value at time t^mon time step m. The above equation reduces into

$CR_{i,j-\frac{1}{2},k}\left(h^m{}_{i,j-1,k} - h^m{}_{i,j,k}\right) + CR_{i,j+\frac{1}{2},k}\left(h^m{}_{i,j+1,k} - h^m{}_{i,j,k}\right) + CC_{i-\frac{1}{2},j,k}\left(h^m{}_{i-1,j,k} - h^m{}_{i,j,k}\right) + CC_{i-\frac{1}{2},j,k}\left(h^m{}_{i-1,j,k} - h^m{}_{i,j,k}\right) + CV_{i,j,k-\frac{1}{2}}\left(h^m{}_{i,j,k-1} - h^m{}_{i,j,k}\right) + CV_{i,j,k+\frac{1}{2}}\left(h^m{}_{i,j,k+1} - h^m{}_{i,j,k}\right) + P_{i,j,k}h^m{}_{i,j,k} + Q_{i,j,k} =$

$S_{S_{i,j,k}}\Delta c_i \Delta r_j v_k \frac{h^m{}_{i,j,k} - h^{m-1}{}_{i,j,k}}{t^m - t^{m-1}}$.....B-11

Note that in this equation, flow terms are evaluated at time m, that is, at the end of the time interval over which the time derivative is simulated. This equation can be used for simulation of groundwater flow. Now, for simplicity we can regroup the terms containing the (unknown) heads at the

end of the current time step, m, on left side and all terms independent of head and the terms with head at the beginning of the current step on the right hand side; also the coefficient of $h^{m}_{i,j,k}$ that do not include conductance between nodes are combined into a single term, HCOF, and all the right hand side terms into a term RHS. Hence, the final finite-difference solution for the MODFLOW is given as

$$CV_{i,j,k-\frac{1}{2}}h^{m}_{i,j,k} + CC_{i-\frac{1}{2},j,k}h^{m}{}_{i-1,j,k} + CR_{i,j-\frac{1}{2},k}h^{m}{}_{i,j-1,k} + (-CV_{i,j,k-\frac{1}{2}} - CC_{i-\frac{1}{2},j,k} - CR_{i,j-\frac{1}{2},k} - CR_{i,j+\frac{1}{2},k} - CC_{i+\frac{1}{2},j,k} - CV_{i,j,k+\frac{1}{2}} - HCOF_{i,j,k})h^{m}{}_{i,j,k} + CR_{i,j+\frac{1}{2},k}h^{m}{}_{i,j+1,k} + CC_{i+\frac{1}{2},j,k}h^{m}{}_{i+1,j,k} + CV_{i,j,k+\frac{1}{2}}h^{m}{}_{i,j,k+1} = RHS_{i,j,k} \quad \text{.....B-12}$$

where, $HCOF_{i,j,k} = P_{i,j,k} - \frac{S_{S_{i,j,k}}\Delta r_j \Delta c_i \Delta v_k}{t^{m} - t^{m-1}}$, and $RHS_{i,j,k} = -Q_{i,j,k} - S_{S_{i,j,k}}\Delta r_j \Delta c_i \Delta v_k \frac{h^{m}_{i,j,k}}{t^{m} - t^{m-1}}$. Using matrix notation the solution can be simplified into:

$$[A]\{h\} = \{q\}$$

where [A] = matrix coefficient of head on LHS of the equation for all active nodes

{h} = vector head values at the time step m

{q} = vectors of the constant terms, RHS

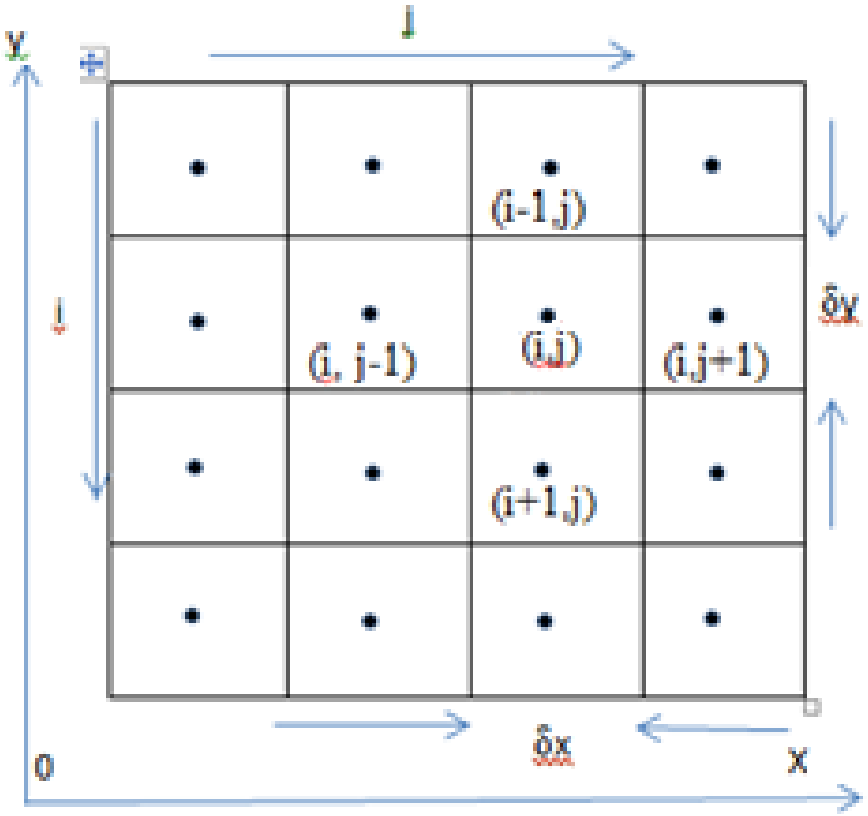

Figure B-4 Finite-difference grid representation for the flow in MODFLOW depicting the numbering convention (Wang and Anderson, 1982)

After the simulation of the head by iterative method using MODFLOW program, the final array of the head is given as a hydrograph, 3-dimensional plots, contour map or a table of the head values as shown in Figures B-3, 6-1, and 6-2.

Appendix C

Miscellaneous Graphs Developed During the Research as Indicators of Urban Impact

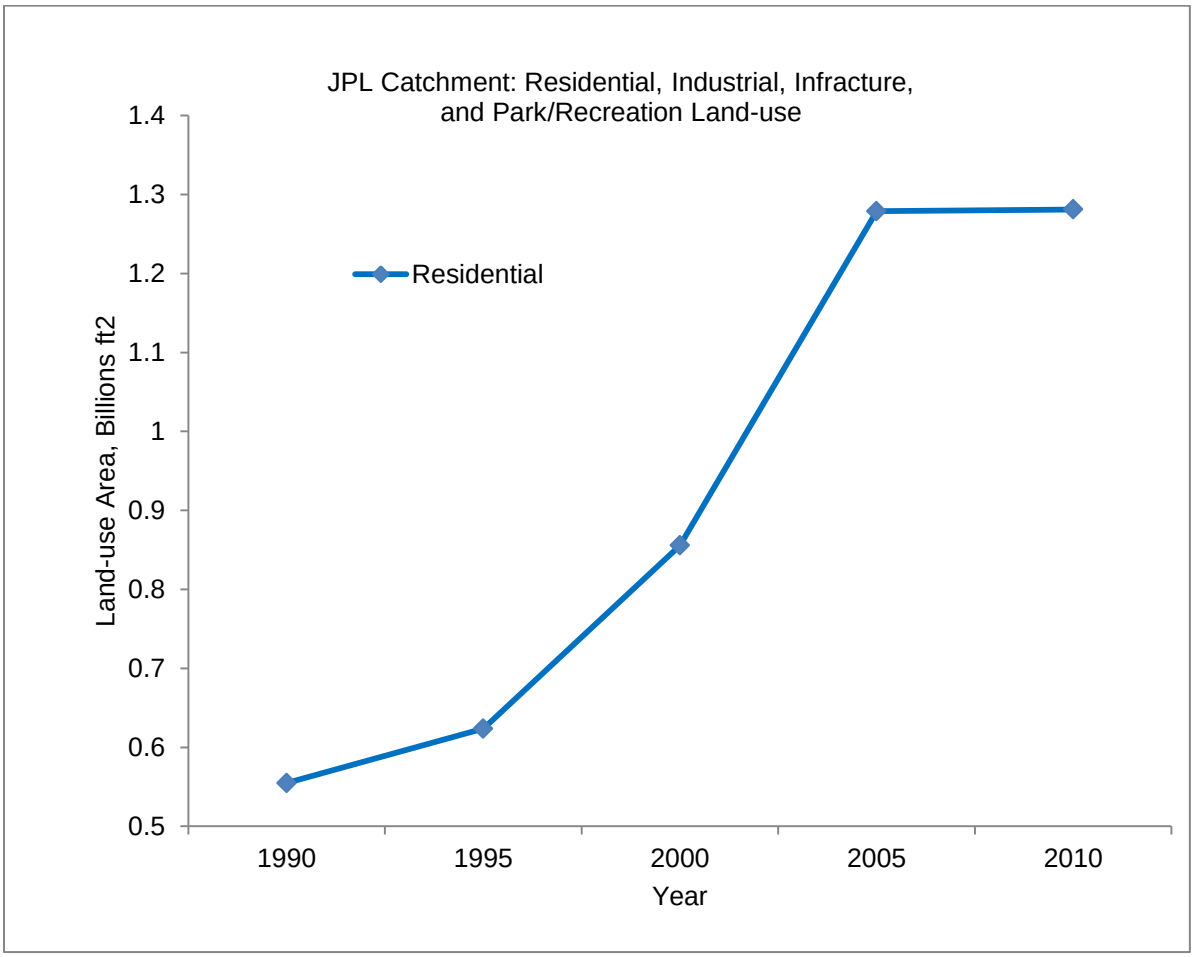

Figure C-1 The developed land-use change inside the JPL catchment as a function of time

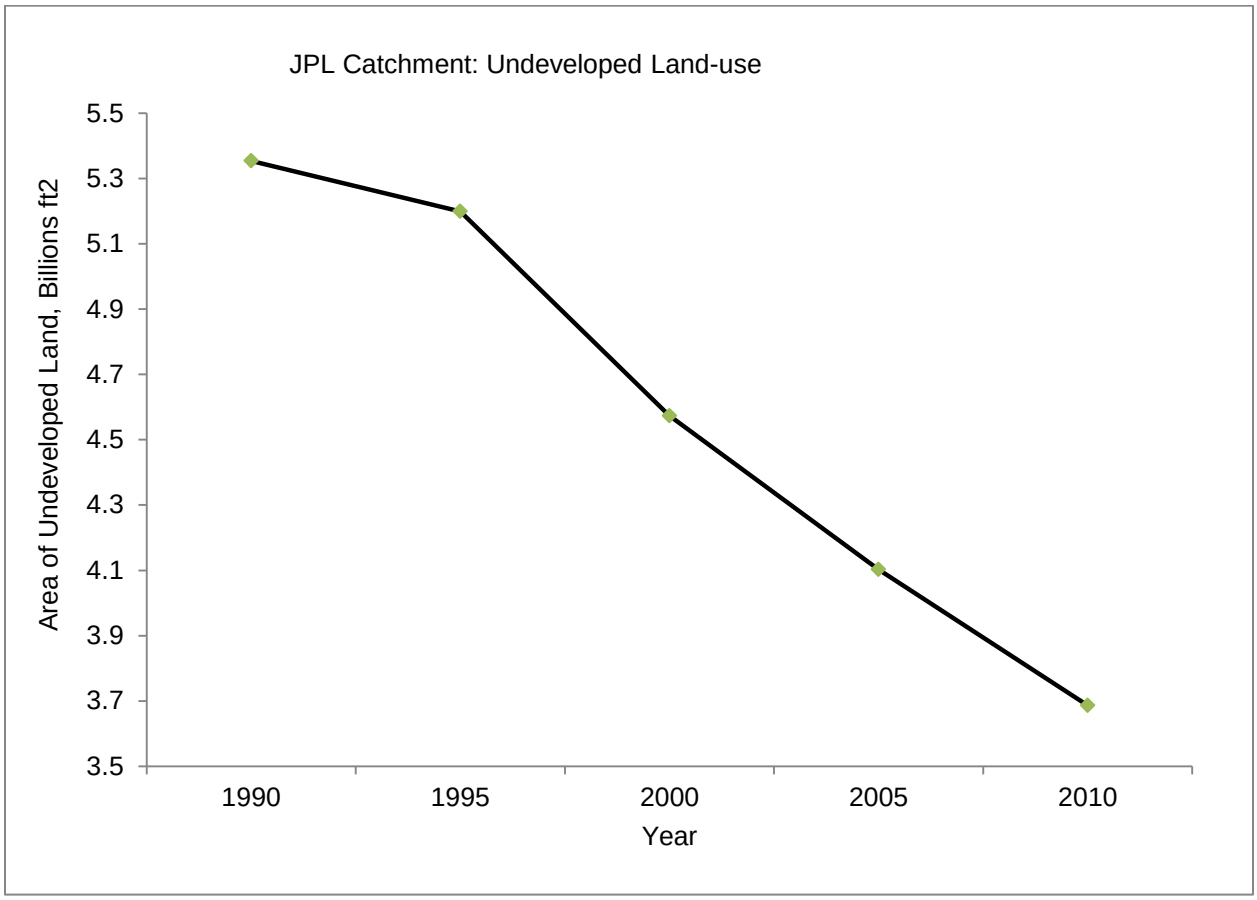

Figure C-2 The undeveloped land-use change inside the JPL catchment as a function of time

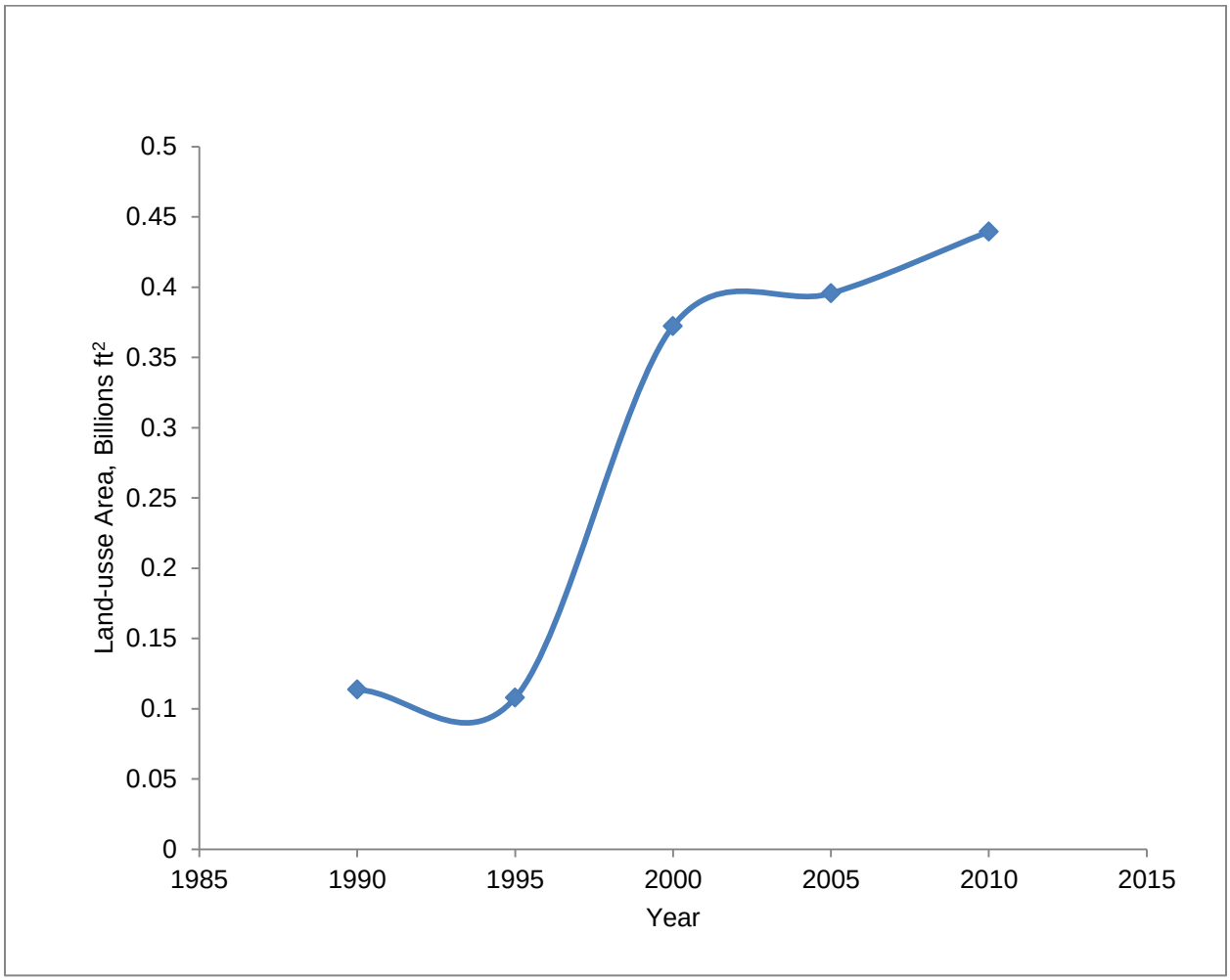

Figure C-3 The infrastructural land-use change inside the JPL catchment as a function of time

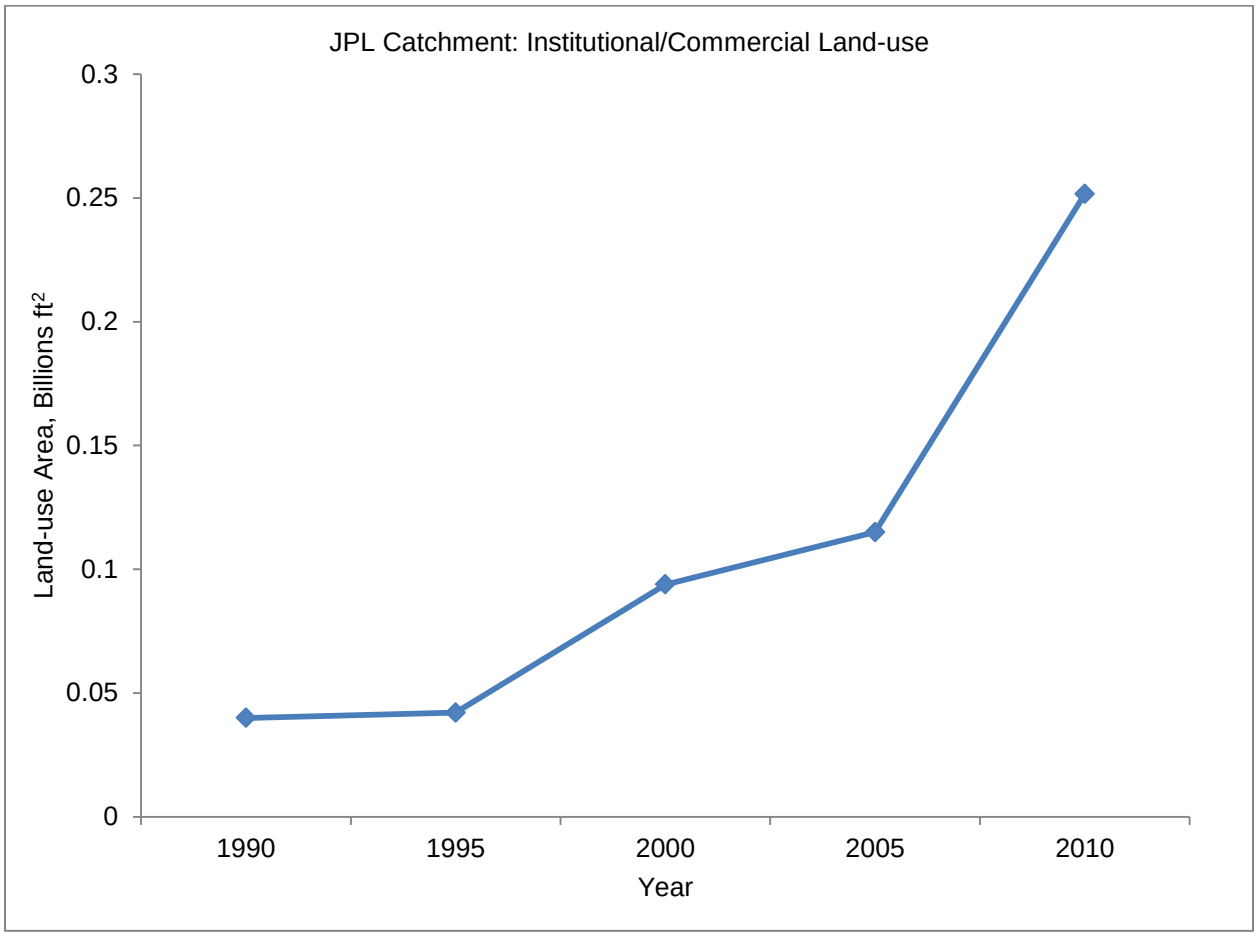

Figure C-4 The institutional/commercial land-use change inside the JPL catchment as a function of time

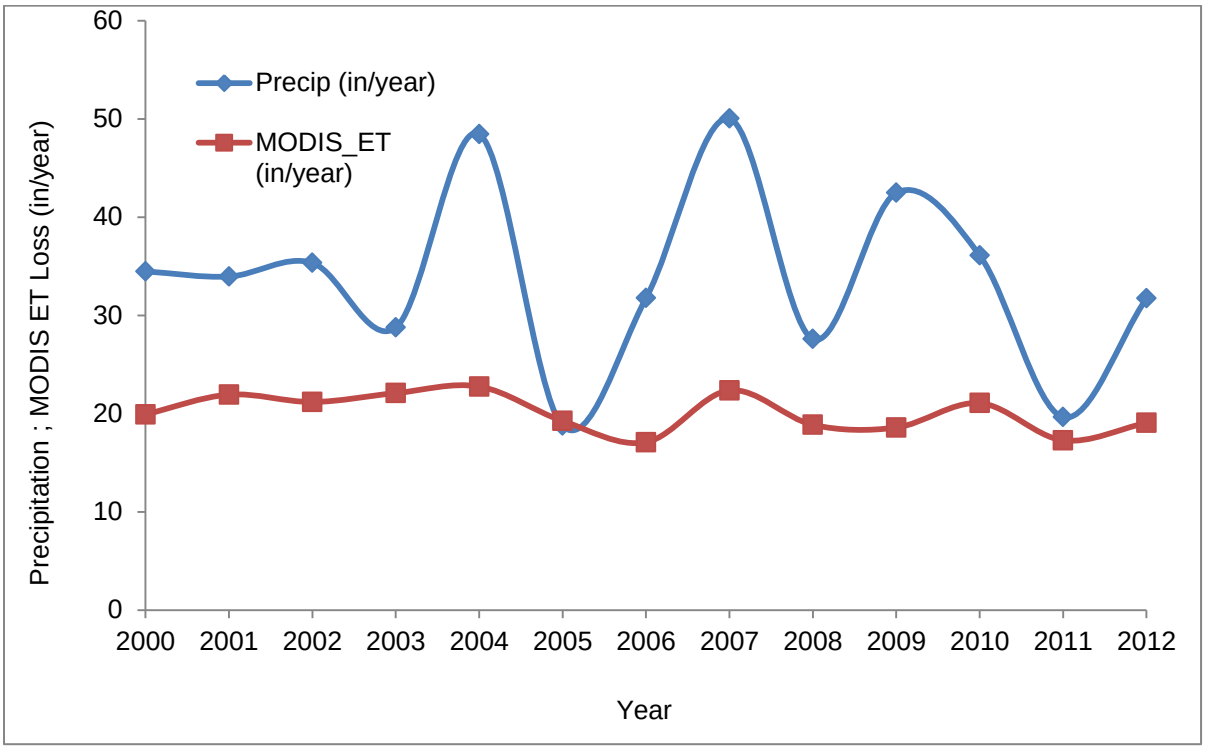

Figure C-5 Time series plot of the MODIS ET and basin precipitation vs. year

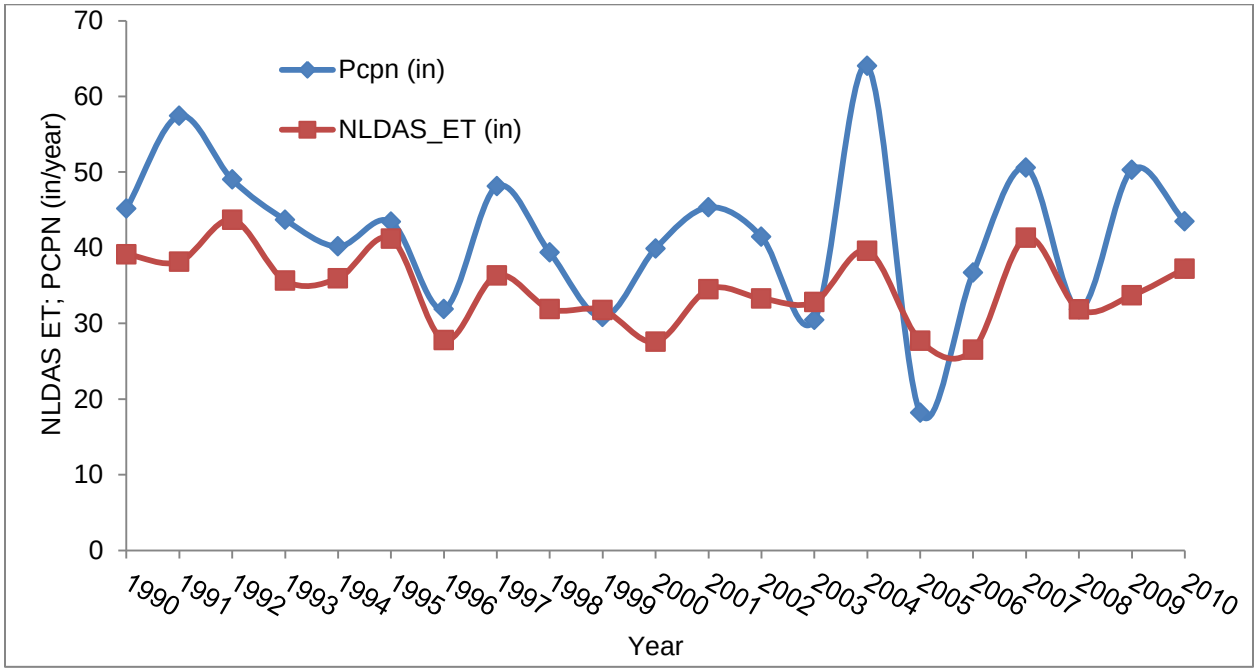

Figure C-6 Time series plot of the NLDAS ET and basin precipitation vs. year

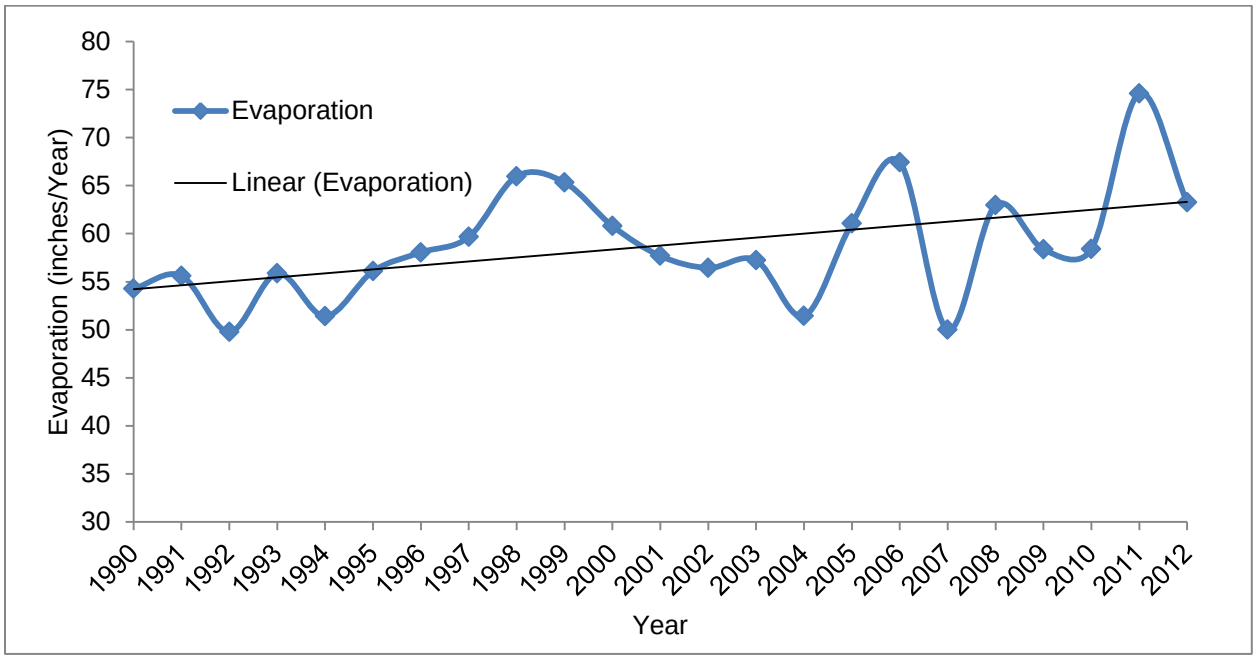

Figure C-7 The time series plot of JPL evaporation loss (in/year) vs. year

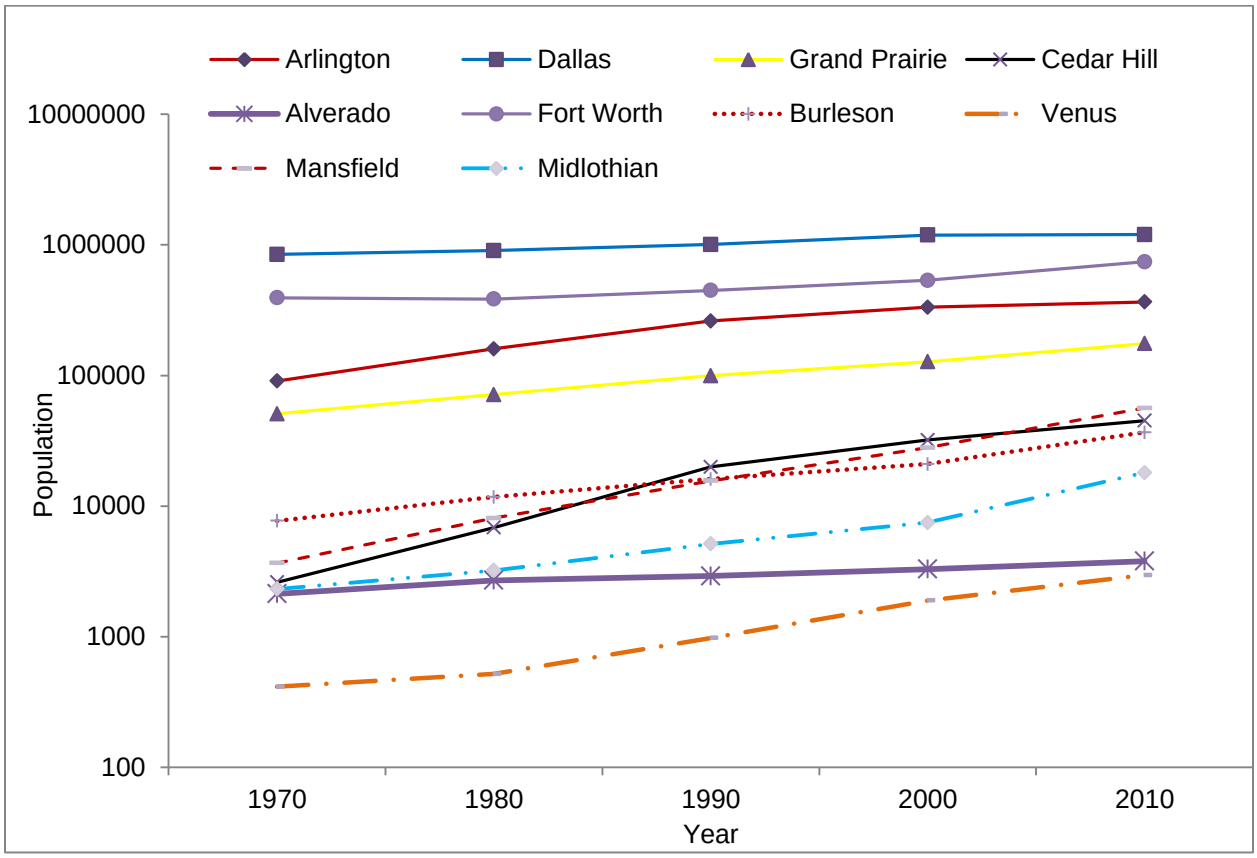

Figure C-8 Population trend of cities inside the project area (1970-2010). Source (NCTCOG population bulletin, March 2007; U. S. Census, 1990-2010)

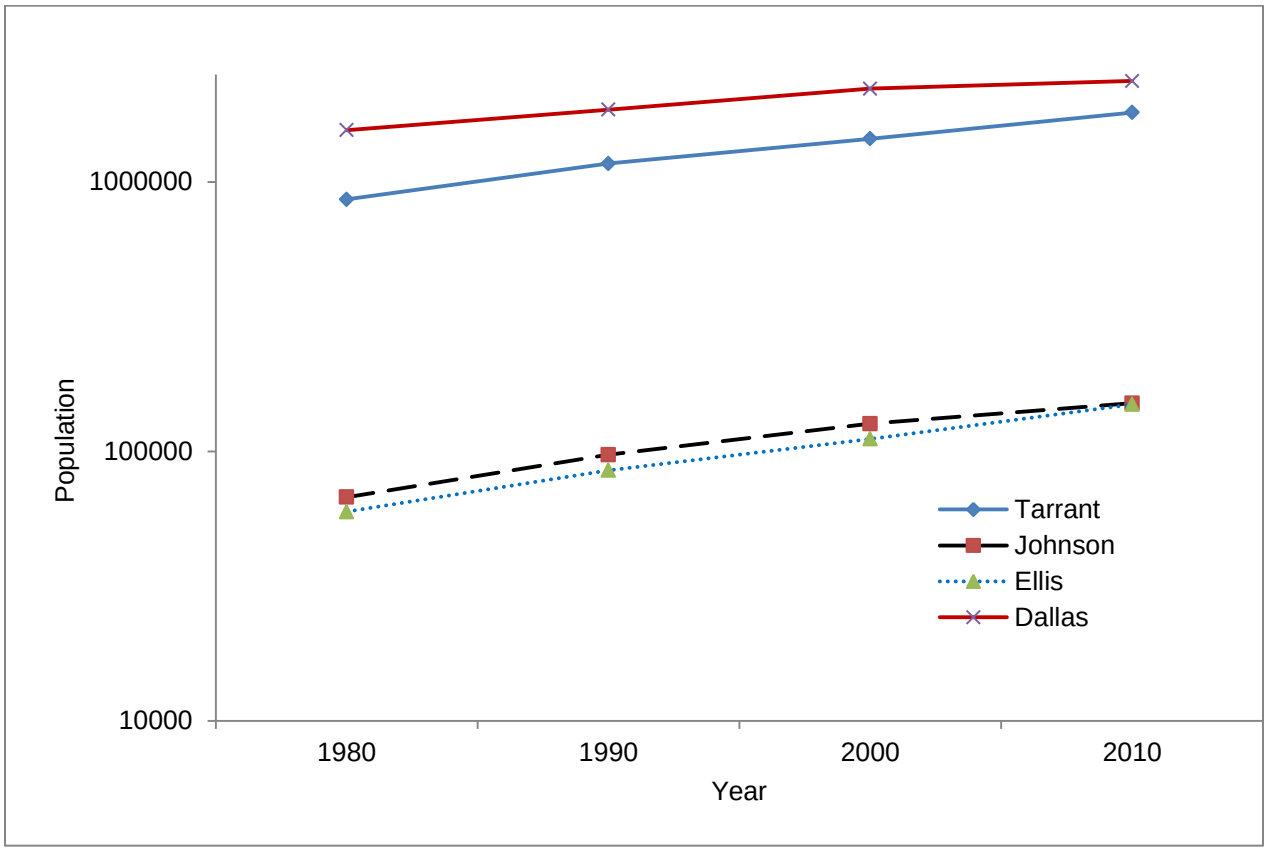

Figure C-9 Population trend of cunties inside the project area (1970-2010). In semi-log scale

References

Ajami, H., and Maddock, T., 2009. RIPGIS-NET: an ArcGIS custom application for the RIP-ET Package in MODFLOW-2000 and MODFLOW-2005. HWR Report no. 10-010, 247, Department of Hydrology and Water Resources, University of Arizona, Tucson, Arizona.

Ajami, H., Maddock, T. (3rd), Meixner, T., Hogan, J.F., and Guertin, D.P., 2012. RIPGIS-NET: a GIS tool for riparian groundwater ET in MODFLOW, Groundwater, Vol. 50, No. 1, p. 154–15. DOI: 10.1111/j.1745-6584.2011.00809.x.

Anderson, M.P., and Woessner, W.W., 1992. Applied groundwater modeling: simulation of flow and advective transport: San Diego, Calif., Academic Press, 381 pp.

Barker, R.A., and Braun, C.L., 2000. Computer-model analysis of ground-water flow and simulated effects of contaminant remediation at Naval Weapons Industrial Reserve Plant, Dallas, Texas. U.S. Geological Survey Water-Resources Investigations Report 00–4197.

Bene, J., Harden, B., Griffin, S.W., and Nicot, J. P., 2007. Northern Trinity/Woodbine GAM assessment of groundwater use in the Northern Trinity Aquifer due to urban growth and Barnett Shale development: contract report prepared for the Texas Water Development Board, 278 pp.

Bené, J., Harden, B., O'Rourke, D., Donnelly, A., and Yelderman, J., 2004. Northern Trinity/Woodbine groundwater availability model: prepared for the TWDB by R.W. Harden & Associates, Inc., with Freese and Nichols, Inc, HDR Engineering, Inc., LBG Guyton Associates, USGS, and Dr. Joe Yelderman, Jr., 391 p. http://www.twdb.state.tx.us/groundwater/models/gam/trnt_n/TRNT_N_Model_Report.pdf.

B.E.G., 1972. Geologic Atlas of Texas, Dallas Sheet: Bureau of Economic Geology (BEG), University of Texas at Austin, Austin, Texas 78713-8924.

B.E.G_____, Digital 15-minute GAT (Geologic Atlas of Texas) Quads for the State of Texas (Projection: TSMS (NAD 83)).

Bennett, G.D., 1989. Introduction to ground-water hydraulics, a programmed text for self-instruction, U.S. Geological Survey, Techniques of Water-Resources Investigations, Book 3, Chapter B2.

Bernard, E. A., and Steward, D. R., 2006. AEM integration in a geodatabases for groundwater modeling, 5th International Conference on the Analytic Element Method, Manhattan, KS, May 14-17, 2006.

Bernard, E. A., Steward, D. R., and Le Grand, P. A., 2005. Geodatabase for groundwater modeling in MLAEM and MODFLOW, ESRI International User Conference 2005, San Diego, CA, July 25–29, 2005.

Celia, M.A., and Williams, G.G., 1992. Numerical methods for differential equations: fundamental concepts for scientific & engineering applications, Prentice Hall, Inc. New Jersey 07632.

Cheng, X., and Anderson, M.P., 1993. Numerical simulation of ground-water interaction with lakes allowing for fluctuating lake levels: Groundwater, Vol. 31, No. 6, pp 929-933.

Chow, V.T., (Ed.) 1964. Handbook of applied hydrology: a compendium of water resources technology. New York: McGraw-Hill.

Collins, R.E., 1961. Flow of fluids through porous materials: New York, Reinhold Publishing Corp., 270 pp.

Collins, E.W., Hovorka, S.D., and Laubach, S.E., 1992. Fracture systems of the Austin Chalk, north-central Texas, in Schmoker, J. W.,Coalson, E.B., and Brown, C.A., eds., Geological studies relevant to

horizontal drilling: examples from western North America: Rocky Mountain Association of Geologists, pp 129-142.

Council, G.W., 1998. A lake package for MODFLOW: Proceedings of MODFLOW 98 Conference, October 4-8, 1998, Golden, Colorado, Vol. 2, pp 675-682.

Council, G.W.,1997. Simulating lake-groundwater interaction with MODFLOW. Proceedings of the 1997 Georgia Water Resources Conference, (March 20-22) at The University of Georgia, Kathryn J. Hatcher, Editor, Institute of Ecology, The University of Georgia, Athens, Georgia.

Czarnecki, J.B., and Waddell, R.K., 1984. Finite-element simulation of ground-water Flow in the vicinity of Yucca Mountain, Nevada-California USGS Water-Resources Investigations Report: 84-4349.

Dong, L., Chen, J., Fu, C., and Jiang, H., 2011. Analysis of groundwater-level fluctuation in a coastal confined aquifer induced by sea-level variation. Hydrogeology Journal, Volume 20, Issue 4, pp.719-726. DOI: 10.1007/s10040-012-0838-2.

Douherty, J.P., 1975. Evaporation data in Texas, Texas water Development Board, Report No. 192.

Dowell, C.L., 1964. Dams and reservoirs in Texas, historical and descriptive information, Texas Water Commission Bulletin No. 6408, July 1964.

EnSafe/Allen & Hoshall 1996a. Draft RCRA facility investigation report, Naval Weapons Industrial Reserve Plant, Dallas, Texas- Volume I (Sections 1–5): Memphis, Tenn., EnSafe/Allen & Hoshall.

EnSafe/Allen & Hoshall 1996b. Interim RFI report category B NAS, Dallas, Texas- Volume III (Sections 7–10): Memphis, Tenn., EnSafe/Allen & Hoshall.

EnSafe/Allen & Hoshall 1997a. Interim RFI report category C NAS, Dallas, Texas: Memphis, Tenn., EnSafe/Allen & Hoshall.

EnSafe/Allen & Hoshall 1997b. Interim RFI report category F NAS, Dallas, Texas: Memphis, Tenn., EnSafe/Allen & Hoshall.

Feinstein, D.T., Hunt, R.J., and Reeves, H.W., 2010. Regional groundwater-flow model, Lake Michigan Basin, Great Lakes Water Availability and Use Studies—Scientific Investigations Report 2010–5109.

Fitts, C., 2002. Groundwater science. Academic Press 525 B Street, Suite 1900, San Diego, CA. 2002. 450 pp. ISBN 0-12-257855-4.

Flugel, W.A., and Micht, C., 1995. Using MODFLOW/MODPATH combined with GIS analysis for groundwater modeling in the alluvial aquifer of the River Sieg, Germany, IAHS Publication, 227 (1995), pp. 117–123.

Freeze, R.A., and Cherry, J.A., 1979. Groundwater, Prentice- Hall, Englewood Cliff, NJ.

Foster, S.S.D., Morris, B.L. and Lawrence, A.R., 1994. Effects of urbanization on groundwater recharge, pp. 43–63. In: Groundwater Problems in Urban Areas, Proceedings of the Institution of Civil Engineers (Wilkinson, W.B., Ed.). Institution of Civil Engineers, London, UK.

Garcia-Fresca, B., 2004. Urban effects on groundwater recharge in Austin, Texas: unpublished M.S thesis, University of Texas, Austin, TX, 173pp.

Garcia-Fresca, B., and Sharp, J.M. (Jr)., 2005. Hydrogeologic considerations of urban development – urban-induced recharge: in Humans as Geologic Agents (Ehlen, J., Haneberg, W.C., and Larson, R.A., (eds.), Geol. Soc. America, Reviews in Engineering Geology, Vol.. XVI, pp 123-136.

George, P.G., Mace, R.E. and Petrossian, R., 2011. Aquifers of Texas: TWDB, Report 380, Austin, TX.

Grischek, T., Nestler, W., Piechniczek, D., and Fischer, T., 1996. Urban groundwater in Dresden, Germany, Hydrogeology Journal: 4(1), 48-63.

Haitjema, H.M., and Hunt, R.J., 2002. Modeling lake-aquifer interactions with analytic elements, AGU Spring Meeting, Washington DC.

Haitjema, H.M., 2005. Modeling lake-groundwater interactions in GFLOW, accessed September 14, 2012, at http://www.haitjema.com/documents/ModelinglakegroundwaterinteractionsinGFLOW.pdf

Haitjema, H.M, and Mitchell-Bruker, S., 2005. Are water tables a subdued replica of the topography? Groundwater Vol. 43, No. 6:781–786.

Hall, F.R., 1968. Base-flow recessions-a review, Water Resource. Research 4, 973 983.

Hamer de, W., Love, D., Owen, R., Booij, M.J., and Hoekstra, A.Y., 2007. Potential water supply of a small reservoir and alluvial aquifer system in Southern Zimbabwe. In: 8th WATERNET/WARFSA/GWP-SA Symposium, 31 October-2 November 2007, Lusaka, Zambia, 31 October-2 November 2007, Lusaka, Zambia.

Harbaugh, A.W. and McDonald, M.G., 1996. User's documentation for MODFLOW–96, an update to the U.S. Geological Survey modular finite-difference ground-water flow model: U.S. Geological Survey Open-File Report 96–485, 56 pp.

Harbaugh, A.W., 1990. A computer program for calculating subregional water budgets using results from the U.S. Geological Survey modular three-dimensional finite-difference groundwater flow model: U.S. Geological Survey Open-File Report 90-392, 46 pp.

Harbaugh, A.W., 2005. MODFLOW-2005, the U.S. Geological Survey modular ground-water model - the ground-water flow process: U.S. Geological Survey Techniques and Methods 6–A16.

Harbaugh, A.W., Banta, E.R., Hill, M.C., and McDonald, M.G., 2000. MODFLOW – 2000, the U.S. Geological Survey modular ground-water model - user guide to modularization concepts and the ground-water flow process: U.S. Geological Survey Open-File Report 00 - 92, 121 pp.

Harbaugh, A.W., 2010. A data-input program (MFI2005) for the U.S. Geological Survey modular groundwater model (MODFLOW-2005) and parameter estimation program (UCODE_2005): U.S. Geological Survey Open-File Report 2010–1057, 35 pp.

Hernandez, J.E., Gowda, P.H., Howell, T. A., Steiner, J. L., Mojarro, F., Núñez , E. P., and Avila, J.R., 2011. Modeling groundwater levels on the Calera Aquifer region in Central Mexico using MODFLOW. Journal of Agricultural Science and Technology B 2 (2012): 52-61.

Hill, M.C., 1990. Preconditioned conjugate-gradient 2 (PCG2), a computer program for solving ground-water flow equations: U.S. Geological Survey Water-Resources.

Hill, M.C., Banta, E.R., Harbaugh, A.W., and Anderman, E.R., 2000. MODFLOW-2000, the U.S. Geological Survey Modular Ground-Water Model - user guide to the observation, sensitivity, and parameter-estimation processes and three post-processing programs: U.S. Geological Survey Open-File Report 00-184, 209 pp.

Horton, R.E., 1933. Role of infiltration in the hydrologic cycle. Transactions, American Geophysical Union 14:446-460.

Howard, K. W. F., 2002. Urban groundwater issues – An introduction, in current problems of hydrogeology in urban areas, urban agglomerates, and industrial centres, edited by K.W. F. Howard and R. G. Israfilov, pp 1–15, Kluwer, Dordrecht.

Hsieh, P.A., and Winston, R.B., 2002. User's guide to model viewer, a program for three-dimensional visualization of ground-water model results: U.S. Geological Survey Open-File Report 02-106, 18 pp.

Hubbert, M.K., 1940. The theory of ground-water motion. The Journal of Geology, v 48, no. 8: 785–944.

Istok, J. D., 1989. Groundwater modeling by the finite-element method, American Geophysical Union, Water Resources Monograph-13: ISBN 0-87590-317-7.

Jobson, H.E., and Harbaugh, A.W., 1999. Modifications to the diffusion analogy surface-water flow model (DAFLOW) for coupling to the modular finite-difference groundwater flow model (MODFLOW): U.S. Geological Survey Open-File Report 99-217,107.

Johnson, S.B., Schindel, G.M., and Veni, G., 2005. Tracing flowpaths in the Edwards Aquifer Recharge Zone in northern Bexar County, Texas, from National Ground Water Association 2005 Summit, San Antonio, TX, USA, April 17-20, 2005, in Abstract Book of the 2005 Ground Water Summit, pp 230-231.

Jones, S. A., and Paillet, F. L., 1995. Integrity of production wells and confining unit at the Naval Weapons Industrial Reserve Plant, Dallas, Texas U.S. Geological Survey Water-Resources Investigations Report 97–4047.

Kalthoff, K., (29 July 2011). “Government Peddles Property as Congress Fights Over Debt” Retrieved 10 July 2013. http://www.nbcdfw.com/news/politics/Government-Peddles-Property-as-Congress-Fights-Over-Debt-126425633.html

Kelley, V. A., Ewing, J., Jones, T.L., Young, S.C., Deeds, N., and Hamlin, S., 2014. Updated groundwater availability model of the Northern Trinity and Woodbine Aquifers: prepared for the TWDB by Intera, Geoscience & Engineering Solutions, in association with Bureau of Economic Geology, University of Texas at Austin and LBG Guyton Associates, http://ntwgam.intera.com/reports.html.

Kuiper, L. K., 1987. Computer program for solving ground-water flow equations by the preconditioned conjugate gradient method: U.S. Geological Survey Water-Resources Investigations Report 87–4091, 34 pp.

Kuniansky, E. L., and Hamrick, T.S., 1998. Hydrogeology and simulation of ground-water flow in the Paluxy Aquifer in the Vicinity of Landfills 1 and 3, U.S. Air Force Plant 4, Fort Worth, Texas: U.S. Geological Survey Water-Resources Investigations Report 98–4023. In cooperation with the U.S. Air Force, Aeronautical Systems Center, Environmental Management Directorate, Wright-Patterson Air Force Base, Ohio.

Lake Products, L.L.C., 2003. Topographic and recreational map of Joe Pool Lake, P.O. Box. 2000744 Arlington, Texas 76006. Phone 1-800-886-MAP1.

Lambert, P. M., Marston, T., Kimball, B. A., and Stolp, B. J., 2011. Assessment of groundwater/surface-water interaction and simulation of potential streamflow depletion induced by groundwater withdrawal, Uinta River near Roosevelt, Utah—Scientific Investigations Report 2011–5044.

Lampayan, R., Ghassemi, F., and White, I., 2001. Groundwater modeling of an irrigated area of the Lachlan catchment for salinity management', International Congress on Modeling and Simulation (MODSIM 2001), (ed.) Ghassemi, F. and others, Modelling and Simulation, Society of Australia and New Zealand Inc., Canberra, pp. 541-548.

Lapidus, L., and Pinder, G.F., 1982. Numerical solutions of partial differential equations in science and engineering. Wiley-Interscience, New York.

Leake, S.A., and Prudic, D.E., 1991. Documentation of a computer program to simulate aquifer-system compaction using the modular finite-difference ground-water flow model: U.S. Geological Survey Techniques of Water-Resources Investigations, Book 6, Chap. A2, 68 pp.

Lerner, D.N., 2002. Identifying and quantifying urban recharge: a review, Hydrogeology Journal, Volume 10, pp 143 – 152, Springer-Verlag.

Lerner, D.N., Issar, A., and Simmers, I., 1990. Groundwater recharge; a guide to understanding and estimating natural recharge. International contributions to hydrogeology, Vol. 8. Heise, Hannover, Germany, 345 pp.

Lerner, D.N., 1997(b). Too much or too little: recharge in urban areas: in groundwater in the urban environment: problems, processes and management (Chilton, J., ed.), Proceedings of the 27th Congress, International Association of Hydrogeologists, Balkema, Rotterdam, pp 41-47.

Leggat. E. R., 1957. Geology and ground-water resources of Tarrant County, Texas: United States Geological Survey and Texas Board of Water Engineers and the City of Fort Worth Report 5709, 1957.

Lim, K.J., Engel, B.A., Tang, Z., Choi, J. Kim, K., Muthukrishnan, S., and Tripathy, D., 2005. Web GIS-based Hydrograph Analysis Tool, WHAT. JAWRA, 41(6): 1407-1416.

Lindgren, R.J., Houston, N.A., Musgrove, M., Fahlquist, L.S., and Kauffman, L.J., 2011. Simulations of groundwater flow and particle-tracking analysis in the zone of contribution to a public-supply well in San Antonio, Texas: U.S. Geological Survey Scientific Investigations Report 2011–5149, 93 pp.

Linsley, R.K. Jr., Kohler, M.A., and Paulhus, J.L.H., 1958. Hydrology for engineers. McGraw-Hill, New York, pp. 482.

Luo, Y., and Sophocleous, M., 2011. Two-way coupling of unsaturated-saturated flow by integrating the SWAT and MODFLOW models with application in an irrigation district in arid region of West China[J]. Journal of Arid Land, 2011, 3(3): 164-173. doi 10.3724/SP.J.1227.2011.00164.

Mace, R. E., Dutton, A. R., and Nance, H. S., 1994, Water-level declines in the Woodbine, Paluxy, and Trinity aquifers of North-Central Texas: Gulf Coast Association of Geological Societies Transactions, Vol. 44, pp 413-420.

Mace, R.E., and Dutton, A.R., 1994. Hydrogeologic controls on contaminant transport in weathered and fractured chalk, Toxic Substances and Hydrologic Sciences, American Institute of Hydrology, pp.535-546.

Maidment, D.R. (Ed.), 2002. ArcHydro : GIS for water resources, Redlands, California, ESRI Press 2002

Malik, V. S., Singh, R.K., and Singh, S. K., 2012. Groundwater modeling with processing MODFLOW for windows, (PMWIN) for the water balance study and suitable recharge site: case of Gurgaon District, Haryana, India. International Journal of Engineering Science and Technology (IJEST), Vol. 4, No.09, pp 72-8. ISSN : 0975-5462.

McDaniels, L.L., 1960. Consumptive use of water by major by major crops in Texas. Bulletin No. 6019. Texas Water Development Board, Surface Water Division, Texas Board of Water Engineers.

McDonald, M.G., and Harbaugh, A.W., 1988. A modular three-dimensional finite-difference ground-water flow model. Techniques of Water-Resources Investigations of the United States Geological Survey, Book 6, Chapter Al. US Department of the Interior, US Geological Survey, Denver, Colorado.

Mehl, S.W., and Hill, M.C., 2005. MODFLOW-2005, the U.S. Geological Survey modular ground-water model - documentation of shared node local grid refinement (LGR) and the Boundary Flow and Head (BFH) Package: U.S. Geological Survey Techniques and Methods 6-A12, 68 pp.

Memon, A.A., and Memon, M.A., 2006. Simulation of unsteady flow in the left bank outfall drain unconfined aquifer in the Lower Indus Basin, Proceedings of The 2006 IJME - INTERTECH Conference, Session: IT P501-125.

Merritt, M.L., and Konikow, L.F., 2000. Documentation of a computer program to simulate lake-aquifer interaction using the MODSFLOW groundwater flow model and the MOC3D solute-transport model: U.S. Geological Survey Water-Resources Investigations Report 00-4167,146 pp.

Miller, R.S., 1988. User's guide for RIV2: a package for routing and accounting of river discharge for a modular three-dimensional finite-difference, groundwater flow model. U.S. Geological Survey Open-File Report 88-345.

Mirlas, V., 2009. Applying MODFLOW model for drainage problem solution: a case study from Jahir Irrigated Fields, Israel Journal of Irrigation and Drainage Engineering, Vol. 135, No. 3. ISSN 0733-9437/2009/3-269–278. DOI: 10.1061/(ASCEIR).1943-4774.0000003.

Monteith, J.L., 1965. Evaporation and environment. Proc. Symp. Soc. Exp. Biol. 19:205–234.

Nance, H.S., Laubach, S.E., and Dutton, A.R., 1994. Fault and joint measurements in Austin Chalk, superconducting super collider site, Texas: Gulf Coast Association of Geological Societies, Transactions, Vol. 44, pp 521-532.

Nathan, R.J., and McMahon, T.A., 1990. Evaluation of automated techniques for base flow and recession analyses. Water Resources Research 26:1465–1473.

NCTCOG, 2010. Land Use Classification. www.nctcog.org/ris/.../landuse/LandUseClassification.pdf

NHGIS.ORG, 2011. Minnesota Population Center, National Historical Geographic Information System: Version 2.0. Minneapolis, MN: University of Minnesota 2011. http://www.nhgis.org

Niswonger, R.G. and Prudic, D.E., 2005. Documentation of the streamflow routing (SFR2) package to include unsaturated flow beneath streams - a modification to SFR1: U.S. Geological Survey Techniques and Methods, Book 6, Chap. A13,47 pp.

Niswonger, R.G., Panday, S., and Ibaraki, M., 2011. MODFLOW-NWT, a Newton formulation for MODFLOW-2005: U.S. Geological Survey Techniques and Methods 6–A37, 44 pp.

Panday, S., Langevin, C.D., Niswonger, R.G., Ibaraki, Motomu, and Hughes, J.D., 2013. MODFLOW-USG version 1: an unstructured grid Version of MODFLOW for simulating groundwater flow and tightly coupled processes using a control volume finite-difference formulation: U.S. Geological Survey Techniques and Methods, Book 6, Chap. A45, 66 pp.

Penman, H.L., 1948. Natural evaporation from open water, bare soil, and grass. Proceedings of the Royal Society of London, 193 (1948), pp. 120–145.

Pinder, G. F., 1970. A digital model for aquifer evaluation. U. S. Geological Survey, Techniques of Water-Resources Investigations, Book 7, Chapter Cl.

Pinder, G.F., 2003. Groundwater modeling using geographical information system, John Wiley& sons, Inc., New York USA.

Pinder, G.F., and Gray, W.G., 1977. Finite-element simulation in surface and subsurface hydrology: New York, Academic, 295 pp.

Pinder, G.F., and Leon, L., 1982. Numerical solution of partial differantial equations in science and engineering, Wiley-Interscience Publication John Wiley & Sons Publishing Company 1982.

Poeter, Eileen P. and Hill, M. C., 2008. SIM_ADJUST -- A Computer Code that Adjusts Simulated Equivalents for Observations or Predictions, International Ground Water Modeling Center Report GWMI 2008-01, 28p.

Pollock, D.W., 1989. Documentation of a computer program to compute and display pathlines using results from the U.S. Geological Survey modular three-dimensional finite-difference ground-water flow model: U.S. Geological Survey Open-File Report 89–381, 188 pp.

Pollock, D.W., 1994. User's guide for MODPATH/MODPATH-PLOT, version 3: a particle-tracking post-processing package for MODFLOW, the U.S. Geological Survey finite-difference ground-water flow model: U.S. Geological Survey Open-File Report 94–464, 249 pp.

Pollock, D.W., 2012. User guide for MODPATH version 6—A particle-tracking model for MODFLOW: U.S. Geological Survey Techniques and Methods, Book 6, Chap. A41, 58 pp.

Prickett, T. A., and Lonnquist, C. G., 1971. Selected digital computer techniques for groundwater resource evaluation. Illinois State Water Survey Bulletin 55.

Prudic, D.E., 1989. Documentation of a computer program to simulate stream-aquifer relations using a modular, finite-difference, ground-water flow model: U.S. Geological Survey Open-File Report 88–729, 113 pp.

Prudic, D.E., Konikow, L.F., and Banta, E.R., 2004. A new streamflow-routing (SFR1) package to simulate stream-aquifer interaction with MODFLOW–2000: U.S. Geological Survey Open-File Report 2004–1042, 95 pp.

Putra, D., and Baier, K., 2008. Impact of urbanization on groundwater recharge - the Example of the Indonesian Million City Yogyakarta, In: UN Habitat- United Nations Settlement Programs: Fourth session of the World Urban Forum, Nanjing, China, Documentations of Germany's Contribution to a Sustainable Urban Future.

Raney, J.A., Allen, P.M., Reaser, D.F., and Collins, E.W., 1987. Geology and Geotechnical Considerations of the SSC Site in Texas: Geologic review of proposed Dallas - Fort Worth area site for the superconducting super collider (SSC), SSC-N-620, April 1989, Material Presented at the meeting of

the Underground Tunnelling Advisory Panel, April 30, 1989 at the SSC Laboratory at Lawrence Berkeley Laboratory.

Reaser, D.F., 1957. Geology of the Ferris quadrangle, Dallas and Ellis Counties, Texas, Field and Laboratory Volume 25 (4):83-93.

Reaser, D.F., and Collins, E.W., 1988. Style of faults and associated fractures in Austin Chalk. Northern extension of the Balcones Fault Zone, Central Texas, Transactions - Gulf Coast. Association of Geological Society 38:267-276.

Reaser, D.F., 1991. Structural features near proposed site for the Superconducting Super collider in north-central Texas, in S. Chuber, ed., Austin Chalk Exploration Symp: Abstracts and short paper of the South Texas Geological Society pp 119-122.

Romero, V., Bull, J., Stapleton, G., Baker, S., Goss, D., and Coulson, L., 1994. Superconducting Super collider (SSCL) Groundwater Model, Superconducting Super Collider Laboratory 2550 Beckleymeade Ave. Dalla, Texas. SSCL-SR-1233, Operated by the Universities Research Association, Inc., for the U.S. Department of Energy under Contract No. DE-AC35-89ER40486.

Rushton, K.R., and Redshaw, S.C., 1979. Seepage and groundwater flow: numerical analysis by analogue and digital methods: New York, John Wiley and Sons, 339 pp.

Rutledge, A. T., 2007a. Program user guide for PART; U.S. Geological Survey Water-Resources Investigations Report: http://water.usgs.gov/ogw/part/UserManualPART.pdf (January 30, 2007).

Rutledge, A.T., 1998. Computer programs for describing the recession of ground-water discharge for estimating mean ground-water recharge and discharge from streamflow data – Update: U.S. Geological Survey Water-Resources Investigations Report 98-4148, 43 pp.

Scanlon, B.R., Mace, R.E., and Barrett, M.E., 2001. Comparison of distributed and lumped approaches to simulating water flow in a karst aquifer, from 2001 Annual Meeting of the Geological Society of America (GSA) annual meeting, November1-10, 2001, Boston, MA, *in* Geological Society of America Abstracts with Programs, Volume 33, No. 6, pp. 411.

Shuler, E.W., 1918. Geology of Dallas County. Texas University Bulletin. 1818, 48 pp.

Smakhtin, V.U., 2001. Low flow hydrology: a review. Journal of Hydrology 240, 147-186.

Stanton, J.S., Peterson, S.M., and Fienen, M.N., 2010. Simulation of groundwater flow and effects of groundwater irrigation on stream baseflow in the Elkhorn and Loup River Basins, Nebraska, 1895–2055 Phase Two: U.S. Geological Survey Scientific Investigations Report 2010–5149, 78 pp. with app.

Sterner, R.W., 1994. Seasonal and spatial patterns in macro- and micronutrient limitation in JPL, Texas. American Society of Limnology and Oceanography, Inc. Limnology Oceanography, 39 (3):535-550.

Stone, D.B., and Fontaine, R.C., 1998. Simulation of groundwater fluxes during open-pit filling and under steady state pit lake conditions, in Proceedings of the Conference on Hazardous Waste Research Snow Bird, Utah, May 1998), pp. 32-42 (1998).

Strassberg, G., Jones, N.L., and Maidment, D. R., 2011. Arc hydro groundwater: GIS for hydrogeology, ESRI Press, 2011.

Sun, A., Painter, S., and Green, R., 2005. Modeling Barton Springs segment of the Edwards Aquifer using MODFLOW-DCM. in Schindel, G., ed., Proceedings of the 10th Multidisciplinary Conference on Sinkholes and the Engineering and Environmental Impacts of Karst (ed. G. Schindel), San Antonio, Texas, 2005.

Swain, E.D., and Wexler, E.J., 1996. A coupled surface-water and ground-water flow model (MODBRANCH) for simulation of stream-aquifer interaction: U.S. Geological Survey Techniques of Water-Resources Investigations, Book 6, Chapter A6, 125 pp.

Takounjou, A.F., Gurunadh Rao, V.V.S., Ngoupayou, N.J., Nkamdjou, L. S., and Ekodeck, G. E., 2009. Groundwater flow modeling in the Upper Anga'a River Watershed, Yaounde, Cameroon. African Journal of Environmental Science and Technology Vol. 3 (10), pp. 341-352. Academic Journals, ISSN 1991-637X.

Tallaksen, L.M., 1995. A review of baseflow recession analysis. Journal of Hydrology 165:349-370.

Tetra Tech NUS, Inc., 2004. Final MNA groundwater modeling report for category B Naval Air Station Dallas, Dallas, Texas Southern Division Naval Facilities Engineering Command Contract Number N62467-94-D-0888, Contract Task Order 0163; Anderson Dr. Foster Plaza 7 Pittsburgh, Pennsylvania 15220.

The PB/MK Team, 1991. Characterization of the state of in situ stresses by hydraulic fracturing method at the Exploratory Shaft site, Ellis County, TX for the Superconducting Super Collider project, Kunsoo Kim, Henry Krumb School of Mines, Columbia University, New York, NY 10027.

Thompson, G. L., 1967. Ground-water resources of Ellis County, Texas: United States Geological Survey and Texas Water Development Board Report 62, 1967.

Thompson, G. L., 1969. Ground-water resources of Johnson County, Texas: United States Geological Survey and Texas Water Development Board Report 94, 1969.

Thornton, J., 2002, Water loss control manual: McGraw-Hill, New York, 526 pp.

Thornthwaite, C.W., 1948. An approach toward a rational classification of climate Geographical Review, 38 (1948), pp. 55–94.

Tonkin, M.J., Tiedeman C.R., Ely, D.M., and Hill, M.C., 2007. OPR-PPR, a Computer Program for Assessing Data Importance to Model Predictions Using Linear Statistics: Reston Virginia, USGS, Techniques and Methods Report TM –6E2, 115 p.

Torres-González, Sigfredo, Gómez-Gómez, Fernando, and Warne, A.G., 2002. Ground-water resource assessment in the Río Grande de Manatí Alluvial Plain, Río Arriba Saliente Area, Puerto Rico—USGS Water-Resources Investigations Report 02-4132.

Trescott, P.C., 1975. Documentation of finite-difference model for simulation of three-dimensional groundwater flow: U.S. Geological Survey Open-File Report 75–438, 32 pp.

Trescott, P.C., and Larson, S.P., 1976. Supplement to open-file report 75-438, documentation of finite-difference model of three-dimensional groundwater flow; U.S. Geological Survey Open-File Report 76-591, 21 pp.

Trescott, P.C., Pinder, G.F., and Larson, S.P., 1976. Finite-difference model for aquifer simulation in two dimensions with results of numerical experiments: U.S. Geological Survey Techniques of Water-Resources Investigations, Book 7, Chap. C1, 116 pp.

U.S. Geological Survey, 2014. Water-resources Data for the United States, Water Year 2013: U.S. Geological Survey Water-Data Report WDR-US-2013, site 08049700, accessed at http://wdr.water.usgs.gov/wy2013/pdfs/08049700.2013.pdf.

USACE, 1979. Trinity River Basin Design Memorandum No.1, Lake View Reservoir, Hydrology. Trinity River Basin Fort. Worth District Design Memos Volume Number 8-1.

USACE, 1988. Completion of embankment and spillway, Joe Pool Lake, Mountain Creek, Texas, Army Engineer District Fort Worth, TX, U.S. Department of Commerce National Technical Information Service, Alexandria, VA 22312.

USACE, 1991. Joe Pool Lake and Mountain Creek, Texas Trinity River Basin, embankment criteria and performance report: U.S. Army Corps of Engineers, Fort Worth.

Van Lanen, H. A. J., and Van Weered, B. D., 1994. Groundwater flow from a Cretaceous Chalk Plateau: impact of groundwater recharge and abstraction. FRIEND: Flow Regimes from International Experimental and Network Data (Proceedings of the Braunschweig Conference, October 1993). IAHS Publ. No. 221, 1994.

Van Metre, P.C., Jones, S.A., Moring, J.B., Mahler, B.J., and Wilson, J.T., 2003. Chemical quality of water, sediment, and fish in Mountain Creek Lake, Dallas, Texas, 1994-97 USGS Water-Resources Investigations Report 2003 - 4082.

Vazquez-Sune, 2003. Urban groundwater, Barcelona City, case study: Polytechnic University of Catalonia, Barcelona, Doctoral Thesis.

Wang, H.F., and Anderson, M.P., 1982. Introduction to groundwater modeling: finite-difference and finite-element methods, W.H. Freeman, San Francisco, 1982.

Weeks, A.W., 1945. Balcones, Luling, and Mexia fault zones in Texas, American Association of Petroleum Geologists Bulletin, Volume 29 (12):1733-1737.

Wickham, M.K., 1991. Hydrogeology and water resources of an unconfined aquifer in a Pleistocene, terrace deposit, Ellis County, Texas, M. S. thesis, the University of Texas at Austin.

Winston, R.B., 2009. ModelMuse—A graphical user interface for MODFLOW–2005 and PHAST: U.S. Geological Survey Techniques and Methods 6–A29, 52 pp.

Winton, W.M., and Scott, G., 1922. The geology of Johnson County, University of Texas Bulletin No. 2229: August 1, 1922. Bureau of Economic Geology and Technology Division of Economic Geology.

Xu, X., Huang, G.H., Qu, Z.Y., and Pereira, L.S., 2011. Using MODFLOW and GIS to assess changes in groundwater dynamics in response to water saving measures in irrigation districts of the upper Yellow River basin. Water Resources Management.doi:10.1007/s11269-011-9793-2.

Yager, R.M., and Metz, P.A., 2004. Simulated effects of ground-water augmentation on the hydrology of Round and Halfmoon Lakes in northwestern Hillsborough County, Florida, U. S. Geological Survey Water-Resources Investigations Report 03-4322, 50 pp.

Yang, Y., Learner, D.N., Barret, M., and Tellam, J., 1999. Quantification of groundwater recharge in the city of Nottingham, UK. Environmental Geology, 38(3), 183-198.

Zheng, C., and Wang, P. P., 1999. MT3DMS, a modular three-dimensional multi-species transport model for simulation of advection, dispersion and chemical reactions of contaminants in groundwater systems; Documentation and user's guide, U.S. Army Engineer Research and Development Center Contract Report SERDP-99-1, Vicksburg, MS, 202 pp.

Zheng, C., 1990. MT3D, a modular three-dimensional transport model for simulation of advection, dispersion and chemical reactions of contaminants in groundwater systems, report to the U.S. Environmental Protection Agency, 170 pp.

Zheng, C., 2010. MT3DMS v 5.3 supplemental user's guide, technical report to the U.S. Army Engineer Research and Development Center, Department of Geological Sciences, University of Alabama, 51 pp.

Zheng, C., Hill, M. C., and Hsieh, P. A., 2001. MODFLOW-2000, the U.S. Geological Survey modular ground-water model - user's guide to the LMT6 Package, the linkage with MT3DMS for multi-species mass transport modeling, U.S. Geological Survey Open-File Report 01-82, 43 pp.

Zheng, C., Weaver, J., and Tonkin, M., 2010. MT3DMS, a modular three-dimensional multispecies transport model user guide to the hydrocarbon spill source (HSS) Package. Athens, Georgia: U.S. Environmental Protection Agency.

Biographical Information

Manoj Kumar Ghimire is raised in Kathmandu, Nepal. He has M.S. degrees (1996) in Hydrology and Meteorology from Tribhuvan University (TU), Nepal and M.S.degree (2007) in Earth and Environmental Sciences from University of Texas at Arlington.

Mr. Ghimire worked at the National Academy of Science and Technology (NAST) Nepal as a research scientist from December 1993–August 1996. He had also worked at the Central Department of Hydrology and Meteorology at TU, Kirtipur, Nepal; Tri-chandra Campus Ghantaghar, Kathmandu, Nepal; and at Kathmandu University, Dhulikhel, Nepal as a lecturer from February 1997 to January 2000, December 1997 to January 2000, and February 2000 to August 2005, respectively. He taught courses such as meteorology, climatology, hydrology, environmental aspect of hydrometeorology, geology, and glacier environment to the graduate and undergraduate students of Environmental Science and Hydrology and Meteorology Program. Mr. Ghimire was employed as the Graduate Teaching Assistant at the Department of Earth and Environmental Sciences at University of Texas at Arlington from January 2006 to December 2014 and taught lab section of the Meteorology, Oceanography, and Physical Geology. Mr. Ghimire is a member of Association of Environmental and Engineering Geologists (AEG) Texas Section, American Association of Petroleum Geologists (AAPG), Geological Society of America (GSA), and National Ground Water Association (NGWA).

Mr. Ghimire is interested in research and teaching of Hydrogeology, Groundwater Modeling, Contaminant Transport Modeling, and Reservoir Modeling, Geographical Information System (GIS), Sedimentology, and Geomorphology. He plans to be a professor and teach courses like Hydrogeology, Environmental Modeling, Geology, GIS, and Geomorphology.